

Sheffield Hallam University

Bioremediation of selenium species in solution by methanotrophic bacteria

ESWYAH, Abdurrahman S.

Available from the Sheffield Hallam University Research Archive (SHURA) at:

<http://shura.shu.ac.uk/21457/>

A Sheffield Hallam University thesis

This thesis is protected by copyright which belongs to the author.

The content must not be changed in any way or sold commercially in any format or medium without the formal permission of the author.

When referring to this work, full bibliographic details including the author, title, awarding institution and date of the thesis must be given.

Please visit <http://shura.shu.ac.uk/21457/> and <http://shura.shu.ac.uk/information.html> for further details about copyright and re-use permissions.

Bioremediation of Selenium Species in Solution by Methanotrophic Bacteria



Abdurrahman S. Eswayah

A thesis submitted in partial fulfilment of the requirements of
Sheffield Hallam University
for the degree of Doctor of Philosophy

January 2018
Sheffield, UK

Abstract

Selenium species, particularly the oxyanions selenite and selenate, are significant pollutants in the environment that leach from rocks and are also released by anthropogenic activities. In the environment, microbial transformations of selenium play important roles in the biogeochemical cycles of the element. For instance, microbial reduction of the toxic and water-soluble selenium oxyanions to nanoparticulate elemental selenium greatly reduces the toxicity and bioavailability of selenium and has a major role in bioremediation. Also, microbial methylation after reduction of selenium oxyanions is another potentially effective detoxification process if limitations with low reaction rates and capture of the volatile methylated selenium species can be overcome.

Methane-oxidizing bacteria are well known for their role in the global methane cycle and their potential for microbial transformation of wide range of hydrocarbon and chlorinated hydrocarbon pollution. Recently, it has also emerged that methane-oxidizing bacteria interact with inorganic pollutants in the environment. Here, the selenium-transforming properties of methane-oxidizing bacteria have been investigated for the first time. The interaction of selenium containing chemical species has been studied with pure strains of the commonly used laboratory model strains of methane-oxidizing bacteria, *Methylococcus capsulatus* (Bath) and *Methylosinus trichosporium* OB3b.

The two strains were both able to convert the toxic selenite but not selenate or DL-selenocystine to extracellular red spherical nanoparticulate elemental selenium, which was confirmed by X-ray absorption near-edge structure (XANES) and extended X-ray absorption fine structure (EXAFS). The selenium nanoparticles were characterized by a variety of techniques, including transmission electron microscopy (TEM) energy dispersive X-ray (EDX) spectrometry, high-angle annular dark-field (HAADF) scanning TEM (STEM), X-ray photoelectron spectroscopy (XPS), SDS-PAGE analyses, Fourier-transform infrared spectroscopy (FTIR), zeta potential and Raman spectroscopy. The results showed that the reduction process is an enzymatic reaction and mediated by cell wall-associated proteins. The elemental red selenium nanoparticles formed during selenite reduction were found to be amorphous containing a certain amount of sulfur.

The results also indicated that the produced selenium nanoparticles are coated with organic materials, likely to be proteins and extracellular polymeric substances (EPS).

The cultures also produced volatile selenium-containing species when challenged with selenite, which shows that both strains have an additional activity that can transform either elemental selenium or selenite into volatile methylated forms of selenium, including dimethyl selenide, dimethyl diselenide, dimethyl selenenyl sulphide, methylselenol and methylselenoacetate. Selenate (at concentrations higher than 100 $\mu\text{g mL}^{-1}$) or DL-selenocystine-amended cultures of *Methylococcus capsulatus* (Bath) (but not *Methylosinus trichosporium* OB3b) produced volatile selenium-containing species. From a biotechnological standpoint, these results are promising for the use of methane-oxidizing bacteria for bioremediation of selenium-contaminated environments and suggest possible uses in the production of selenium nanoparticles for technological applications.

Acknowledgements

Praise is due to almighty Allah, the sole Lord of the universe, whose mercy and blessings are being bestowed constantly upon the author. Equally, peace and blessings be upon His final messenger Mohammed.

I would like to express my sincere gratitude to my esteemed supervisor Dr Philip Gardiner, for his continued guidance which helped me accomplish the goals of my research. Dr Gardiner has been a great source of inspiration, for his patience and perseverance has helped embed confidence in myself to explore new opportunities. He has always been happy and willing to help me and support me during the course of research. My thanks also to my second supervisor Prof Thomas Smith, for listening, having an open door, the countless conversations and always being happy to support, even at the busiest of times.

I would like to thank Dr Nicole Hondow at School of Chemical and Process Engineering, University of Leeds for assistance with the TEM-EDX measurements. I would also like to thank Dr Emma Wharfe at Department of Geography, University of Sheffield for Raman analysis. I would also like to convey my thanks to Dr Tamim Chalati at Department of Chemistry, University of York for assistance with the zeta potential measurements. I am highly thankful to Dr Andreas Scheinost at the Rossendorf Beamline at the European Synchrotron Radiation Facility (ESRF), Grenoble, France for assistance with the X-ray absorption spectroscopy measurements. Thank you to Dr Debbie Hammond at Sheffield Surface Analysis Centre, University of Sheffield for assistance with the X-ray photoelectron spectroscopy (XPS) analysis. I take this opportunity to express my thanks to Dr Mohamed Merroun at the “Centro de Instrumentación Científica”, University of Granada, Spain for assistance with the TEM-EDX thin section analyses. I am highly thankful to Dr Sarah Haywood-Small (Sheffield Hallam University) for assistance with the flow cytometric analysis. I extend my sincere thanks to Michael Cox (Sheffield Hallam University) for assistance with the HPLC-ICP-MS measurements and Jonathan Foster (Sheffield Hallam University) for assistance with the GC-MS analysis.

My thanks are extended to all staff and colleagues at Biomolecular Science Research Centre, Sheffield Hallam University for their advice and friendship. Big thanks go to my

friends, Yasin AL-Luaibi, Mohammed Tawfiq, Hasan Aldewachi, Mootaz Salman, Guma Beleid and Salaheldeen Enbaia for their help and cooperation as well as their friendship.

The acknowledgement would be incomplete without the mention of constant encouragement as well as support of Prof Nicola Woodroffe, Head of the Biomolecular Sciences Research Centre.

My special thanks are due to my beloved wife, children, brothers, sisters, relatives and all my friends either in the UK or back home in Libya, whose encouragements have been invaluable. Finally, my professional thanks go to the Libyan Government for funding and supporting my Ph. D. studies.

Dissemination: Publications during Ph. D.

Published:

Eswayah, A.S., Smith, T.J. and Gardiner, P.H., 2016. Microbial transformations of selenium species of relevance to bioremediation. *Applied and Environmental Microbiology*, 82(16), pp.4848-4859.

Eswayah, A.S., Smith, T.J., Scheinost, A.C., Hondow, N. and Gardiner, P.H., 2017. Microbial transformations of selenite by methane-oxidizing bacteria. *Applied Microbiology and Biotechnology*, 101(17), pp.6713-6724.

In preparation:

Eswayah A.S., Smith T.J., Hondow, N. Hammond D. and Gardiner, P.H. Characterization of Selenium Nanoparticles Produced by Methane-oxidizing Bacteria.

Dissemination: Conferences during Ph. D.

Poster Presentation entitled “Reduction of Selenite to Red Elemental Selenium by Methane-oxidizing Bacteria” at the VI International Conference on Environmental, Industrial and Applied Microbiology - BioMicroWorld2015, Barcelona, Spain, 28-30 October 2015.

Poster Presentation entitled “Transformation of Selenium Species by Methane-oxidising Bacteria for Bioremediation” at the ECO-BIO 2016 Conference, Rotterdam, Netherlands, 6-9 March 2016.

Poster Presentation entitled “Transformation of Selenium Species by Methane-oxidising Bacteria” at Mini C1 Symposium UEA 2016, University of East Anglia, Norwich, UK, Thursday 5th May 2016.

Oral Presentation entitled “Remediation of Selenium (IV) by Methane-oxidising Bacteria” at the 2nd International Conference on Environmental Science and Technology (ICOEST), Belgrade, Serbia 27 September-4 October 2016.

Oral Presentation entitled “Microbial Transformations of Selenite by Methane-Oxidizing Bacteria” at the 3rd International Conference on Environmental Science and Technology (ICOEST), Budapest, Hungary 19-23 October 2017.

Dissemination: Collaboration

I have been collaborating with Dr Maria Romero-Gonzales (University of Sheffield) and Dr Mohamed Merroun and Miguel Angel Ruiz Fresneda (University of Granada, Spain) on a project entitled "Effect of bacterial surface layer proteins in coating and controlling the size and shape of Se NPs" in which the methods I have developed in my research are being applied to the study of the recently described new species *Stenotrophomonas bentonitica*, isolated from Spanish bentonite.

Declaration

I hereby declare that the work presented in the thesis entitled “Bioremediation of Selenium Species in Solution by Methanotrophic Bacteria” in fulfilment of the requirements for the award of the Degree of Doctor of Philosophy, Biomolecular Science Research Centre, Sheffield Hallam University, is an authentic record of my own work carried out under the supervision of Dr Philip Gardiner and Prof Tom Smith. The matter embodied in this thesis has not been submitted in part or full to any other university or institute for the award of any degree in the UK or abroad.

Abdurrahman S. Eswayah

January 2018

Table of contents

Abstract.....	i
Acknowledgements.....	iii
Dissemination: Publications during Ph. D.	v
Dissemination: Conferences during Ph. D.	vi
Dissemination: Collaboration.....	vii
Declaration.....	viii
List of figures.....	xiv
List of tables.....	xviii
List of abbreviations.....	xix
1 Introduction and review of literature.....	1
1.1 Selenium.....	2
1.1.1 Biochemical functions of selenium.....	3
1.1.1.1 Selenium deficiency.....	6
1.1.1.2 Selenium toxicity.....	6
1.2 Microbial transformations of selenium species for bioremediation.....	8
1.2.1 Background.....	8
1.2.2 Microbial reduction of selenium species.....	10
1.2.2.1 Reduction of selenate.....	16
1.2.2.2 Reduction of selenite.....	17
1.2.2.3 Reduction of selenium species to selenide.....	20

1.2.3	Oxidation of selenium compounds.....	21
1.2.4	Methylation of selenium species.....	22
1.2.4.1	Selenium methylation pathways	23
1.2.5	Demethylation of selenium compounds	27
1.2.6	Selenium bioremediation	27
1.3	Methane-oxidizing bacteria.....	33
1.3.1	Remediation of toxic chemicals by methanotrophs.....	38
1.4	Aims of the work reported in this study.....	40
2	Materials and methods	42
2.1	Materials.....	43
2.2	Methods	43
2.2.1	Bacterial strains and growth conditions.....	43
2.2.2	Determination of the minimum inhibitory concentration (MIC) of selenite and selenate for methanotrophs	44
2.2.3	Bacterial growth under selenite or selenate stress.....	45
2.2.3.1	Changes in cell size of cell population under Se oxyanions stress (Flow Cytometry).....	46
2.2.4	Reduction of selenium oxyanions by methanotrophs.....	46
2.2.5	Evaluation of selenium oxyanions reduction and elemental selenium formation by methanotrophs	47
2.2.5.1	Quantitation of aqueous selenium species	47
2.2.5.2	Quantitation of elemental selenium	48

2.2.5.3	Analysis of total selenium content in dry cell biomass of DL-selenocystine amended cultures	49
2.2.6	Investigation into the role of s/pMMO in the reduction of selenium oxyanions	50
2.2.7	Investigation of the involvement of methanobactin in selenite/selenite reduction.....	50
2.2.8	Cell fractionation.	51
2.2.9	Reductase activity assay	52
2.2.10	Transmission electron microscopy (TEM) and energy dispersive X-ray (EDX) spectrometry/high-angle annular dark-field (HAADF) scanning TEM (STEM) analysis	52
2.2.11	X-ray absorption spectroscopy measurements.....	53
2.2.12	Extraction of selenium nanoparticles produced by methanotrophs	55
2.2.13	X-ray photoelectron spectroscopy (XPS) analysis	56
2.2.14	Raman spectroscopy analysis of SeNPs.....	56
2.2.15	Fourier transform infrared (FT-IR) spectroscopy measurements of SeNPs	57
2.2.16	Dynamic light scattering (DLS) and zeta potential analysis of the SeNPs ...	58
2.2.17	Bacteria protein-associated SeNPs.....	58
2.2.18	Detection of volatile selenium species.....	59
3	Interaction of methanotrophs with selenium oxyanions and evaluation of their reducing ability	61
3.1	Bacterial response to selenium oxyanions.....	62

3.1.1	Minimum inhibitory concentrations of selenium for methanotrophs.....	62
3.1.2	Bacterial growth under selenite/selenate stress	63
3.1.3	Flow cytometric studies.....	68
3.2	Optimization of the separation and detection conditions of selenium species by HPLC-ICP-MS.....	70
3.3	Colour and concentration changes in selenium oxyanion-amended cultures	71
3.4	Transformation of selenium oxyanions and elemental selenium content of cultures.....	77
3.5	Conversion of DL-selenocystine by methanotrophs	78
3.6	EXAFS and XANES measurements	83
3.7	Confirmation of the site of selenite reduction and role of methane.....	85
3.8	Search for enzymes with possible selenite reductase activity in <i>Mc. capsulatus</i> OB3b and <i>Ms. trichosporium</i> OB3b contains genome	88
3.9	The role of methanobactin in the reduction of selenium oxyanions.....	89
3.10	Conclusions.....	90
4	Characterization of elemental selenium produced by methanotrophs	91
4.1	TEM and HAADF-STEM imaging of cell-associated selenium.....	92
4.2	Time course experiments for the formation of elemental selenium nanoparticles.....	95
4.3	Extraction and purification of SeNPs.....	98
4.4	SDS-PAGE analyses of selenium nanoparticles	99
4.5	X-ray photoelectron spectroscopy analysis	100

4.6 Fourier transform infrared (FTIR) analysis	106
4.7 Raman spectroscopy	110
4.8 Zeta potential and average particle size values of selenium nanoparticles	112
4.9 Application of SeNPs	114
4.10 Conclusions.....	119
5 Detection and identification of volatile selenium species	120
5.1 Volatile selenium species of selenite-amended cultures.....	121
5.2 Volatile selenium species of selenate-amended cultures.....	125
5.3 Volatile selenium species of DL-selenocystine-amended cultures	127
5.4 Conclusions.....	129
6 General discussion and future directions.....	130
6.1 General discussion.....	131
6.2 Future directions	141
References.....	143

List of figures

Figure 1-1 Effects of selenium deficiency and excess in animals and humans.....	4
Figure 1-2 Selenium metabolism in mammalian organisms.....	5
Figure 1-3 Schematic Se cycle in soil, and the influence of microbial processes on the transformation of the element.	9
Figure 1-4 The biosynthesis of selenocysteine and decoding of the UGA codon via a quaternary complex.	11
Figure 1-5 Challenger's pathway for the microbial transformations of selenium.....	24
Figure 1-6 Reamer and Zoller's pathway for the microbial transformations of selenium.	25
Figure 1-7 Doran's pathway for the microbial transformations of selenium.....	26
Figure 1-8 Primary structure of methanobactin from <i>Ms. trichosporium</i> OB3b.....	37
Figure 3-1 Time course of bacterial growth of <i>Mc. capsulatus</i> (Bath) and <i>Ms. trichosporium</i> OB3b in the presence of various concentrations of sodium selenate... ..	64
Figure 3-2 Bacterial growth profile of <i>Mc. capsulatus</i> (Bath) and <i>Ms. trichosporium</i> OB3b under different selenite concentrations.....	66
Figure 3-3 Forward scattering analysis of <i>Mc. capsulatus</i> (Bath) and <i>Ms. trichosporium</i> OB3b grown in the presence of selenate.....	69
Figure 3-4 Forward scattering analysis of methanotroph cultures grown in the presence of selenite.....	69
Figure 3-5 Chromatogram of a standard containing of selenite, selenate and DL-selenocystine.....	71
Figure 3-6 Reduction of SeO_3^{2-} to red Se^0 by the methanotrophs.	73

Figure 3-7 Reduction of selenite (10mg L^{-1}) to red Se^0 by sMMO-deleted mutant of <i>Ms. trichosporium</i> OB3b (SMDM) without and with selenite.	73
Figure 3-8 Time course of selenite reduction after an initial addition of 10 mg L^{-1} of the oxyanion to the culture containing <i>Mc. capsulatus</i> and <i>Ms trichosporium</i> OB3b.	74
Figure 3-9 The effect on the time course of selenite reduction after an initial addition of different concentrations of the oxyanion to the culture containing <i>Mc. capsulatus</i> and <i>Ms trichosporium</i> OB3b.	74
Figure 3-10 Reduction of SeO_3^{2-} to red putative Se^0 by <i>Mc. capsulatus</i> (Bath) without and with methane.	75
Figure 3-11 The variation of the mean selenate concentrations with time after incubation in the cultures containing <i>Mc. capsulatus</i> (Bath) and <i>Ms trichosporium</i> OB3b.	75
Figure 3-12 Time course of selenite reduction and elemental selenium production by <i>Mc. capsulatus</i> and <i>Ms. trichosporium</i> OB3b.	78
Figure 3-13 Time course of DL-selenocystine change and total selenium content in the bacterial biomass.	80
Figure 3-14 HAADF-STEM imaging of <i>Mc. capsulatus</i> (Bath) cultures exposed to DL-selenocystine and selenite.	81
Figure 3-15 HAADF-STEM imaging of <i>Ms. trichosporium</i> OB3b cultures exposed to DL-selenocystine and selenite.	82
Figure 3-16 K-edge X-ray absorption spectra of cultures of <i>Mc. capsulatus</i> and <i>Ms. trichosporium</i> and selected references.	84
Figure 3-17 Results of experiments showing selenite reduction after an initial addition of 100 mg L^{-1} of the oxyanion incubated in the reaction mixture without methane in the presence of different cell factions.	86

Figure 3-18 Results of experiments showing loss of selenite reduction after an initial addition of 100 mg L ⁻¹ of the oxyanion incubated in the reaction mixture without methane in the presence of boiled cell wall and cell membrane factions.....	87
Figure 4-1 TEM of <i>Mc. capsulatus</i> and <i>Ms. trichosporium</i> OB3b cultures exposed to SeO ₃ ²⁻ , and EDX analysis within the electron dense regions.....	93
Figure 4-2 HAADF-STEM imaging of <i>Mc. capsulatus</i> and <i>Ms. trichosporium</i> OB3b showing Se nanospheres attached to the cells.....	94
Figure 4-3 Time course of Se nanospheres growth and SeO ₃ ²⁻ reduction by <i>Mc. capsulatus</i> and <i>Ms. trichosporium</i> OB3b.	97
Figure 4-4 The frequency distribution histogram of the selenium nanoparticles produced from the TEM images after the formation in the cultures containing the methanotrophs <i>Mc. capsulatus</i> and <i>Ms trichosporium</i> OB3b.....	97
Figure 4-5 TEM micrographs of the cells and selenium nanoparticles at different incubation times..	98
Figure 4-6 Extraction of purified SeNPs by a two-phase water-octanol extraction system..	99
Figure 4-7 SDS-PAGE gel images of SeNPs of proteins associated with biogenic selenium nanoparticles produced by <i>Mc. capsulatus</i> and <i>Ms. trichosporium</i> OB3b.. .	100
Figure 4-8 Wide scan X-ray photoelectron spectra of the SeNPs produced by <i>Mc. capsulatus</i> , and high resolution spectra for Se 3d, C 1s,O 1s and N 1s.....	102
Figure 4-9 Wide scan x-ray photoelectron spectra of the SeNPs produced by <i>Ms. trichosporium</i> OB3b and high resolution spectra for Se 3d, C 1s,O 1s and N 1s.....	104
Figure 4-10 The FTIR spectra of freeze dried Bio-SeNPs and bacterial biomass of <i>Mc. capsulatus</i> and <i>Ms. trichosporium</i> OB3b..	107

Figure 4-11 The Raman spectra of purified Se nanospheres from <i>Mc. capsulatus</i> and <i>Ms. trichosporium</i> OB3b..	112
Figure 4-12 Structure of selenium-sulfur nanoparticles produced by <i>Azospirillum brasilense</i> ..	117
Figure 5-1 GC-MS chromatograms of the headspace gas of the <i>Mc. capsulatus</i> (Bath) cultures amended with and without selenite.....	122
Figure 5-2 GC-MS chromatograms of the headspace gas of the <i>Ms. trichosporium</i> OB3b cultures amended with and without selenite.....	123
Figure 5-3 GC-MS chromatograms of the headspace gas of the <i>Mc. capsulatus</i> (Bath) cultures amended with selenate (600 mg L ⁻¹).....	126
Figure 5-4 Mass chromatograms of the headspace gas of the <i>Mc. capsulatus</i> (Bath) cultures amended with DL-selenocystine at different time intervals..	128

List of tables

Table 1-1 Chemical Forms of Selenium in the Environment.	3
Table 1-2 Cultured SeO_4^{2-} - and SeO_3^{2-} -reducing microorganisms and observed Se transformation reactions.	15
Table 1-3 Se-methylating organisms, showing the Se-containing substrate and methylated product.	23
Table 1-4 Classification of aerobic methanotrophic bacteria.....	35
Table 2-1 The operating conditions for ICP-MS and HPLC instruments	48
Table 3-1 Minimum inhibition concentrations of selenium for methanotrophs..	62
Table 3-2 Se-K edge EXAFS data of Se(IV)-reacted methanotrophs.	84
Table 4-1 Results of curve-fitting Se 3d spectra	105
Table 4-2 Results of curve-fitting C 1s spectra.....	105
Table 4-3 Results of curve-fitting O1s spectra	105
Table 4-4 Results of curve-fitting N 1s spectra	105
Table 4-5 Tentative assignments of main bands to the relevant functional groups....	108
Table 4-6 Time course of growth and Zeta potential of Se nanoparticles produced by <i>Mc. capsulatus</i> and <i>Ms. trichosporium</i> OB3b.	114
Table 5-1 Volatile selenium species produced by methanotrophs from different selenium-containing substrates.....	123

List of abbreviations

AdhP	Propanol-preferring alcohol dehydrogenase
BioSeNPs	Biogenic elemental selenium nanoparticles
bTPMT	Bacterial thiopurine methyltransferase
CheSeNPs	Chemically produced selenium nanoparticles
DIO	Iodothyronine deiodinases
DMDSe	Dimethyldiselenide
DMDSeS	Dimethyl diselenenyl sulfide
DMSe	Dimethylselenide
DMSeDS	Dimethyl selenyl disulfide
DMSeS	Dimethylselenenylsulfide
DMSO	Dimethyl sulfoxide
DMTSe	Dimethyl triselenide
DNA	Deoxyribonucleic acid
DNBP	Dinitrobutylphenol
EPS	Extracellular polymeric substances
EXAFS	Extended X-ray absorption fine structure
FNR	Fumarate nitrate reduction
GPx	Glutathione peroxidases
GR	Glutathione reductase
GSH	glutathion
HPLC	High performance liquid chromatography
ICP-MS	Inductively coupled plasma mass spectrometry
Idh	Isocitrate dehydrogenase (NADP)
KED	kinetic energy discrimination
LC	Liquid chromatography
MeSeH	Methane selenol/methylselenol
MIC	Minimum inhibitory concentrations
MMO	Methane monooxygenase
MSA	Methylseleninic acid
NADH	Nicotinamide Adenine Dinucleotide
NADPH	Nicotinamide Adenine Dinucleotide Phosphate

Nap	Periplasmic nitrate reductase
Nar	Membrane-bound nitrate reductase
NIST	The National Institute of Standards and Technology
NMS	Nitrate mineral salts
OYE	Old yellow enzyme
PAGE	Polyacrylamide gel electrophoresis
PEEK	Polyetheretherketone
PLFA	Phospholipid fatty acid
pMMO	Particulate methane monooxygenase
QD	Quantum dot
RuMP	Ribulose monophosphate
S	Sulfur
SDS	Sodium dodecyl sulphate
Se	Selenium
Se ⁰	Elemental selenium
SECIS	selenocysteine insertion sequence
Selenate	Se (VI)
Selenite	Se (IV)
Se-Met	Selenomethionine
SeNPs	Selenium nanoparticles
Ser	Selenate reductase
sMMO	Soluble methane monooxygenase
TrxR	Thioredoxin reductases
XANES	X-ray absorption near-edge structure
XAS	X-ray absorption spectroscopy

Chapter 1

Introduction and review of literature

1.1 Selenium

Selenium (Se) is a chemical element that was discovered in 1817 by the Swedish chemist Jöns Jakob Berzelius, when he was working on the oxidation of sulfur dioxide from selenium-bearing copper pyrites. The element was given the name selenium, derived from Selene (the Greek goddess of the moon) (Weeks 1932; Kieliszek & Błażej 2013). Selenium has an atomic number of 34 and atomic mass of 78.96, and belongs to Group VIA of the Periodic Table; it thus displays chemical behaviour similar to sulfur. The element has been classified as a metalloid, having properties of both a metal and nonmetal. It ranks 69th in elemental abundance in the Earth's crust, where it occurs in concentration of 0.05-0.09 mg kg⁻¹ (Janz 2011; Fordyce 2013).

Selenium exists in several natural oxidation states and in a variety of chemical forms (inorganic and organic) (Table 1-1). Inorganic Se species found in water and soils are mainly selenite [Se (IV), SeO₃²⁻] and selenate [Se (VI), SeO₄²⁻], which are both known to be highly soluble and the most mobile Se forms (Tolu *et al.* 2011). Both oxyanionic species are of major concern, because they are toxic and known to bioaccumulate (Presser & Ohlendorf 1987; Weres *et al.* 1989). Organic Se-containing compounds that can be found in air or in the aqueous environment include volatile methyl species such as dimethylselenide (DMSe, CH₃SeCH₃), dimethyldiselenide (DMDSe, CH₃SeSeCH₃), dimethylselenenylsulfide (DMSeS, CH₃SeSCH₃) and methane selenol (CH₃SeH, MeSeH) (Pyrzynska 1998).

The main sources of selenium in the environment are natural and anthropogenic. The natural sources include volcanic activity, weathering of rocks, sea spray, atmospheric flux, volatilization, and recycling from biota. The anthropogenic activities may include

industrial uses such as electric component, glass manufacture, pigments, rubber, metal alloys, and photocopier component, as well as burning of fossil fuels. The agricultural sources of selenium are mainly pesticides; manure; lime; phosphate fertilizers (National Research Council (US). Subcommittee on Mineral Toxicity in Animals 1980; Haygarth 1994).

In natural environments, selenium like many other elements is subject to microbial transformations. Microorganisms play a crucial role in Se bio-transformations by changing its chemical forms. Many of these transformations are important components of the biogeochemical cycle of the element. Microbial transformations of selenium, in particular; ones that may be applicable in bioremediating selenium-contaminated environments are discussed in section 2 of this chapter (1.2).

Table 1-1 Chemical Forms of Selenium in the Environment. Adapted from (Fordyce 2013).

Oxidative state	Chemical forms
Se ²⁻	Selenide (Se ²⁻ , HSe ⁻ , H ₂ Se _{aq})
Se ⁰	Elemental selenium (Se ⁰)
Se ⁴⁺	Selenite (SeO ₃ ²⁻ , HSeO ₃ ⁻ , H ₂ SeO _{3aq})
Se ⁶⁺	Selenate (SeO ₄ ²⁻ , HSeO ₄ ⁻ , H ₂ SeO _{4aq})
Organic Se	Methylated selenium species, selenomethionine, selenocysteine

1.1.1 Biochemical functions of selenium

Since its discovery, the metalloid was considered as only a toxic element and its essential role in biology was not established until the 1950s. In 1954 Pinsent observed that certain bacteria grew faster in selenium-amended media (Pinsent 1954). In 1957, selenium was first identified as an essential micronutrient element in mammals during pioneering work by Schwarz and Foltz into selenium-responsive diseases (Schwarz &

Foltz 1957). As a consequence of those findings, selenium has been recognized as an essential trace element for growth and metabolism in most living organisms. Minute quantities of Se are essential for normal biological functions in diverse life forms, mainly as selenocysteine, a genetically encoded amino acid incorporated into the active centres of selenoenzymes including glycine reductases, formate dehydrogenases, glutathione peroxidases (GPx), iodothyronine deiodinases (DIO) and thioredoxin reductases (TrxR), which play key roles in prokaryotic and eukaryotic cells (Stadtman 1991; Heider & Bock 1993; Patching & Gardiner 1999; Birringer *et al.* 2002; Johansson *et al.* 2005; Taylor *et al.* 2009; Shamberger 2012). However, excessive amounts of selenium can be toxic to animals and humans (Birringer *et al.* 2002; Lenz & Lens 2009; Qin *et al.* 2013). Indeed, there is a very narrow margin between the concentration at which the element exerts beneficial effects on an organism and the level at which the element exerts toxic effects (dietary deficiency $< 40 \mu\text{g day}^{-1}$ and toxic levels $> 400 \mu\text{g day}^{-1}$) (Figure 1-1). The recommended dietary allowance is 55-70 μg per day, based on a reference dose of $0.005 \text{ mg kg}^{-1} \text{ body weight day}^{-1}$ (Pyrzynska 1998; National Research Council 2005; Fordyce 2013).

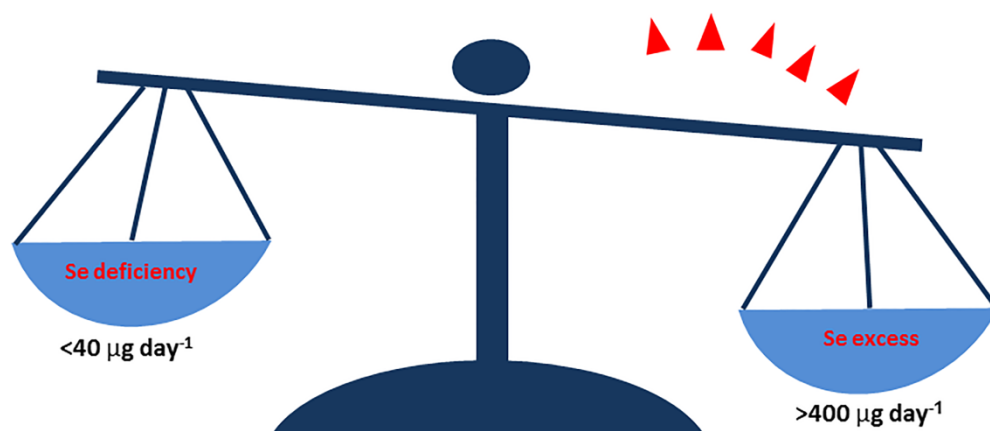


Figure 1-1 Effects of selenium deficiency and excess in animals and humans. Adapted from (Nancharaiah & Lens 2015a).

To date, selenium has been identified in at least 25 selenoproteins that commonly occur in the human organism as well as in 12 selenoproteins in yeast cells (Letavayová *et al.* 2008; Tastet *et al.* 2008; Lenz & Lens 2009; Fairweather-Tait *et al.* 2010). Historically, glutathione peroxidase was the first enzyme identified as containing selenium (Flohe *et al.* 1973; Rotruck *et al.* 1973). The biochemical function of GPxs is to catalyze the reduction of hydrogen peroxide and organic hydroperoxides, thus protecting the cell against oxidative damage (Papp *et al.* 2007; Lenz & Lens 2009). The selenoamino acid selenomethionine (Se-Met) has radioprotective properties and protects against UV-light-induced cell damage (Schrauzer 2000). A simplified overview of selenium metabolism in mammals is shown in Figure 1-2.

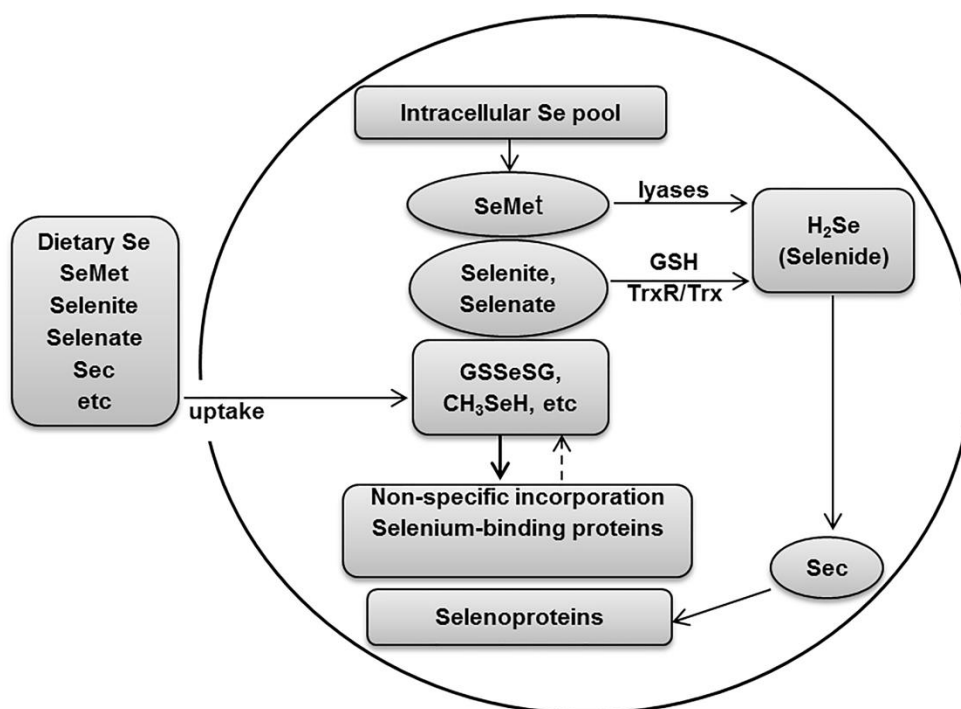


Figure 1-2 Selenium metabolism in mammalian organisms.

Dietary selenium metabolites are taken up into the cell, where, together with the existing intracellular pool, they become metabolized by different pathways, ultimately to yield selenide, which serves as the selenium source for Sec biosynthesis. (Se, selenium; GSSeSG, selenodiglutathione; CH₃SeH methylselenol; H₂Se selenide; SeMet, selenomethionine; Sec, selenocysteine; GSH, glutathione; TrxR, thioredoxin reductase; Trx, thioredoxin). Adapted from (Papp *et al.* 2007).

1.1.1.1 Selenium deficiency

Although the biological significance of selenium was initially recognized with its toxicity to livestock, selenium deficiency is a more widespread practical problem. It has been reported that selenium deficiency is associated with several metabolic diseases in animals such as liver necrosis in rats, exudative diathesis in chicks, white muscle disease in ruminants, and reproduction failure in various species (National Research Council 1983). In humans, selenium deficiency is regarded as a major health problem for 0.5 to 1 billion people all over the world (Haug *et al.* 2007). Although the pathological condition resulting from selenium deficiency alone has not been fully understood, the element has been implicated in a number of diseases. In this context, selenium deficiency has been linked to a heart disorder termed “Keshan disease” (Chen *et al.* 1980) and bone and joint condition (Kashin-Beck disease) (Ge & Yang 1993) in humans in some areas of China. In a study by Clark and co-workers (1996) supplementation of free-living people with selenized brewer’s yeast was capable of decreasing the overall cancer morbidity and mortality by approximately 50%.

1.1.1.2 Selenium toxicity

Selenium toxicity had been recorded in the 13th century in livestock, by the Italian merchant traveller Marco Polo during his journey from Venice to China in 1295. He reported that his horses suffered from hoof disease after eating poisonous plants which are now known as selenium accumulators (Birringer *et al.* 2002). Selenium poisoning in livestock causes two main syndromes, “alkali disease” and “blind staggers”. The syndromes occur when an animal consumes selenium accumulating plants. “Alkali disease” often presents with emaciation, loss of hair, deformation and

shedding of hooves. The symptoms of “blind staggers” include impaired vision, depressed appetite, and the tendency to wander in circles (Moxon 1937; Oldfield 2002).

Selenium toxicity in humans is far less widespread than selenium deficiency. The toxicity is characterized as short-term (acute) or long term symptoms (chronic or selenosis). Acute poisoning typically involves a single dose that produces symptoms within minutes to hours, causing stomach upsets including vomiting, nausea, diarrhea, and intestinal cramps. Whereas chronic poisoning involves smaller doses given repeatedly, producing symptoms that become apparent over days or longer, resulting in hair loss, brittle nails, deformed nails, and discoloration of teeth and skin (Nuttall 2006). The precise mechanism of selenium toxicity remains unclear, but it has been speculated that it is linked to the generation of free radical species, which induce DNA damage, and its reactivity with thiols, affecting the integrity and/or function of DNA repair proteins (Letavayová *et al.* 2006). Selenium toxicity in humans depends on its chemical forms, concentration and on a number of compounding factors. For example, ingestion of any significant quantity of selenious acid (H_2SeO_3) is usually fatal to humans, preceded by stupor, severe hypertension, and respiratory depression (Matoba *et al.* 1986; Quadrani *et al.* 2000; Hunsaker *et al.* 2005). Whereas the toxicity of methylated selenium compounds depends not only on the dose administered but also on the previous level of selenium intake (Fordyce 2013).

1.2 Microbial transformations of selenium species for bioremediation

1.2.1 Background

Since the discovery in 1954 by Pinsent that the oxidation of formate by cell suspensions of *Escherichia coli* requires growth medium containing molybdate and selenite, there has been a growing interest in the biochemical role of selenium in microorganisms (Pinsent 1954). Se is an essential component of selenoamino acids, such as selenomethionine and selenocysteine (the 21st proteinogenic amino acid) that occur in certain types of prokaryotic enzymes. Indeed, the requirement for selenite in *E.coli* growing on formate is linked to the fact that dehydrogenase contains selenocysteine. Other prokaryotic enzymes containing selenocysteine include glycine reductase in several clostridia, formate dehydrogenases in diverse prokaryotes including *Salmonella*, *Clostridium*, and *Methanococcus*, as well as hydrogenases in *Methanococcus* and other anaerobes. In addition, other bacterial Se-dependent enzymes, in which the selenium is part of the active site molybdenum-containing cofactor, include nicotinic acid dehydrogenase and xanthine dehydrogenase, which is present in certain clostridial species (Stadtman 1991; Heider & Bock 1993; Johansson *et al.* 2005).

Reactions that are involved in the cycling of Se in soil, including those influenced by microbes, are diagrammatically summarized in Figure 1-3. Of the four transformation reactions, dissimilatory reduction and methylation are considered the most important in terms of bioremediation. For example, the microbial reduction of toxic Se oxyanions (SeO_4^{2-} and SeO_3^{2-}) to the insoluble and less biologically available elemental selenium (Se^0) results in its removal from solution. Microbial transformation of non-volatile Se

forms to volatile compounds is a significant pathway of Se transfer from aquatic and terrestrial environments to the atmosphere. Moreover, the reduction and methylation of SeO_4^{2-} and SeO_3^{2-} are an effective detoxification processes because the product (dimethylselenide or dimethyldiselenide) is 500 to 700 times less toxic than SeO_4^{2-} or SeO_3^{2-} (Franke & Moxon 1936; Wilber 1980; Dungan & Frankenberger 1999; Ranjard *et al.* 2003).

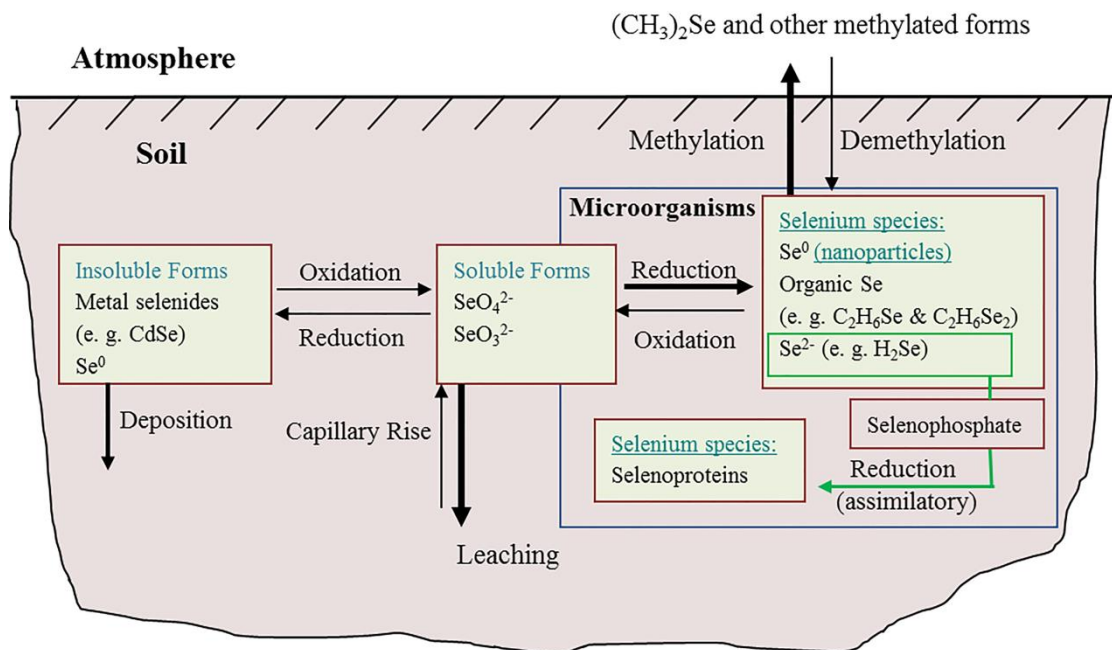


Figure 1-3 Schematic Se cycle in soil, and the influence of microbial processes on the transformation of the element. The bold arrows indicate the preferred direction of the process (Eswayah *et al.* 2016).

Zehr and Oremland (1987) tested the assumption that microorganisms involved in the S cycle can also reduce Se oxyanions since Se is adjacent to S in group 6 of the periodic table and both commonly occur in the +6, +4 and -2 oxidation states. Washed cell suspensions of *Desulfovibrio desulfuricans* (a sulfate-reducing bacterium) were found to be capable of reducing small (nanomolar) amounts of SeO_4^{2-} to Se^{2-} at the same time as reducing SO_4^{2-} to S^{2-} . The reduction was dependent on the relative

concentrations of SeO_4^{2-} and SO_4^{2-} . Increasing concentrations of SO_4^{2-} inhibited rates of SeO_4^{2-} reduction but enhanced SO_4^{2-} reduction rates (Zehr & Oremland 1987). Subsequently, however, Oremland *et al.* (1989) reported a novel bacterial dissimilatory reduction of SeO_4^{2-} which occurs by pathways different from those for SO_4^{2-} , and was spatially separated from sulfate reduction in the environment despite the presence of substantial concentrations of sulfate where it occurred. Thus, it can be concluded that Se and S have different reductive biogeochemical cycles and appear to involve distinct populations of microorganisms (Oremland *et al.* 1989).

With respect to the remediation of seleniferous environments, microbial oxidation and demethylation of Se compounds are not often considered because of the low rates at which these reactions proceed. Microbial demethylation of Se compounds occurs when some microorganisms utilize methylated Se forms as their sole source of carbon and energy (Doran & Alexander 1977; Dungan & Frankenberger 1999). The aim of this review is to discuss the reactions involved in the microbial transformation of different forms of selenium and to consider these in an environmental context, with reference to the bioremediation of the element in polluted environments.

1.2.2 Microbial reduction of selenium species

During microbial assimilation of Se oxyanions, selenate (SeO_4^{2-}) and selenite (SeO_3^{2-}) are transported into the cells by different permeases. In the cell, both oxyanions are reduced through assimilatory reduction to selenide (Se^{2-}) (Karle & Shrift 1986). In bacteria, selenophosphate is then produced by selenophosphate synthase (Figure 1-4). Selenocysteine is subsequently synthesised via enzyme-catalysed reaction of serine with selenophosphate, whilst the serine is attached to the tRNA^{Sec} specific for insertion

of selenocysteine into ribosomally synthesized proteins (Forchhammer & Bock 1991). Also, in the presence of excess available Se, cells begin to incorporate Se instead of S into cellular components that normally contain S (Dungan & Frankenberger 1999).

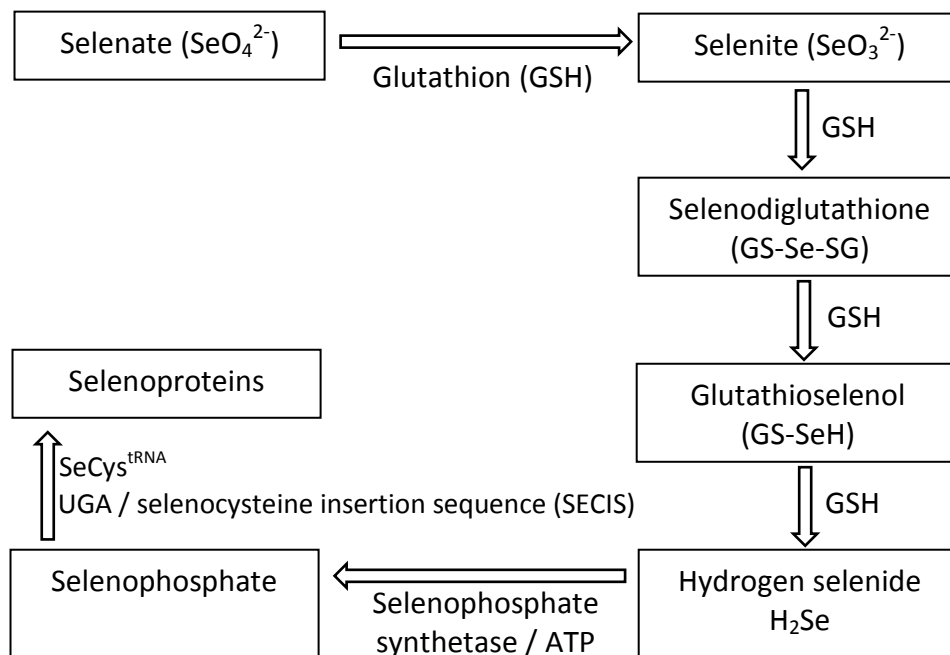


Figure 1-4 The biosynthesis of selenocysteine and decoding of the UGA codon via a quaternary complex. Adapted from (Taylor *et al* 2009).

In soil, sediment and water, microbial reduction of SeO_3^{2-} and SeO_4^{2-} is known to be an important process for removing toxic soluble Se oxyanions (Staicu & Barton 2017). In dissimilatory Se reactions, the reduction of Se oxyanions is a mechanism by which certain microorganisms can obtain metabolic energy (Nancharaiah & Lens 2015b). Dissimilatory Se-reducing microorganisms are known to use a number of different electron donors such as alcohols, sugars, organic acids, humic substances, and

hydrogen (Lovley *et al.* 1999; Kashiwa *et al.* 2000; Astratinei *et al.* 2006; Chung *et al.* 2006; Zhang *et al.* 2008). In terms of bioremediation of seleniferous environments, assimilatory reduction of Se is expected to make only a minor contribution because of the small selenium fluxes involved. In contrast, the dissimilatory reduction of Se is considered to be the more important process for bioremediation. Assimilatory reduction is the process whereby selenite and selenate are reduced and incorporated into organic compounds, whereas dissimilatory reduction generally refers to reduction of compounds as terminal electron acceptors in energy metabolism.

The reduction of selenium oxyanions, including reduction that is apparently not linked to respiration or assimilation, is a highly active reaction among many bacterial isolates and may play an important role in the environment (Wilber 1980; Staicu *et al.* 2017). Research into dissimilatory reduction of Se is receiving increasing attention, not least because results from these investigations offer a potentially cost-effective means of remediating selenium pollution. In contrast to insoluble Se^0 , SeO_4^{2-} and SeO_3^{2-} are environmentally problematic in aqueous phases because of their high solubility. However, they become immobilized when the selenate and selenite are microbially reduced to Se^0 (Schröder *et al.* 1997). Microbial reduction of Se^0 to selenide (Se^{2-}) has received limited attention, but it is noteworthy that partially soluble Se^0 can be reduced microbiologically to soluble selenide (Herbel *et al.* 2003; Pearce *et al.* 2009).

Certain bacteria are able to grow anaerobically through the dissimilatory reduction of selenium oxyanions. The product from dissimilatory reduction of selenite is generally Se^0 , which appears in the form of Se nanoparticles. Microbial reduction occurs either in the periplasmic space (intracellularly) (Debieux *et al.* 2011; Sonkusre *et al.* 2014; Li *et al.* 2014b) or extracellularly (Oremland *et al.* 2004; Zhang *et al.* 2012; Jiang *et al.* 2012).

The reduction of Se oxyanions to Se^0 nanoparticles can also be mediated aerobically by diverse species of bacteria, namely, selenium-resistant bacteria (Prakash *et al.* 2009; Wang *et al.* 2010; Dhanjal & Cameotra 2010; Bajaj *et al.* 2012).

Several investigations have dealt with the mechanisms of microbial formation of Se nanoparticles (Zhang *et al.* 2001; Dobias *et al.* 2011; Jain *et al.* 2015b; Wadhvani *et al.* 2016; Jain *et al.* 2017; Song *et al.* 2017). The Se nanoparticles are known to have microbial proteins associated with them, which play a role in the formation and growth of the Se nanoparticles (Wang *et al.* 2010) as well as in controlling their size distribution (Dobias *et al.* 2011). Jain *et al.* (2015b) used biogenic elemental selenium nanoparticles (BioSeNPs), which were produced by anaerobic granular sludge in the treatment of pulp and paper wastewater, in an investigation of a presence of extracellular polymeric substances (EPS) on the BioSeNPs. Functional group characteristic of proteins and carbohydrates were detected on the BioSeNPs, suggesting that EPS form a coating that determines the surface charge on these BioSeNPs. It is probable that EPS contribute to the colloidal properties of the BioSeNPs, and thereby influence their fate in the environment and consequently the efficiency of bioremediation technologies (Jain *et al.* 2015b). Microbial reduction of Se may not only be exploited in Se bioremediation but also in the production of selenium nanoparticles for biotechnological applications (Dobias *et al.* 2011; Jain *et al.* 2014). However, the mechanisms involved in the formation of the nanoparticles, and more importantly, in their physical and chemical properties are yet to be fully elucidated.

Microorganisms that reduce the Se oxyanions SeO_3^{2-} and SeO_4^{2-} are not confined to any particular group of prokaryotes and are widely distributed throughout the bacterial and archaeal domains (McCready *et al.* 1966; Oremland *et al.* 1994; Macy

1994; Tomei *et al.* 1995; Yanke *et al.* 1995; Fujita *et al.* 1997; Losi & Frankenberger 1997; Ike *et al.* 2000; Siddique *et al.* 2006; Hunter 2007; Han & Gu 2010; Kuroda *et al.* 2011; Slobodkina *et al.* 2015). However, compared to the SeO_3^{2-} -reducing microorganisms that have been isolated, the number of known SeO_4^{2-} reducers is relatively small.

The reduction of SeO_4^{2-} to Se^0 is generally a two-step process in which SeO_3^{2-} is an intermediate product. Some bacteria are capable of reducing both SeO_4^{2-} and SeO_3^{2-} to Se^0 (Doran 1982; Lortie *et al.* 1992; Turner *et al.* 1998), while other bacterial species can only reduce SeO_3^{2-} to Se^0 (Bebien *et al.* 2001; Roux *et al.* 2001). In some instances, dissimilatory reduction of SeO_4^{2-} supports growth via anaerobic respiration. In other cases, reduction of selenium oxyanions may serve a detoxifying function or be an adventitious reaction of enzymes with a different function. The reductions of SeO_4^{2-} and SeO_3^{2-} are considered in detail below. Major cultured selenium-reducing prokaryotes and their properties are summarised in Table 1-2.

Table 1-2 Cultured SeO_4^{2-} - and SeO_3^{2-} -reducing microorganisms and observed Se transformation reactions.

Microorganism(s)	Se transformation	Reference
Bacteria – dissimilatory Se reduction supporting anaerobic respiration		
<i>Thauera selenatis</i>	Respiration via reduction of SeO_4^{2-} to SeO_3^{2-} in the absence of NO_3^- , minor reduction of SeO_3^{2-} to Se^0 . In the presence of NO_3^- , SeO_4^{2-} completely reduced to Se^0	(Macy 1994)
<i>Chrysiogenetes</i> S5 <i>Deferribacteres</i> S7 <i>Deltaproteobacteria</i> KM	Respiration via reduction of SeO_4^{2-} to Se^0	(Narasingarao & Haggblom 2007)
<i>Sulfurospirillum barnesii</i> SES-3 <i>Bacillus arsenicoselenatis</i> E-1H	Respiration via reduction of SeO_4^{2-} and SeO_3^{2-} to Se^0 Respiration via reduction of SeO_4^{2-} to SeO_3^{2-} .	(Oremland <i>et al.</i> 1994) (Switzer Blum <i>et al.</i> 1998)
<i>Bacillus selenitireducens</i> MLS10	Respiration via reduction of SeO_3^{2-} to Se^0	(Switzer Blum <i>et al.</i> 1998)
<i>Selenihalanaerobacter shriftii</i> DSSe-1	Respiration via reduction of SeO_4^{2-} to Se^0	(Switzer Blum <i>et al.</i> 2001)
Archaea – dissimilatory Se reduction supporting anaerobic respiration		
<i>Pyrobaculum arsenaticum</i> ; <i>Pyrobaculum aerophilum</i>	Anaerobic chemolithotrophs that also grow organotrophically with SeO_4^{2-} as electron acceptor. Hyperthermophiles.	(Huber <i>et al.</i> 2000)
<i>Pyrobaculum ferrireducens</i>	Anaerobic organotrophic growth on SeO_4^{2-} and SeO_3^{2-} . Produces Se^0 . Hyperthermophile.	(Slobodkina <i>et al.</i> 2015)
Bacteria – dissimilatory Se reduction not clearly supporting respiration		
<i>Rhodospirillum rubrum</i>	Extracellular reduction of SeO_3^{2-} to Se^0 ; reduction under anoxic conditions greater than under oxic conditions.	(Kessi <i>et al.</i> 1999)
<i>Rhodobacter sphaeroides</i>	Reduction of SeO_3^{2-} to Se^0 with intracellular accumulation under aerobic and anaerobic conditions	(Bebien <i>et al.</i> 2001)
<i>Shewanella oneidensis</i> MR-1	Extracellular reduction of SeO_3^{2-} to Se^0 under aerobic or anaerobic conditions	(Klonowska <i>et al.</i> 2005)
<i>Clostridium pasteurianum</i> <i>Enterobacter cloacae</i> SLD1a-1	Enzymatic reduction of SeO_3^{2-} using hydrogenase I Reduction of SeO_4^{2-} to Se^0 through SeO_3^{2-} as intermediate in the presence of NO_3^-	(Yanke <i>et al.</i> 1995) (Losi & Frankenberger 1997)
<i>Azospira oryzae</i>	Reduction of SeO_4^{2-} and SeO_3^{2-} to Se^0 under anaerobic and microaerobic conditions, using O_2 or NO_3^- as terminal electron acceptors for growth.	(Hunter 2007)
<i>Desulfovibrio desulfuricans</i>	Reduction of SeO_4^{2-} and SeO_3^{2-} to Se^0 , with formate as electron donor and fumarate or sulfate as electron acceptor	(Tomei <i>et al.</i> 1995)
<i>Enterobacter cloacae</i> SLD1a-1	Reduction of SeO_4^{2-} to Se^0 through SeO_3^{2-} as intermediate in the presence of NO_3^- .	(Losi & Frankenberger 1997)
<i>Pseudomonas stutzeri</i> NT-1	Aerobic reduction of SeO_4^{2-} and SeO_3^{2-} to Se^0	(Kuroda <i>et al.</i> 2011)
<i>Rhodopseudomonas palustris</i> N	Aerobic reduction of SeO_4^{2-} and SeO_3^{2-} to Se^0	(Li <i>et al.</i> 2014a)
<i>Wolinella succinogenes</i>	Aerobic reduction of SeO_4^{2-} and SeO_3^{2-} to Se^0	(Tomei <i>et al.</i> 1992)
<i>Salmonella heidelberg</i>	Reduction of SeO_3^{2-} to intracellular granules Se^0	(McCready <i>et al.</i> 1966)
<i>Ralstonia metallidurans</i> CH34	Aerobic reduction of SeO_3^{2-} to Se^0	(Roux <i>et al.</i> 2001)
<i>Salmonella heidelberg</i>	Aerobic reduction of SeO_3^{2-} to Se^0	(McCready <i>et al.</i> 1966)
<i>Azospirillum brasilense</i>	Reduction of SeO_3^{2-} to Se^0 nanoparticles	(Tugarova <i>et al.</i> 2014)
<i>Pseudomonas sp.</i> CA-5	Reduction of SeO_3^{2-} to Se^0 under aerobic conditions	(Hunter & Manter 2009)
<i>Bacillus cereus</i> CM100B	Reduction of SeO_3^{2-} to Se^0 under aerobic conditions	(Dhanjal & Cameotra 2010)
<i>Bacillus megaterium</i> BSB6, BSB12.	Aerobic reduction of SeO_3^{2-} to Se^0 at high salt concentrations	(Mishra <i>et al.</i> 2011)
<i>Duganella sp.</i> C1 and C4	Reduction of SeO_3^{2-} to Se^0 nanoparticles	(Bajaj <i>et al.</i> 2012)
<i>Agrobacterium sp.</i> C 6 and C 7		
<i>Pseudomonas sp.</i> strain RB	Reduction of SeO_3^{2-} in the presence of cadmium producing CdSe nanoparticles	(Ayano <i>et al.</i> 2014)
<i>Burkholderia fungorum</i> DBT1 <i>Burkholderia fungorum</i> 95	Reduction of SeO_3^{2-} to Se^0 nanoparticles under aerobic conditions	(Khoei <i>et al.</i> 2017)
Archaea – dissimilatory Se reduction not clearly supporting respiration		
<i>Halorubrum xinjiangense</i>	Aerobic reduction of SeO_3^{2-} to Se^0 . Halophile.	(Güven <i>et al.</i> 2013)
Bacteria – a well-studied example of assimilatory Se reduction		
<i>Escherichia coli</i>	Reduction of SeO_4^{2-} and SeO_3^{2-} to Se^0 , incorporation of Se into proteins	(Turner <i>et al.</i> 1998)

1.2.2.1 Reduction of selenate

The mechanism of selenate reduction varies among the cultured microorganisms studied to date. Several selenate-respiring bacterial species (i.e. bacteria that can use selenate as the terminal electron acceptor to support growth) including *Thauera selenatis*, *Sulfurospirillum barnesii*, and *Bacillus arseniciselenatis* have been well-characterized and shown to respire anaerobically by using SeO_4^{2-} as the terminal electron acceptor (Macy *et al.* 1993; Switzer Blum *et al.* 1998; Stolz *et al.* 1999). Membrane-bound nitrate reductase (Nar), periplasmic nitrate reductase (Nap) and selenate reductase (Ser) have all been shown able to catalyse reduction of SeO_4^{2-} to SeO_3^{2-} .

Current evidence from *Enterobacter cloacae* (Watts *et al.* 2003) and other organisms indicates that selenate reductases have evolved specifically for the reduction of selenate and are more important in cultures of specific strains and, by implication, environmentally than adventitious capacity of nitrate reductases to reduce selenate. Selenate reductase (Ser) has been purified and characterized from *T. selenatis* (Schröder *et al.* 1997). It is a heterotrimer that is located in the periplasm, forming a complex of approximately 180 kDa containing the subunits SerA (96 kDa), SerB (40 kDa) and SerC (23 kDa). It contains molybdenum, iron and acid-labile sulfur as prosthetic groups (Schröder *et al.* 1997). Ser has been demonstrated to be specific for SeO_4^{2-} reduction to SeO_3^{2-} and does not use nitrate, nitrite, chlorate, or sulfate as electron acceptors. In contrast, the selenate reductase complex in *S. barnesii* is found in the membrane. It is a heterotetramer with subunits of 82, 53, 34 and 21 kDa and also contains molybdenum at the active site (Stolz *et al.* 1997; Stolz & Oremland 1999; Barton 2005).

In the facultative anaerobe *Enterobacter cloacae* SLD1a-1, which can reduce selenate under aerobic conditions, the selenate reductase is located in the membrane fraction. It discriminates between SeO_4^{2-} and NO_3^- and is expressed under aerobic and anaerobic conditions. It is located in the cytoplasmic membrane, with its active site facing the periplasmic compartment (Watts *et al.* 2003). The enzyme is a heterotrimeric ($\alpha\beta\gamma$) complex with an apparent molecular mass of approximately 600 kDa. The individual subunit masses are 100 kDa (α), 55 kDa (β), and 36 kDa (γ). It contains molybdenum, heme, and nonheme iron in its prosthetic groups and displays activity on chlorate and bromate but none on nitrate (Ridley *et al.* 2006; Han & Gu 2010). It is noteworthy that the reductase of *E. cloacae* SLD1a-1 is similar to periplasmic Ser from *T. selenatis*. Both have active sites located in the periplasm, both are molybdo-enzymes with catalytic α subunits of similar sizes (SerA is ~96 kDa), and both possess *b*-type cytochromes. Yee *et al.* (2007) investigated the mechanisms of SeO_4^{2-} reduction by the Se-reducing bacterium *E. cloacae* SLD1a-1 in order to identify gene(s) required for SeO_4^{2-} reduction. They demonstrated that the selenate reductase of the bacterium is controlled at the genetic level by the global anaerobic fumarate nitrate reduction (FNR) regulator and is induced under suboxic conditions.

1.2.2.2 Reduction of selenite

Microorganisms can carry out the conversion of SeO_3^{2-} to Se^0 via a number of different mechanisms (Kessi *et al.* 1999; Kessi & Hanselmann 2004; Kessi 2006). SeO_3^{2-} reduction can be catalysed by reductases, including the periplasmic nitrite reductase, sulfite reductase, and dimethyl sulfoxide (DMSO) reductase (Harrison *et al.* 1984; DeMoll-Decker & Macy 1993; Afkar *et al.* 2003). A number of thiol mediated reactions have

also been observed to reduce selenite to elemental selenium (Nancharaiah & Lens 2015b).

In *T. selenatis*, which is able to grow anaerobically with SeO_4^{2-} as the electron acceptor, little of the SeO_3^{2-} produced is reduced to Se^0 when SeO_4^{2-} is supplied as the sole electron acceptor. In contrast, SeO_3^{2-} formed during SeO_4^{2-} respiration is completely reduced to Se^0 by the same bacterium when NO_3^- and SeO_4^{2-} are available as electron acceptors. Mutants of *T. selenatis* that lack periplasmic NO_3^- reductase activity are unable to reduce either SeO_3^{2-} or NO_3^- , while mutants with increased nitrate reductase activity show rapid reduction of NO_3^- and SeO_3^{2-} . Together, these observations suggest that the nitrate reductase is required for the reduction of SeO_3^{2-} to Se^0 by *T. selenatis* (DeMoll-Decker & Macy 1993).

Pseudomonas selenitipraecipitans strain CA-5 is capable of reducing both SeO_3^{2-} and SeO_4^{2-} to Se^0 . The strain is resistant to selenite at high concentrations (>150 mM). Two activities capable of reducing selenate were detected by zymography, one of which may correspond to nitrate reductase (Hunter & Manter 2009). Analyses of fractions from this strain indicate the presence of two reductases that can reduce SeO_3^{2-} to Se^0 in the presence of NADPH and that (based upon proteomics analysis of mixed protein samples) may correspond to glutathione reductase and thioredoxin reductase, both of which are able to reduce SeO_3^{2-} to Se^0 when derived from other sources (Hunter 2014a). Similar zymography and proteomic analysis of fractions from *Rhizobium selenitireducens* suggest that a protein belonging to the old yellow enzyme (OYE) family of flavoproteins is capable of reducing SeO_3^{2-} to Se^0 using NADH as the electron donor (Hunter 2014b).

In a study by Li *et al.* (2014), *Shewanella oneidensis* MR-1, an organism that shows substantial metabolic versatility and is known for its ability to perform biological electrons transfer to solid minerals, is also able to reduce SeO_3^{2-} to Se^0 . Specific mutants of *S. oneidensis* MR-1 have been used to investigate the contribution of the anaerobic respiration system to microbial reduction of SeO_3^{2-} . Deletions of the genes that encode nitrate reductase (*napA*), nitrite reductase (*nrfA*), and two other periplasmic mediators of electron transfer for anaerobic respiration (*mtrA* and *dmsE*) were not impaired in their ability to reduce SeO_3^{2-} , which indicated that neither nitrate reductase nor nitrite reductase was essential for selenite reduction. In contrast, in the fumarate reductase (*fccA*) mutant of *S. oneidensis* MR-1, selenite reduction was decreased by 60% compared to that of the wild-type strain. This suggests that FccA contributes substantially to selenite reduction in the organism (Li *et al.* 2014b).

Deletion of *cymA*, which encodes a membrane-anchored c-type cytochrome that transfers electrons from the quinol pool in the cell membrane to various reductases (including fumarate reductase) that are involved in anaerobic respiration, resulted in a strain that exhibited only 9.6% of the selenite-reducing rate of the wild-type strain. Whilst this indicates that a respiratory electron transport chain is involved in supplying electrons for reduction of selenite, it is unclear whether this could support growth in *S. oneidensis* MR-1. In these experiments, the culture actually lost biomass when it reduced selenite anaerobically, using lactate as electron donor. Thus, the culture may have employed fumarate reductase to reduce the selenite and used it as a means of detoxifying selenite in the periplasm to prevent it from entering the cytoplasm, where it could be toxic (Li *et al.* 2014b; Nancharaiah & Lens 2015b).

Reduction of selenite to elemental selenium has also been observed in living systems via a reaction that appears to be partly abiotic. Here, the selenite reacts chemically with biological thiol compounds, such as glutathione, via Painter-type reactions to produce molecules containing an S-Se-S bridge moiety known as a selenotrisulfide. It may break down spontaneously with the generation of reactive oxygen species, but it may also be reduced enzymatically by thioredoxin reductase or glutathione reductase, whose natural principal function is to regenerate the thiols in glutathione and thioredoxin by oxidation of S-S bridges. When the substrate is a selenotrisulfide, the selenium is liberated as Se^0 (Zannoni *et al.* 2007). This may, of course, be the reaction via which glutathione and thioredoxin reductases are involved in reduction of selenite to elemental selenium in *Pseudomonas selenitipraecipitans* (Hunter 2014a) detailed above. Other reports of reduction of SeO_3^{2-} to Se^0 by bacterial cultures include a detoxification mechanism in *Salmonella* (McCready *et al.* 1966). The reduction of selenite to elemental selenium is clearly of pivotal importance to bioremediation of selenium species, so further work is needed to provide information about the role and mechanisms of selenite reductases.

1.2.2.3 Reduction of selenium species to selenide

Dissimilatory reduction of selenium species to selenide (Se^{2-}) has been observed in a limited extent in environmental microorganisms. The obligate acidophile, *Thiobacillus ferroxidans* can convert Se^0 to hydrogen selenide (H_2Se) under anaerobic conditions (Bacon & Ingledew 1989). The selenite-respiring bacterium *Bacillus selenitireducens* produces significant amounts of selenide when supplemented with Se^0 . The strain is also able to reduce SeO_3^{2-} through Se^0 to Se^{2-} (Herbel *et al.* 2003; Pearce *et al.* 2009).

1.2.3 Oxidation of selenium compounds

The oxidation of reduced selenium species may be relevant with respect to availability of selenium as a trace nutrient for crop plants. It is not, however, considered of major relevance to environmental toxicity of selenium species because of the low rates of transformation involved. Various studies indicate that microorganisms are capable of aerobic oxidation of Se^0 and SeO_3^{2-} in soil (Lipman & Waksman 1923; Torma & Habashi 1972; Sarathchandra & Watkinson 1981). A photosynthetic purple sulfur bacterium has been reported to use the oxidation of Se^0 to selenic acid (H_2SeO_4) as a sole source of energy (Doran 1982), and *Acidithiobacillus ferrooxidans* has been shown to use copper selenide oxidation as a source of energy (Torma & Habashi 1972). Oxidation of Se^0 by an aerobic heterotrophic bacterium, a strain of *Bacillus megaterium*, that was isolated from soil via an enrichment procedure using elemental selenium has also been found to be capable of oxidizing Se^0 to SeO_3^{2-} and a trace of SeO_4^{2-} (< 1 % of SeO_3^{2-}) (Sarathchandra & Watkinson 1981). The genes and enzymes and the pathways involved in the biological oxidation of selenium species have not yet been reported.

Studies with bulk soil have indicated that oxidation of Se^0 in soils is largely biotic in nature, occurs at relatively slow rates, and produces SeO_3^{2-} and SeO_4^{2-} (Losi & Frankenberger 1998). In a study of the oxidation of Se^0 in oxic soil slurries, SeO_3^{2-} was the predominant product, with small amounts of SeO_4^{2-} also produced. The oxidation rate constants were found to be between 0.0009 and 0.0117 day^{-1} in unamended soil slurries (at 25°C). Oxidation of Se^0 may have been carried out by heterotrophic bacteria, sulfur-oxidising bacteria, and possibly fungi (Dowdle & Oremland 1998). These rates indicate that the removal of Se^0 from soil via biological oxidation would take hundreds of days. In contrast, field studies have shown that the SeO_4^{2-} pool of

contaminated anoxic sediments can have turnover times of less than 1 hour due to reductive processes that are much more rapid (Oremland *et al.* 1991). Oxidation, as well as reduction, of the selenium species also occurs during the methylation of the selenium species, which is considered in the next section.

1.2.4 Methylation of selenium species

Environmental microorganisms can use the Se methylation process as mechanism to remove SeO_3^{2-} and SeO_4^{2-} by converting them to volatile compounds, such as dimethyl selenide (DMSe) and dimethyl diselenide (DMDS_e). They may also be important in the natural cycling of Se to the atmosphere and play a role as a detoxification mechanism (McConnell & Portman 1952). Although the biological significance of Se methylation is not clearly understood, once volatile Se compounds are released to the atmosphere and diluted, Se has lost its hazardous potential.

A number of studies have shown microbial production of DMSe and DMDS_e in various environmental samples, including soil, sewage sludge, and water, from selenium sources, including SeO_4^{2-} , SeO_3^{2-} , selenocysteine, and selenomethionine (Francis *et al.* 1974). A substantial number of cultured microorganisms, both bacteria and fungi, are now recognised as being able to produce methylated forms of selenium. Methylated forms of selenium produced by microorganisms also include dimethyl selenone $[(\text{CH}_3)_2\text{SeO}_2]$, also known as methyl methylselenite] (Reamer & Zoller 1980), dimethyl triselenide (DMTSe, $\text{CH}_3\text{SeSeSeCH}_3$), and mixed selenium/sulfur-methylated species, dimethyl selenyl sulfide (DMSeS, $\text{CH}_3\text{SeSCH}_3$), dimethyl selenyl disulfide (DMSeDS, $\text{CH}_3\text{SeSSCH}_3$), and dimethyl diselenenyl sulfide (DMDS_eS, $\text{CH}_3\text{SeSeSCH}_3$) (Burra *et al.* 2010). Known cultured microorganisms that are capable of producing methylated

selenium species are summarised in Table 1-3. The predominant groups of Se-methylating organisms that can be found in soils and sediments are bacteria and fungi, while bacteria are the active Se-methylating organisms in the aquatic environments (Doran 1982; Dungan & Frankenberger 1999).

Table 1-3 Se-methylating organisms, showing the Se-containing substrate and methylated product.

Organisms	Substrate	Product	Reference
Bacteria			
<i>Corynebacterium sp.</i>	SeO ₄ ²⁻ , SeO ₃ ²⁻ , Se ⁰	DMSe	(Doran & Alexander 1977)
<i>Aeromonas sp.</i>	SeO ₄ ²⁻	DMSe, DMDSe	(Chau <i>et al.</i> 1976)
<i>Rhodocyclus tenuis</i>	SeO ₄ ²⁻ , SeO ₃ ²⁻	DMSe, DMDSe	(McCarthy <i>et al.</i> 1993)
<i>Aeromonas veronii</i>	SeO ₄ ²⁻ , SeO ₃ ²⁻ , Se ⁰ , SeS ₂ , H ₂ SeO ₃ , NaSeH	DMSe, DMDSe, methyl selenol, DMSeS	(Rael & Frankenberger 1996)
<i>Bacillus sp.</i>	SeO ₃ ²⁻ , SeO ₄ ²⁻ , selenocyanate	DMSe, DMSeS, DMDSe, DMSeDS, DMDSeS, DMTSe	(Burra <i>et al.</i> 2010)
<i>Rhodospirillum rubrum S1</i>	SeO ₃ ²⁻ , Se ⁰	DMSe, DMDSe	(Van Fleet-Stalder & Chasteen 1998)
<i>Desulfovibrio gigas</i>	SeO ₃ ²⁻	DMSe, DMDSe	(Michalke <i>et al.</i> 2000)
<i>Methanobacterium formicicum</i>	SeO ₃ ²⁻	DMSe, DMDSe	(Michalke <i>et al.</i> 2000)
<i>Pseudomonas fluorescens K27</i>	SeO ₄ ²⁻	DMSe, DMDSe, DMSeS	(Chasteen & Bentley 2003)
<i>Citrobacter freundii KS8</i>	SeO ₄ ²⁻	DMSe, DMDSe, DMSeS	(Chasteen & Bentley 2003)
<i>Pseudomonas strain Hsa.28</i>	SeO ₄ ²⁻ , SeO ₃ ²⁻	DMSe, DMDSe	(Chasteen & Bentley 2003)
<i>Stenotrophomonas maltophilia</i>	SeO ₄ ²⁻ and SeO ₃ ²⁻	DMSe, DMDSe, DMSeS	(Dungan <i>et al.</i> 2003)
<i>Pseudomonas stutzeri NT-1</i>	SeO ₄ ²⁻ , SeO ₃ ²⁻ , Bio-Se ⁰	DMSe, DMDS	(Kagami <i>et al.</i> 2013)
Fungi			
<i>Scopulariopsis brevicaulis</i>	SeO ₄ ²⁻ , SeO ₃ ²⁻	DMSe	(Challenger & North 1934)
<i>Penicillium notatum and p. chrysogenum</i>	SeO ₄ ²⁻ , SeO ₃ ²⁻	DMSe	(Bird & Challenger 1939)
<i>Penicillium sp.</i>	SeO ₄ ²⁻	DMSe	(Fleming & Alexander 1972)
<i>Cephalosporium sp.</i>	SeO ₄ ²⁻ , SeO ₃ ²⁻	DMSe	(Barkes & Fleming 1974)
<i>Fusarium sp.</i>	SeO ₄ ²⁻ , SeO ₃ ²⁻	DMSe	(Barkes & Fleming 1974)
<i>Candida humicola</i>	SeO ₄ ²⁻ , SeO ₃ ²⁻	DMSe	(Cox & Alexander 1974)
<i>Alternaria alternata</i>	SeO ₄ ²⁻ , SeO ₃ ²⁻	DMSe	(Thompson-Eagle <i>et al.</i> 1989)
<i>Penicillium citrinum</i>	SeO ₃ ²⁻	DMSe, DMDSe	(Chasteen <i>et al.</i> 1990)
<i>Acremonium falciforme</i>	SeO ₃ ²⁻	DMSe, DMDSe	(Chasteen <i>et al.</i> 1990)

1.2.4.1 Selenium methylation pathways

If the initial form of selenium is one of the selenium oxyanions or elemental selenium, Se-methylation must involve both reduction and methylation reactions. To date, a number of pathways have been suggested for biomethylation of selenium, with

evidence from proposed intermediates. Methyltransferases capable of methylating selenium species have been identified. The original pathway proposed by Challenger (1945) suggested that methylation of SeO_3^{2-} by fungi involved the methylation and reduction of the Se atom in four steps to form DMSe as the final product (Figure 1-5).

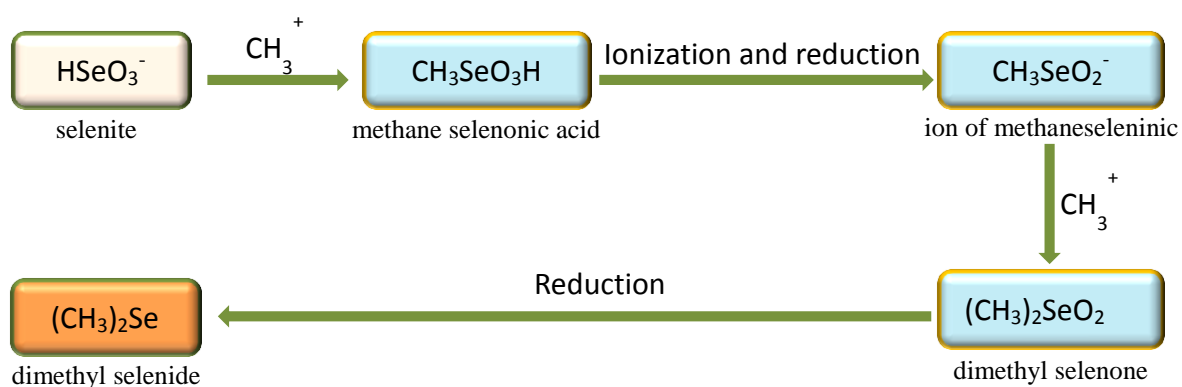


Figure 1-5 Challenger's pathway for the microbial transformations of selenium (Challenger 1945).

Reamer and Zoller (1980) subsequently reported that inorganic selenium compounds (SeO_3^{2-} or Se^0) are converted into DMDS_e, DMS_e, and dimethyl selenone [or possibly DMS_eS (Chasteen 1993)] by microorganisms in soil and sewage sludge. Challenger's proposed scheme was modified to introduce a branch that yielded DMDS_e (Figure 1-6). In this pathway, the methaneseleninic ion intermediate can form either methaneselenol or methaneselenenic acid, which would then be reduced to DMDS_e. It was found that at low concentrations of SeO_3^{2-} (1 - 10 mg L⁻¹ Se), DMS_e was the predominant product, while DMDS_e or dimethyl selenone was produced at high concentrations of SeO_3^{2-} (10 - 1000 mg L⁻¹). In contrast, when Se^0 was added to sewage

sludge, DMSe was the only product. There was a direct dependence of the production of DMSe on the concentration of added SeO_3^{2-} as at high concentrations of Se, DMSe production was inhibited. During the 30-day period of the experiment, the maximum proportion of selenium across the tested concentration range that was volatilised was 7.9 % (Reamer & Zoller 1980).

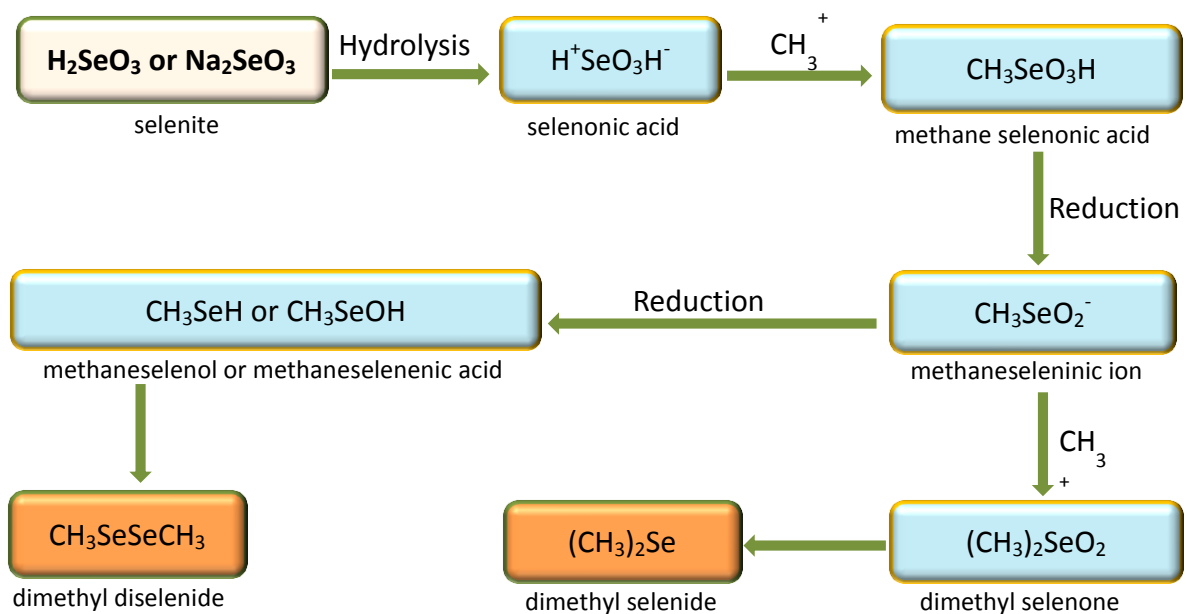


Figure 1-6 Reamer and Zoller's pathway for the microbial transformations of selenium (Reamer & Zoller 1980).

Zhang and Chasteen (1994) observed that the amounts of DMSe and DMDSe released from cultures of the Se-resistant bacterium *Pseudomonas fluorescens* K27 amended with dimethyl selenone were more than those formed from SeO_4^{2-} . This finding suggested that dimethyl selenone may be an intermediate in the reduction and methylation of selenium oxyanions, which is consistent with the proposed pathway for production of DMSe (Figure 1-5).

In the scheme proposed by Doran (1982), the methylation of inorganic Se by soil *Corynebacterium* involved the reduction of SeO_3^{2-} to Se^0 and then a reduction to the selenide. The selenide was then methylated to form DMSe (Figure 1-7). Although hydrogen selenide and methane selenol were not identified as intermediates, the roles of selenide and methane selenol as intermediates have been suggested in other investigations (Bird & Challenger 1942; Bremer & Natori 1960; Hsieh & Ganther 1975).

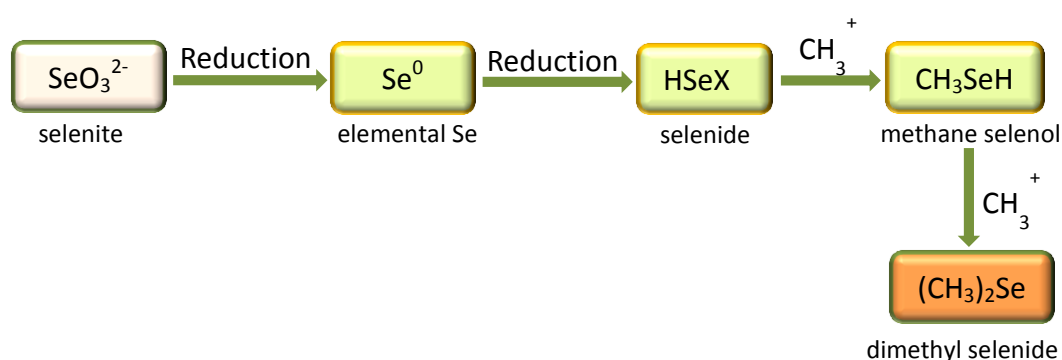


Figure 1-7 Doran's pathway for the microbial transformations of selenium (Doran 1982).

The bacterial thiopurine methyltransferase (bTPMT) from *Pseudomonas syringae*, which catalyses methyl transfer reactions using S-adenosyl methionine (SAM) as the methyl donor, confers upon *Escherichia coli* the ability to transform selenite into DMSe and selenomethionine or (methyl)selenocysteine into DMSe and DMDS (Ranjard *et al.* 2002). Production of methylated selenium species was also observed with an *E. coli* that was transformed with a methyltransferase gene (*amtA*) from a freshwater isolate of *Hydrogenophaga* sp. that produced DMSe and DMDS (Ranjard *et al.* 2004).

While rates for biological production of methylated selenium species are generally low, applications of selenium-methylating microorganisms in bioremediation and

biotechnology have been suggested, such as for recovery of selenium from seleniferous water via biovolatilization. A fermenter culture of *Pseudomonas stutzeri* NT-I under aerobic conditions was able to produce methylated selenium species at rate of $14 \text{ mol L}^{-1} \text{ h}^{-1}$. The selenium could be recovered from the gas phase via a simple gas trap containing nitric acid (Kagami *et al.* 2013), and preserving the selenium in the (-II) oxidation state in each of these compounds: DMSe and DMDS₂ as dimethylselenoxide [(CH₃)₂SeO or DMSeO] and methylseleninic acid (MSA) [CH₃Se(O)OH or Methylseleninic acid], respectively.

1.2.5 Demethylation of selenium compounds

Doran and Alexander (1977) isolated from seleniferous clay a pseudomonad able to grow on DMSe as well as strains of *Xanthomonas* and *Corynebacterium* that were able to grow on DMDS₂ as sole carbon and energy sources. The pathways for breakdown of methylated selenium compounds, which presumably involve demethylation in such organisms, are currently unknown. In anoxic sediments, DMSe undergoes rapid demethylation. It has been suggested that DMSe could be anaerobically transformed to methane (CH₄), carbon dioxide (CO₂), and hydrogen selenide (H₂Se) by sediment organisms (methanogens and sulfate-reducing bacteria) in a pathway similar to dimethyl sulfide (DMS) degradation in freshwater and estuarine sediments (Oremland & Zehr 1986).

1.2.6 Selenium bioremediation

As its industrial and agricultural usage increases, increasing amounts of selenium (particularly in the forms of SeO₃²⁻ and SeO₄²⁻) will be discharged into the environment, posing a threat to the aquatic and terrestrial environments. Indeed, of the 2,700

tonnes of selenium that is produced annually only about 15% is recycled (Haug *et al.* 2007). Therefore, there is a need to develop efficient, eco-friendly and cost-effective methods for remediation of Se pollution and also, where possible, for recovery of this valuable element. As more stringent regulations come into force in order to limit the discharge of Se containing waste, the use of bioremediation technologies are preferable because they will offer more cost effective approaches for the removal of the pollutant. There has been a growing interest in the use of microorganisms in remediating Se-contaminated environments (Higashi *et al.* 2005; Soda *et al.* 2012; Williams *et al.* 2013; Santos *et al.* 2015; Jain *et al.* 2016; Barlow *et al.* 2017; Ike *et al.* 2017). In this context, a number of studies have been carried out in order to exploit the use of Se-oxyanion-reducing microorganisms in small/large-scale remediation schemes. These studies have demonstrated that many microorganisms may be used in remediation approaches designed for the treatment of Se-contaminated soil, sediments, and wastewater. Selenium is to a large extent immobilized and can be recovered in solid form after biological reduction of selenium oxyanions to Se^0 . Alternatively, if limitations due to slow reaction rates can be overcome, the biological conversion of Se^0 to volatile methylated forms potentially permits remediation and subsequent removal and collection in a controlled manner.

A range of carbon and energy sources have been tested as electron donors for the microbial reduction of selenium species. These included inexpensive algal biomass, which has been explored as an electron donor and carbon source for bacterial reduction of SeO_4^{2-} to Se^0 as well as reduction of NO_3^- to N_2 in agricultural drainage (Gerhardt *et al.* 1991). In another study, the SeO_4^{2-} -respiring bacterium *Thauera selenatis* was used to treat Se-oxyanion-containing oil refinery wastewater in a

laboratory-scale bioreactor. A reduction of 95% of the soluble element was achieved from an initial concentration of 3.7 mg L^{-1} (Lawson & Macy 1995). The SeO_4^{2-} -reducing bacterium, *Bacillus* sp. SF-1, has been tested in an anoxic continuous flow bioreactor under steady-state conditions for removing SeO_4^{2-} from a model wastewater containing $41.8 \text{ mg L}^{-1} \text{ SeO}_4^{2-}$, with lactate as the electron donor. The system effectively removed SeO_4^{2-} at short cell retention times (2.9 h), but there was accumulation of SeO_3^{2-} under these conditions. As the retention time was increased, more of the selenium was reduced to Se^0 . Conversion of Se^0 was $\geq 99\%$ at a cell retention time of 92.5 h and an Se^0 production rate of $0.45 \text{ mg L}^{-1} \text{ h}^{-1}$ (Fujita *et al.* 2002).

T. selenatis has been employed on a pilot-scale for the remediation of Se-containing drainage water from the San Joaquin Valley, CA. The inflow to the reactor had a Se oxyanion (SeO_3^{2-} plus SeO_4^{2-}) concentration of 0.237 mg L^{-1} . The reactor effected 97.9% conversion to recoverable insoluble Se^0 and left the treated water containing only $5 \mu\text{g L}^{-1}$ of selenium. This high removal of Se^0 was achieved via polymer coagulation with Nalmet 8072, which helped to overcome the general technical challenge of recovering Se^0 due to small particle size (Cantafio *et al.* 1996). The Se-reducing bacterium *Pseudomonas stutzeri* NT-I has also been effectively employed for the bioremediation of a Se-containing refinery wastewater in 256-litre pilot-scale bioreactors via reduction to elemental selenium (Soda *et al.* 2012).

In a high-throughput sequencing study to investigate the effect of an electron acceptor on community structure during respiration of an activated-sludge derived microbial population using hydrogen as the electron donor, principal component analysis revealed a substantial shift in the composition of the microbial population upon first

addition of nitrate as an alternative to selenate as the electron acceptor (Lai *et al.* 2014). This gives additional evidence for the presence of environmental communities of microorganisms that utilize selenite as an electron acceptor and that these are, to a significant extent, distinct from nitrate-reducing microorganisms.

Since some algae can volatilize substantial quantities of inorganic Se compounds (Oyamada *et al.* 1991; Fan *et al.* 1997; Neumann *et al.* 2003), algal methylation of selenium compounds offers a possible way to remove selenium from the aqueous phase. The inclusion of an algal pretreatment unit into a constructed wetland system was investigated in order to remove Se from river water entering the Salton Sea in California. The alga *Chlorella vulgaris* (Cv) removed 96% of Se supplied as selenium oxyanions (1.58 mg L^{-1}) from the microcosm water column within 72 hours. With this arrangement, up to 61% of the selenium was removed by volatilization to the atmosphere, suggesting that an algal pre-treatment stage could be included into constructed wetland systems for selenium bioremediation (Huang *et al.* 2013).

In addition to the problems that it causes as an environmental pollutant, selenium is an essential micronutrient and a valuable metalloid for which there are a dearth of high-yielding geological sources. Hence, the most advantageous systems for remediation of selenium pollution would put the recovered selenium to good nutritional or technological uses. Elemental selenium is used in industry, the growth of some crops, prevention and treatment of certain diseases including cancer, as well as antifungal activities. In this connection, it must be noted that a great diversity of prokaryotes are able to reduce selenium oxyanions to elemental selenium in the form of nanoparticles, which have properties difficult to mimic by chemical technologies. The microbially produced nanoparticles could be used in a variety of technological

applications (Oremland *et al.* 2004; Nancharaiah & Lens 2015b). In effective selenium bioremediation, the selenium may have several acceptable fates. The likely fates of selenate in the presence of a variety of organisms have been demonstrated in an engineered aquatic ecosystem designed for brine shrimp production. In this investigation, selenate was taken up and metabolized differently by microalgae, bacteria, and diatoms to selenite, selenide or elemental Se. Some of the biotransformed selenium species were incorporated and bioaccumulated as organic selenium compounds as they were transferred between the different trophic levels. Organic selenium-enriched invertebrates suitable for human and animal consumption were produced as a result of these metabolic biotransformations (Schmidt *et al.* 2013).

Microbial methylation of inorganic Se oxyanions to volatile species offers a possible approach to bioremediation of selenium compounds in Se-polluted soils and aquatic environments. This has the attraction that the selenium may be completely removed in the vapour phase, although the limitation of low reaction rates would have to be overcome. In principle, organisms that demethylate selenium species may be used to recover vapour-phase selenium, provided reaction rate limitations and possible production of toxic and volatile H₂Se can be overcome. Genetic characterization of the pathways of selenium methylation and demethylation may enable their modification by overexpressing the necessary enzymes, resulting in acceleration of these processes.

Selenium species may be transformed in a diversity of metabolic reactions. Interest in the microorganisms capable of transforming selenium compounds involved in environmental pollution and in making selenium nutritionally available will increase as

the activities of these organisms become better understood. Further characterizations of the mechanisms of selenite reduction to elemental selenium and of selenium methylation and demethylation are needed. Culture-independent analysis will be useful in studying the diversity and distribution of selenium-transforming organisms in a range of environments using a combination of functional gene analysis and metagenomics. Sequencing with 16S rRNA gene analysis should be fruitful in unraveling the role of microorganisms in the global selenium cycle. Their ability to produce selenium nanoparticles will be industrially exploited. Their ability to transform different selenium species by reduction, methylation, and demethylation will be harnessed further in the remediation of selenium-containing wastewater.

As discussed above the microbial transformation of selenium has been demonstrated in a wide range of bacteria under aerobic and anaerobic conditions (Switzer Blum *et al.* 1998; Switzer Blum *et al.* 2001; Bebien *et al.* 2001; Klonowska *et al.* 2005). However, the potential contribution of aerobic methane-oxidizing bacteria, which are widespread in the environment, has not been assessed until recently. The ecology, taxonomy, physiology and biochemistry of methane-oxidizing bacteria, as well as their potential in remediation of environments contaminated with toxic chemicals are discussed in section 1.3.

1.3 Methane-oxidizing bacteria

Methane-oxidizing bacteria (methanotrophs) are a diverse and ubiquitous group of Gram-negative bacteria within the environment that are able to grow using methane as their sole source of carbon and energy (Hanson & Hanson 1996; Smith & Murrell 2009). This group of bacteria exist in a variety of habitats including soils, peatlands, rice paddies, sediments, freshwater and marine systems, acidic hot springs, mud pots, alkaline soda lakes, cold environments, and tissues of higher organisms (Pester *et al.* 2004; Abell *et al.* 2009; Moussard *et al.* 2009; Smith & Murrell 2009; Antony *et al.* 2010; Semrau *et al.* 2010), as well as in a wide range of pH, temperature, oxygen concentrations, salinity, heavy metal concentrations, and radiation (Pandey *et al.* 2014). Methanotrophs are of great interest for their role in the global carbon cycle as the largest biological sink for atmospheric methane (Singh *et al.* 2010; Finn *et al.* 2015; Tiwari *et al.* 2015).

Although methanotrophs were first described in 1906 by Söhngen (Rasigraf *et al.* 2014), their classification was not until 1970, when Whittenbury *et al.* (1970) isolated and characterized over 100 new strains of methane-oxidizing bacteria. Whittenbury *et al.* (1970) established the fundamental construction of current classification of these organisms. Methanotrophs are currently classified into two broad taxonomic groups, namely type I and type II methanotrophs, based on cell morphology, phenotypic traits including carbon assimilation pathways, 16S rRNA gene phylogeny, phospholipid fatty acid (PLFA) profiles and intracellular membrane system architecture (Hanson & Hanson 1996; Smith & Murrell 2009; Bissett *et al.* 2012). Type I methanotrophs belong to the *Gammaproteobacteria* and are further divided into the type Ia and type Ib (or type X) methanotrophs. The type Ia comprises the genera *Methylomicrobium*, *Methylomonas*,

Methylobacter, *Methylosarcina*, *Methylosphaera*, *Methylosoma*, *Crenothrix*, and *Clonothrix*, while the type Ib includes *Methylococcus*, *Methylocaldum*, *Methylohalobius*, *Methylothermus*. The type II belongs to the *Alphaproteobacteria* and comprises the genera *Methylosinus*, *Methylocystis*, *Methylocapsa* and *Methylocella* (Table 1-4).

Table 1-4 Classification of aerobic methanotrophic bacteria. Adapted from (Smith & Murrell 2009; Bissett *et al.* 2012).

Type	Phylum	Genus	MMO type	C1 assimilation	Tropic niche	
Type I	γ -Proteobacteria type Ia	<i>Methylobacter</i>	pMMO	RuMP	some psychrophilic	
		<i>Methylomonas</i>	pMMO+/-sMMO	RuMP	some psychrophilic	
		<i>Methylosoma</i>	pMMO	not known	not extreme	
		<i>Methylomicobium</i>	pMMO+/-sMMO	RuMP	halotolerant; alkaliphilic	
		<i>Methylosarcina</i>	pMMO	RuMP	not extreme	
		<i>Methylosphaera</i>	pMMO	RuMP	psychrophilic	
		<i>Crenothrix</i>	pMMO		not extreme	
		<i>Clonothrix</i>	pMMO		not extreme	
	γ -Proteobacteria type Ib (X)	<i>Methylococcus</i>	pMMO + sMMO	RuMP/Serine	thermophilic	
		<i>Methylocaldum</i>	pMMO	RuMP/Serine	thermophilic	
		<i>Methylohalobius</i>	pMMO	RuMP	halophilic	
		<i>Methylothermus</i>	pMMO	RuMP	thermophilic	
	Type II	α -Proteobacteria	<i>Methylosinus</i>	pMMO + sMMO	Serine	not extreme
			<i>Methylocystis</i>	pMMO+/-sMMO	Serine	some acidophilic
<i>Methylocapsa</i>			pMMO	Serine	acidophilic	
<i>Methylocella</i>			sMMO	Serine	acidophilic	

Methanotrophs contain the enzyme methane monooxygenase (MMO), which occurs in two forms, namely, copper-dependent membrane-associated or particulate form (pMMO), and iron-containing soluble or cytoplasmic form (sMMO). It is noteworthy that sMMO and pMMO are different their protein components and active-site metals, but more importantly substrate specificity. pMMO is found in all known methanotrophs, except *Methylocella* spp (Theisen *et al.* 2005), while sMMO is only found in a few methanotrophs (Murrell *et al.* 2000). In methanotrophs such as *Methylosinus trichosporium* and *Methylococcus capsulatus* that are able to produce both the copper-containing pMMO and iron-containing sMMO, the switch between expression of pMMO and sMMO is effected by available copper in the culture, with sMMO being expressed at low copper-to-biomass ratio and pMMO at high copper-to-biomass ratio (Stanley *et al.* 1983).

The copper demand for proteobacterial methanotrophs expressing pMMO is high, approximately 10-fold higher than the copper requirement observed in other microorganisms (Semrau *et al.* 2013). Thus, in order to meet their high copper requirement, γ - and α -*Proteobacteria* methanotrophs synthesize and secrete a small modified peptide, high-affinity copper-binding compound called methanobactin. The compound functions as a chalkophore (siderophore-like molecule, the function of which is to bind copper rather than iron) by binding Cu^{2+} or Cu^+ , then shuttling the copper into the cell (Kim *et al.* 2004; Krentz *et al.* 2010; El Ghazouani *et al.* 2012; Kalidass 2016). Methanobactin uses a unique sulfur and nitrogen coordination system to bind copper (Kim *et al.* 2004). It has been demonstrated that methanobactin can increase the bioavailability of copper for methanotrophs (Knapp *et al.* 2007; Semrau *et al.* 2013). Methanobactin is known to play a significant role in the copper-switch that

controls expression of the two forms of MMO. Indeed, the first form of methanobactin characterized was from *Methylosinus trichosporium* OB3b (Figure 1-8), and it was found to be a small modified polypeptide of 1,154 Da (DiSpirito *et al.* 1998; Tellez *et al.* 1998; Kim *et al.* 2004).

More recently, methanobactins from five other methanotrophs have been structurally characterized, including *Methylocystis* strain SB2, *Methylocystis hirsuta* CSC1, *Methylocystis* strain M, *Methylocystis rosea* SV97T, and *Methylosinus* sp. LW4 (Behling *et al.* 2008; Krentz *et al.* 2010; Bandow *et al.* 2012; El Ghazouani *et al.* 2012; Kenney *et al.* 2016). These methanobactins are all small with molecular mass of 851.20, 910.20, 825.13, 914.13 and 1334.23 Da, respectively. The molecular structures of these methanobactins were characterized via nuclear magnetic resonance and X-ray crystallography. Although copper is the most physiologically relevant metal ion that binds to methanobactin, methanobactin from *Methylosinus trichosporium* OB3b also binds other metal ions including Au^{3+} , Ag^+ , Cd^{2+} , Mn^{2+} , Fe^{3+} , Co^{2+} , Zn^{2+} , Hg^{2+} , Ni^{2+} and U^{4+} (Bandow 2014; DiSpirito *et al.* 2016; Dassama *et al.* 2017).

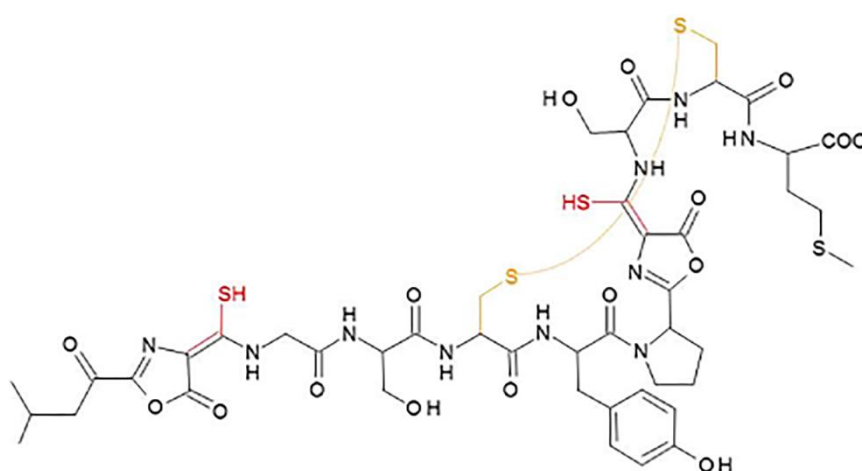
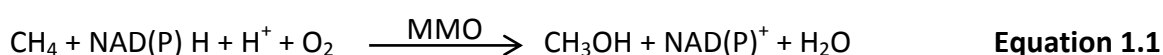


Figure 1-8 Primary structure of methanobactin from *Ms. trichosporium* OB3b. Reprinted with permission from (Semrau *et al.* 2013).

Methanotrophs use the enzyme methane monooxygenase (MMO) to catalyse the oxidation of methane to methanol. They assimilate the formaldehyde produced from the oxidation of methane via the ribulose monophosphate (RuMP) or the serine pathway. The formaldehyde is an important branch point in methylotrophic metabolism. The conversion of methane to methanol by the methanotrophic MMOs is an essential step of methane oxidation, in which an oxygen molecule is incorporated across C-H bond to produce methanol (Dalton 1980; Wallar & Lipscomb 1996; Merckx *et al.* 2001) as in Equation 1.1,



MMO catalyzes a classic monooxygenase reaction in which two reducing equivalents from NAD(P)H are utilized to split the O-O bond of O₂. One atom of oxygen is reduced to water while the second is incorporated into the substrate to yield methanol.

1.3.1 Remediation of toxic chemicals by methanotrophs

The MMOs from methanotrophs have been shown to not only oxidize methane to methanol but also a wide range of other organic substrates, including aromatic compounds, halogenated benzenes, toluene and styrene as well as aliphatic hydrocarbons (Lontoh & Semrau 1998; Kikuchi *et al.* 2002; Jiang *et al.* 2010). Consequently, methanotrophs are well known for their potential in remediating these organic pollutants and, more recently, their capacity for remediating inorganic pollutants has also been recognised. Certain methanotrophs have been found able to reduce chromium (VI) to the less toxic and less bioavailable chromium (III) (Al Hasin *et al.* 2009; Lai *et al.* 2016a) and to reduce mercuric ions to metallic mercury (Boden &

Murrell 2011). During the course of his investigations, Lai *et al* (2016) have reported a mixed culture capable of the bio-reduction of selenate to elemental selenium using methane as the electron donor in a membrane biofilm reactor containing a microbial community including aerobic methanotrophs (Lai *et al.* 2016b).

The research related to bioremediation potential of methanotrophs is still in its infancy. However, with the combination of biotechnology and genetic engineering, methanotrophs can be exploited for in situ bioremediation of a wide range of inorganic and organic pollutants.

1.4 Aims of the work reported in this study

Although a considerable number of studies have been conducted on the microbial transformations of selenium in the environments, no attention has been paid to the role of methane-oxidizing bacteria in transforming selenium species. The present investigation is the first study of the selenium-transforming properties of methane-oxidizing bacteria which are ubiquitous in the environment. If methane-oxidizing bacteria are exposed to the toxic selenium oxyanions, then the bacteria will transform the oxyanions into less toxic selenium species, because this group of bacteria has been shown to degrade/co-oxidize diverse type of heavy metals and organic pollutants. MMOs and methanobactin may play a role in the transformation of selenium oxyanions.

The interaction of selenium containing chemical species has been studied with well characterised representatives of two major groups of methane-oxidizing bacteria, the type I methanotroph *Methylococcus capsulatus* (Bath) and the type II methanotroph *Methylosinus trichosporium* OB3b.

The overall aim of this study was to investigate the microbial transformation of selenium using methane-oxidizing bacteria for developing and implementing successful bioremediation of selenium. As a first step to developing a bioremediation strategy for selenium in the field, it was essential to investigate the mechanisms by which these microorganisms convert selenium into different chemical forms under laboratory conditions.

The main objectives are as follow:

- To investigate the efficiency of soluble selenium species, namely selenite and selenate reduction by methanotrophs.
- To characterise the elemental selenium nanoparticles produced after reduction.
- To detect and identify volatile selenium species that may be produced during the biotransformation reactions.
- To investigate the involvement of methane monooxygenases (MMOs) in the selenium transformations.
- To study the possible mechanism(s) of the reduction.
- To identify and purify the enzyme(s) responsible for selenium biotransformation.

Chapter 2

Materials and methods

2.1 Materials

All reagents used were of analytical grade. All solutions and media were prepared with high-purity deionized water (18.2 M cm, MilliQ, Millipore).

2.2 Methods

2.2.1 Bacterial strains and growth conditions

The methanotrophic bacteria *Mc. capsulatus* (Bath) (NCIBM 11132), *Ms. trichosporium* OB3b (NCIMB 11131) were chosen for investigation in order to establish whether the pure strains of methane- oxidizing bacteria can bio-transform selenium oxyanions. In addition, *Ms. trichosporium* SMDM (a derivative of *Ms. trichosporium* OB3b in which the genes encoding soluble methane monooxygenase [sMMO] have been inactivated via marker exchange mutagenesis) (Borodina, *et al.* 2007) was used to test the hypothesis that MMO may be involved directly in the transformation of the selenium oxyanions.

The strains were grown and propagated aerobically in sterile nitrate mineral salts (NMS) media (Smith & Murrell 2011) using methane (1:4 v/v in air) as the source of carbon and energy. The NMS media contained (per L of deionized water) KNO₃, 1000 mg; MgSO₄·7H₂O, 1000 mg; CaCl₂·2H₂O, 200 mg; NaMoO₄·2H₂O, 0.5 mg; Fe-EDTA, 3.8 mg; CuSO₄·5H₂O 0.1 mg; FeSO₄·7H₂O, 0.5 mg; ZnSO₄·7H₂O, 0.4 mg; H₃BO₃, 0.15 mg; CoCl₃·6H₂O, 0.05 mg; Na₂EDTA, 0.25 mg; MnCl₂·4H₂O, 0.02 mg; NiCl₂·6H₂O, 0.01 mg; Na₂HPO₄, 497 mg; KH₂PO₄, 390 mg. The experiments were performed in 50 mL liquid cultures in 250mL conical Quickfit® flasks capped with Suba-Seals (Sigma-Aldrich) to prevent methane loss while allowing the addition and removal of material using

hypodermic syringes. The *Ms. trichosporium* OB3b and *Mc. capsulatus* (Bath) cultures were incubated at the optimum growth temperature of 30 and 45°C, respectively, on a shaker at 180 rpm and allowed to grow to an OD₆₀₀ of between 0.5-0.8. Under the conditions used in these experiments, the *Mc. capsulatus* (Bath) strain grew substantially faster than the *Ms. trichosporium* OB3b stain, reaching an OD₆₀₀ of 0.7 typically at 24 - 30 hours, whereas cultures of *Ms. trichosporium* OB3b took 50 -72 hours.

2.2.2 Determination of the minimum inhibitory concentration (MIC) of selenite and selenate for methanotrophs

Minimum inhibitory concentrations (MICs) for selenite and selenate were determined. The MIC of selenite for *Mc. capsulatus* (Bath) and *Ms. trichosporium* OB3b in NMS medium was determined by inoculating the two strains with various initial concentrations of selenite salt (Na₂SeO₃): 0 (control), 5, 10, 20, 40, 60, 80 and 100 mg L⁻¹, and 0, 1, 2, 3, 4, 5, 6, 7 and 8 mg L⁻¹ for *Mc. capsulatus* (Bath) and *Ms. trichosporium* OB3b, respectively. While MIC for selenate was determined by inoculating the organisms with various initial concentrations of selenate salt (Na₂SeO₄): 0, 1000, 1500, 2000, 2200, 2300, 2400 and 2500 mg L⁻¹ and 0, 1000, 1200, 1500, 1600, 1700, 1800 and 2000 mg L⁻¹ for *Mc. capsulatus* (Bath) and *Ms. trichosporium* OB3b, respectively. Cultures were then incubated and after 48 and 72 hours for *Mc. capsulatus* (Bath) and *Ms. trichosporium* OB3b, respectively, cultures were assessed visually for turbidity. Cultures, in which growth does not occur, as measured visually by a lack of visible turbidity, represent the MIC for the agent (selenite or selenate). The choice of these concentrations was based on the effect of selenite toxicity on the two strains by carrying out preliminary experiments. The growth profile of the bacteria was

studied by addition of different concentrations of selenite and selenate in the growth medium under the conditions used in these experiments, taking into account the inoculum size and the volume of the media. The *Mc. capsulatus* strain grew in up to 60 and 1700 mg L⁻¹ selenite and selenate, respectively. In contrast, the *Ms. trichosporium* OB3b stain grew in up to 5 and 1600 mg L⁻¹ selenite and selenate, respectively and growth does not occur at higher concentrations.

2.2.3 Bacterial growth under selenite or selenate stress

The effect of selenate on the growth of the two strains was determined in the presence of 0 (control), 100, 400 and 800 mg L⁻¹; and 0, 100, 200 and 600 mg L⁻¹ selenate for *Mc. capsulatus* (Bath) and *Ms. trichosporium* OB3b, respectively. Bacterial growth was measured by recording the optical density at 600 nm (OD₆₀₀).

For selenite, the effect of the oxyanion on the growth of the two strains was determined in the presence of 0, 10 and 20 mg L⁻¹, and 0, 2 and 4 mg L⁻¹ sodium selenite for *Mc. capsulatus* (Bath) and *Ms. trichosporium* OB3b, respectively. Optical density was not used to follow growth of cultures in these experiments because the Se⁰ particles would contribute to the OD₆₀₀ measurements, which would therefore not be an accurate measure of growth. Therefore, the total protein content was measured at different time intervals, and used as a measure of the growth of the microorganisms. Protein concentration in bacterial cell extracts was determined using the bicinchoninic acid (BCA) assay method (Pierce™ BCA Protein Assay Kit, Thermo Scientific, 23227). A 1.5 mL aliquot of bacterial culture was collected at different time intervals of bacterial growth and was centrifuged at 11,000 × *g* for 10 min. The pellet was washed and

resuspended in 200 μ l of extraction buffer (140 mM NaCl; 2.7 mM KCL; 10 mM Na₂HPO₄; 1.8 mM KH₂PO₄; pH 7.3) containing protease inhibitor cocktail (1% v/v) (Sigma-Aldrich, Dorset, UK, P2714). The resulting suspension was sonicated in an ice bucket 4 x 10 sec (Sonics VCX-750 Vibra Cell Ultra Sonic Processor) and centrifuged at 12,000 $\times g$ for 15 min at 4°C. The supernatant was collected and measured for protein content. Flasks with inoculum without the addition of selenite served as control.

2.2.3.1 Changes in cell size of cell population under Se oxyanions stress (Flow Cytometry)

The size of the cell population under selenite or selenate stress was determined by Forward scatter using FACS Calibur™ (Becton-Dickinson) with the help of Dr Sarah Haywood-Small (Sheffield Hallam University). *Mc. capsulatus* (Bath) and *Ms. trichosporium* OB3b were grown in the presence of 50 and 100 mg L⁻¹ sodium selenate. Similarly, the two strains were grown in the presence of 5 and 10 mg L⁻¹, and 1 and 2 mg L⁻¹ sodium selenite for *Mc. capsulatus* (Bath) and *Ms. trichosporium* OB3b, respectively. An aliquot of 1 ml bacterial culture was collected at different time intervals of bacterial growth to determine the cell size. The samples were centrifuged at 1200 $\times g$ for 10 min. The cell pellet was gently washed twice with phosphate buffered saline (PBS) pH 7.2 and re-suspended in the same buffer for analysis. Cultures without addition of selenite or selenate oxyanions served as control.

2.2.4 Reduction of selenium oxyanions by methanotrophs

Under the conditions used in these experiments, the cultures were allowed to grow to an OD₆₀₀ of 0.5-0.8 before addition of either sodium selenite (Na₂SeO₃) or sodium selenate (Na₂SeO₄) (Sigma-Aldrich, Dorset, UK). Selenium stock solutions of 1000 and

10,000 mg L⁻¹ Se as selenite, and selenate were prepared and sterilized by filtration using 0.22 µm syringe filter (Millex®-GP). Addition of the oxyanions to give the desired selenium concentration was done towards the end of the logarithmic growth phase. The initial selenite concentrations used were 20 and 40 mg L⁻¹ for the *Mc. capsulatus* (Bath) and 10 and 20 mg L⁻¹ for the *Ms. trichosporium* OB3b strain, respectively. The initial selenate concentration was 10 mg L⁻¹ for either strain, respectively. Three controls were set up for each experiment, with bacterial inoculum, methane and the selenium species omitted, respectively. In addition to selenite and selenate, selenide in the form of DL-selenocystine (Sigma-Aldrich, Dorset, UK) was investigated.

2.2.5 Evaluation of selenium oxyanions reduction and elemental selenium formation by methanotrophs

Selenite reduction capability and elemental selenium production were determined for *Mc. capsulatus* (Bath) and *Ms. trichosporium* OB3b, respectively.

2.2.5.1 Quantitation of aqueous selenium species

The selenite, selenate and DL-selenocystine concentrations in the amended cultures were determined by using high performance liquid chromatography (HPLC)-inductively coupled plasma mass spectrometry (ICP-MS) system. 0.5 mL aliquots of the amended cultures were collected at intervals and centrifuged (11000 × *g*; 10 min; room temperature), to remove the cells and other debris. An aliquot of the supernatant (20 µl) was injected into HPLC-ICP-MS system using a PerkinElmer LC Flexar autosampler attached to a PerkinElmer Flexar HPLC pump connected to Hamilton PRP-X 100, 5 µm particle size, 250 mm length x 4.6 mm internal diameter (id) column, and coupled to a PerkinElmer ICP-MS NexION 350X. Separation was achieved at a flow rate of 1 mL min⁻¹

¹ using a mobile phase made up of 5 mmol L⁻¹ ammonium citrate buffer containing methanol (2% v/v) with the pH adjusted to 5.2 (Bueno, 2007). The HPLC-ICP-MS interface was a polyetheretherketone (PEEK) tubing. The HPLC and ICP-MS conditions are summarized in Table 2-1. Both the HPLC and ICP-MS were fully controlled by the PerkinElmer Chromera[®] speciation software.

For the DL-selenocystine amended cultures, the cells were harvested and kept for total selenium content analysis (see 2.2.5.3).

Table 2-1 The operating conditions for ICP-MS and HPLC instruments

HPLC	
Column	Hamilton PRP-X 100 PEEK, 4.6 x 250 mm, 5 µm
Mobile phase	5 mmol L ⁻¹ ammonium citrate (pH 5.2)
Flow rate	1 mL min ⁻¹
Separation scheme	Isocratic
Column temperature	Room temperature
Injection volume	20 µl
LC Vials	2 mL-amber glass
ICP-MS	
Nebulizer	SeaSpray, 2 mL min ⁻¹
Spray chamber	Peltier Cooler includes Quartz spray chamber
Interface cones	Nickel
RF power	1600 W
Plasma gas flow	18 L min ⁻¹
Nebulizer gas flow	0.87 L min ⁻¹
Helium gas flow	4.4 mL min ⁻¹
Interference correction	kinetic energy discrimination (KED)
Isotope	⁷⁸ Se, ⁸² Se
Dwell time	1000 ms
Peristaltic pump speed	20 rpm
Sampling rate	1 point second ⁻¹

2.2.5.2 Quantitation of elemental selenium

The pellets were analysed for elemental selenium using a method previously described by Biswas *et al* (2011) with minor modifications, as follows; before analysis the pellets were washed twice with 1 mL of 1 M NaCl in order to remove non-metabolized

selenite. This high concentration of NaCl was employed because it had been previously found to be effective in the collection of colloidal elemental sulfur (Roy & Trudinger 1970). The washed red colloidal selenium was dissolved in 1.5 mL of 1 M Na₂S, and the solution centrifuged to remove bacterial cells and cell debris.

A standard calibration curve for elemental selenium was constructed using red powdered selenium metal (Pfaltz & Bauer, Waterbury, USA). Appropriate volumes of red selenium dissolved in 1 M Na₂S solution to give a 1 g L⁻¹ stock suspension were transferred into 1.5 mL Eppendorf tubes and the volume made to 1 mL with 1 M Na₂S to give concentrations ranging from 10 to 50 mg L⁻¹ of elemental selenium. The absorbance of each of standard solutions and samples were measured at 500 nm.

2.2.5.3 Analysis of total selenium content in dry cell biomass of DL-selenocystine amended cultures

Cells were harvested after centrifugation at 11000 × *g* for 10 min, the supernatant was removed, and cells were washed three times with sterile NMS media by centrifugation (11000 × *g*, 10 min). Biomass was freeze-dried and stored at -20°C until analysis. Prior to the total selenium analysis, samples were digested by concentrated nitric acid using a microwave system (CEM MARS 6) equipped with Xpress vessels. The vessels were heated in the MARS 6 Xpress system to 200°C over 20 min and held at this temperature for 20 min. After the digest vessels were cooled to room temperature the digest solutions were transferred into volumetric flasks and diluted by ultrapure water to a final volume of 25 mL. The total contents of selenium in the bacterial biomass were determined by the ICP-MS according to the ICP-MS conditions summarized in

Table 2-1. The reagent blank solutions were prepared using the same preparation method as for the sample.

2.2.6 Investigation into the role of s/pMMO in the reduction of selenium oxyanions

In order to investigate the involvement of MMOs (sMMO and pMMO), *Ms. trichosporium* OB3b cultures at different stages of expression of the MMOs (sMMO-positive and sMMO-negative cultures) were amended with 10 mg L⁻¹ selenite and selenate, respectively. *Ms. trichosporium* OB3b cultures expressing sMMO activity were identified using the naphthalene oxidation assay reported by Brusseau *et al* (1990). The naphthalene oxidation assay is a well-known biochemical assay for identifying and quantifying sMMO activity. sMMO oxidises naphthalene to a mixture of 1-naphthol and 2-naphthol. The naphthols are detected by reaction with tetrazotized *o*-dianisidine to form purple diazo dyes with large molar absorptivities. Naphthalene is not a substrate for pMMO and all expressiry pMMO do not oxidise naphthalene. The culture of the sMMO-deleted mutant of *Ms. trichosporium* SMDM was amended with either selenite or selenate and then incubated under the above conditions. The *Ms. trichosporium* OB3b and *Mc. capsulatus* (Bath) were also grown in Cu-free NMS media prior to adding selenite or selenate (10 mg L⁻¹).

2.2.7 Investigation of the involvement of methanobactin in selenite/selente reduction

In order to investigate the involvement of methanobactin in the reduction of selenite, a stock solution of 1000 mg L⁻¹ was prepared by dissolving methanobactin in high-purity deionized water. Methanobactin used in these experiments was provided by Dr

Jeremy Semrau (University of Michigan). 270 μL aliquots of various concentration of methanobactin (50, 100 and 200 mg L^{-1}) were transferred into a 96-well microtitre plates. Subsequently, 30 μL of Na_2SeO_3 or Na_2SeO_4 solution (to a final concentration of 100 mg L^{-1} Se[IV] or Se[VI]) was added to each well. The mixture was then incubated at room temperature and 30°C for 96 hours. The mixtures were assessed visually for colour change.

2.2.8 Cell fractionation.

In order to determine the location of reductase activity, the grown culture ($\text{OD}_{600} \sim 0.7$) was centrifuged at $11000 \times g$ for 10 min at 4°C to obtain a pellet. The pellet was washed with ice-cold 50 mM Tris-HCl (pH 7.5) and re-suspended in 10 mL of the same buffer, and protease inhibitor cocktail was added (1% v/v) (Sigma-Aldrich, Dorset, UK). The suspension was passed through a French pressure cell (1500 Psi, 4°C). The lysate was then fractionated by a modification of the method reported by Smith and Foster (1995), as follows: the whole procedure was performed at 0 to 4°C to minimize protein degradation. The lysate was centrifuged ($3,000 \times g$, twice for 2 min each) to remove debris before being centrifuged ($27,000 \times g$, 20 min) to sediment cell wall fragments. The cell walls were washed by resuspension in 50 mM Tris-HCl (pH 7.5), and kept in the same buffer. The supernatant fraction was centrifuged again ($27,000 \times g$, 20 min) to remove remaining cell wall material. Membrane fragments were sedimented by centrifugation ($105,000 \times g$, 60 min) of the supernatant. The pellet (cell membranes) was washed in 50 mM Tris HCl (pH 7.5), centrifuged again under the same conditions, resuspended in the same buffer. The supernatant from the first ultracentrifugation was centrifuged again under the same conditions to remove remaining membranous material, and kept as cytoplasmic fraction.

2.2.9 Reductase activity assay

The total protein content of each fraction was measured using the BCA assay kit. 200 μL aliquots of different cell fraction suspensions (cell walls, cell membrane and cytoplasm) of *Mc. capsulatus* (Bath) and *Ms. trichosporium* OB3b, respectively were transferred into the 96-well plate. Subsequently, SeO_3^{2-} was added to give final concentrations of 100 mg L^{-1} . The mixture was then incubated at 30°C for 72 hours. Reaction mixture without addition of the three fractions served as controls. Additionally, in addressing the hypothesis that NADH may be involved directly in the reduction of the selenium oxyanions, the same mixtures were incubated in the presence of NADH (2.0 mM).

2.2.10 Transmission electron microscopy (TEM) and energy dispersive X-ray (EDX) spectrometry/high-angle annular dark-field (HAADF) scanning TEM (STEM) analysis

Samples of selenite amended culture (1.5 mL) were pelleted by centrifugation ($11000 \times g$; 10 min; room temperature), and washed with 0.1 M sodium phosphate buffer (pH 7.4). The specimens were then fixed in 3% glutaraldehyde in the same buffer overnight at room temperature and washed again in the same buffer. Secondary fixation was carried out in 1% w/v aqueous osmium tetroxide for 1 hour at room temperature followed by the same wash step. Fixed cells were dehydrated through a graded series of ethanol dehydration steps (75%, 95% and 100% v/v), and then placed in a 50/50 (v/v) mixture of 100% ethanol and 100% hexamethyldisilazane for 30 min followed by 30 min in 100% hexamethyldisilazane. The specimens were then allowed to air dry overnight. A small sample of the fixed sample was crushed and dispersed in methanol,

with a drop placed on a holey carbon coated copper grid (Agar Scientific). The samples were examined in an FEI Tecnai F20 field emission gun (FEG)-TEM operating at 200 kV and fitted with a Gatan Orius SC600A CCD camera, an Oxford Instruments X-Max SDD EDX detector and a high angle annular dark field (HAADF) scanning TEM (STEM) detector. The HAADF and TEM measurements were carried out with the help of Dr Nicole Hondow, School of Chemical and Process Engineering, University of Leeds, UK. For thin section analysis, after the ethanol dehydration steps, the cells were embedded in EM bed 812 epoxy resin and cut into thin sections (90 nm, using a diamond knife on a Reichert Ultracut S ultramicrotome). The sections were supported on copper grids and coated with carbon. TEM specimen holders were cleaned by plasma prior to TEM analysis to minimize contamination. Samples were examined with a high-resolution Philips CM 200 transmission electron microscope at an acceleration voltage of 200 kV under standard operating conditions with the liquid nitrogen anticontaminator in place. The thin section analyses were carried out at the “Centro de Instrumentación Científica”, University of Granada, Spain by Dr. Mohamed Merroun.

2.2.11 X-ray absorption spectroscopy measurements

For XAS examination, the cultures were grown as described above followed by supplementation with sodium selenite (final concentration of 20 mg L⁻¹ Se). After the development of the red colour, the cultures were centrifuged at 11,000 x g for 10 min. The pellet was freeze dried and analyzed without further treatment. Selenium K-edge X-ray Absorption Near-Edge Structure (XANES) and Extended X-ray Absorption Fine-Structure (EXAFS) spectra were collected at the Rossendorf Beamline at the European Synchrotron Radiation Facility (ESRF), Grenoble, France with the help of Dr. Andreas Scheinost. The energy of the X-ray beam was tuned by a double crystal

monochromator operating in channel-cut mode using a Si(111) crystal pair. Two rhodium-coated mirrors were used for collimation and suppression of higher harmonics. A 13-element high purity germanium detector (Canberra) together with a digital signal processing unit (XIA XMap) was used to measure reaction samples in fluorescence mode. Reference samples were measured in transmission mode using ionization chambers (300 mm, FMB Oxford) filled with 95% N₂ and 5% Ar (I₀) and with 100% Ar (I₁ and I₂). Spectra were collected at 15 K using a closed cycle He cryostat with a large fluorescence exit window and a low vibration level (CryoVac). Photoinduced redox reactions were effectively prevented by the cold temperature, since XANES edges remained stable during short-term exposure (10 min) as well as during the EXAFS measurements which took up to 8 h. For energy calibration, a gold foil (K-edge at 11919 eV) was chosen because of its greater inertness in comparison to Se. Data in the XANES region were collected in steps of 0.5 eV, i.e. with higher resolution than the resolution of the Si(111) crystal at the given vertical divergence (1.7 eV) and the broadening due to the core-hole life-time (2.3 eV). A comparison of single scans of the same sample showed an accuracy of better than 0.5 eV. Dead time correction of the fluorescence signal, energy calibration and the averaging of single scans were performed with the software package SixPack. (Webb 2005). Normalization, transformation from energy into k space, and subtraction of a spline background was performed with WinXAS using routine procedures (Ressler 1998). The EXAFS data were fit with WinXAS using theoretical backscattering amplitudes and phase shifts calculated with FEFF 8.2 (Ankudinov & Rehr 1997). This method provides a precision of ± 0.01 Å for shell distances and a resolution of about ± 0.1 Å for neighbouring shells. The error of coordination numbers is $\pm 25\%$. Statistical analysis of spectra (Eigen analysis and

iterative target test) was performed with the ITFA program package (Rossberg *et al.* 2003).

2.2.12 Extraction of selenium nanoparticles produced by methanotrophs

Grown cultures (an OD_{600} of 0.5-0.8) were supplemented with SeO_3^{2-} . After the development of the reddish colour, the cultures were pelleted by centrifugation (at $12500 \times g$; 10 min). SeNPs were extracted by a modification of the method of (Sonkusre, 2014). The resultant pellet was washed and resuspended in 10 mL of sterile water followed by addition of lysozyme to give a final concentration of 500 mg mL^{-1} , and the tube was incubated at 37°C for 3 h. The suspension was passed through a French pressure cell (1500 Psi, 4°C). The resultant slurry containing both cell debris and NPs was washed four times at $15000 \times g$ for 10 min with 1.5 M Tris-HCl (pH 8.3) containing 1% sodium dodecyl sulfate (SDS). The resultant pellet containing SeNPs and the insoluble cell wall fraction was washed and resuspended in 4 mL sterile water in 15 mL falcon tube, and 2 mL of 1-octanol were added. The solution was mixed vigorously on a vortex mixture for few min and centrifuged at $2000 \times g$ for 5 min at 4°C . The tubes were then kept undisturbed at 4°C for 24 hours. The upper phase and interface containing the insoluble cell fraction were removed, and the bottom water phase containing SeNPs was transferred to a clean 15 mL centrifuge tube. This was washed sequentially with chloroform, absolute ethanol, 70% ethanol, and water at $16000 \times g$. Collected NPs were resuspended in water and stored at 4°C .

2.2.13 X-ray photoelectron spectroscopy (XPS) analysis

Harvested SeNPs samples were deposited on silicon wafer, left to dehydrate in the load lock of the XPS instrument overnight. The analyses were carried out using a Kratos Axis Ultra DLD instrument with the monochromated aluminium source. The XPS spectra were collected at Sheffield Surface Analysis Centre, University of Sheffield with the help of Dr. Debbie Hammond. Survey scans were collected between 1200 to 0 eV binding energy, at 160 eV pass energy and 1 eV intervals. High-resolution C 1s, N 1s, O 1s, Se 3d and S 2p spectra were collected over an appropriate energy range at 20 eV pass energy and 0.1 eV intervals. The analysis area was 700 μm by 300 μm . Two areas were analysed for each sample, collecting the data in duplicate. Charge neutralisation was used with intention of preventing excessive charging of the samples during analysis. The data collected was calibrated in intensity using a transmission function characteristic of the instrument (determined using software from NPL) to make the values instrument independent. The data can then be quantified using theoretical Schofield relative sensitivity factors. The data was calibrated for binding energy by making the main carbon peak C 1s at 285.0, and correcting all data for each sample analysis accordingly.

2.2.14 Raman spectroscopy analysis of SeNPs

Aliquots of 2 μL of SeNPs suspended in water were transferred onto a calcium fluoride (CaF_2) slide and air-dried prior to Raman analysis. Raman spectra were collected at Department of Geography, University of Sheffield with the help of Dr. Emma Wharfe. Raman spectra were obtained using a Horiba LabRam HR and a modified Horiba LabRam HR (Wellsens Biotech. Ltd., China). Three factors have been modified in this

new Raman system to improve Raman spectral quality. These include shortening the Raman light path, employing a low noise and sensitive EMCCD for the Raman signal detection, and increasing incident laser power. The old and new modified systems are identical except these three factors. The Raman signals were collected by a Newton EMCCD (DU970N-BV, Andor, UK) utilizing a 1600×200 array of $16 \mu\text{m}$ pixels with thermoelectric cooling down to -70°C for negligible dark current. A 532 nm Nd:YAG laser (Ventus, Laser Quantum Ltd., UK) was used as the light source for Raman measurement. A $100\times$ magnifying dry objective ($\text{NA} = 0.90$, Olympus, UK) was used for sample observation and Raman signal acquisition. A 600 l/mm grating was used for the measurements, resulting in a spectral resolution of $\sim 1 \text{ cm}^{-1}$ with 1581 data points. The laser power on sample was measured by a laser power meter (Coherent Ltd.). The Raman spectra were processed by background subtraction (using spectra from cell free region on the same slide) and normalization using the Labspec5 software (HORIBA Jobin Yvon Ltd., UK).

2.2.15 Fourier transform infrared (FT-IR) spectroscopy measurements of SeNPs

In order to determine the functional groups present on the SeNPs, the FTIR spectra of SeNPs were recorded on a PerkinElmer Spectrum 100 FT-IR Spectrometer. Spectra were recorded from 650 to $4,000 \text{ cm}^{-1}$, and 4 scans were averaged at a resolution of 4 cm^{-1} . Extracted SeNPs were freeze dried overnight and analyzed without further treatment. For comparison, the FTIR spectra of samples of bacterial cells (as controls) and chemically synthesized SeNPs (Chem-SeNPs) were also recorded. For the controls,

the grown cultures ($OD_{600} \sim 0.7$) of *Mc. capsulatus* (Bath) and *Ms. trichosporium* OB3b were centrifuged at $11000 \times g$ for 10 min to obtain the cell pellet. Pellet was washed twice with phosphate buffered saline (PBS) pH 7.2, and then freeze dried overnight. The synthesis of Chem-SeNPs was done according to the procedure of (Lampis *et al.* 2017). 1.0 mL of 50 mM L-cysteine (Sigma-Aldrich, Dorset, UK) solution was added dropwise into 1.0 mL of 0.1 M Na_2SeO_3 . The mixed solution was then stirred for 30 min at room temperature. The Chem-SeNPs were pelleted by centrifugation (at $15000 \times g$; 10 min), and then freeze dried overnight.

2.2.16 Dynamic light scattering (DLS) and zeta potential analysis of the SeNPs

The zeta potential and average particle size of the SeNPs were measured by a Nano-ZS instrument (Malvern Instruments Limited, UK). Aliquots of 500 μ L of SeNPs suspended in 1 mM NaCl solution were transferred into cuvettes (Disposable Capillary Cell, Malvern Instruments, DTS-1070). Data recorded at 25°C with equilibrium time of 30 seconds. Each sample was measured at least 3 times to ensure the validity. All the values were obtained using the Malvern software. The measurements were carried out at Department of Chemistry, University of York, UK with the help of Dr. Tamim Chalati.

2.2.17 Bacteria protein-associated SeNPs

In order to investigate the proteins associated with the SeNPs, extracted SeNPs samples were denatured at 95°C for 10 min in Laemmli sample buffer (Bio-Rad, 161-0747) and then separated in a 12% SDS-PAGE gel (Mini-PROTEAN[®] TGX Precast Protein Gels, Bio-Rad, 456-1046) in the presence of 1 x Tris-Glycine running buffer (Sigma) containing 1% SDS (Sigma) at a constant voltage of 120 V. Silver staining (Pierce[®] Silver

Stain Kit, Thermo Scientific, 24612) was performed. The staining was carried out according to manufacturer instructions. To aid molecular weight determination, 5 μL SeeBlue[®] Plus2 Pre-Stained molecular weight marker (Novex, LC5925) was loaded.

2.2.18 Detection of volatile selenium species

The presence of volatile selenium-containing metabolites was detected by GC-MS. Analytical standards of dimethyl selenide (CH_3SeCH_3 , DMSe) and dimethyl diselenide ($\text{CH}_3\text{SeSeCH}_3$, DMDSe) (Sigma-Aldrich, Poole, UK, >99.0 %, 98%, respectively) were used. Since dimethyl selenenyl sulfide ($\text{CH}_3\text{SeSCH}_3$, DMSeS) and methylselenol (CH_3SeH , MeSeH) were not commercially available, the compounds were synthesized as described previously (Chasteen 1993). Cultures of *Mc. capsulatus* (Bath) and *Ms. trichosporium* OB3b were grown as detailed in section 2.2.1 and amended with either selenite (40 and 20 mg L^{-1} , respectively) or selenate (ranging from 100 - 2500 mg L^{-1}). Flasks containing medium inoculated with the bacteria but with no SeO_3^{2-} salts added, were run as controls. Samples (200 mL) of the headspace gas were collected through a needle attached to a sorbent tube (Tenax TA/, SulfiCarb C2-CXXX-5314, Markes International, UK) connected to a hand-held pump (Easy-VOC grab-sampler, Markes International UK) after 24 and 48 hours for *Mc. capsulatus* (Bath) and *Ms. trichosporium* OB3b, respectively. To ensure that the tubes were contamination free, before use the sorbent tubes were preconditioned with helium at flow rate of 90 mL min^{-1} using the following temperature program: 15 min at 100°C, 15 min at 200°C, 15 min at 300°C and 15 min at 335°C.

Samples analyse was performed on a combined thermal desorption GC–MS system. The volatiles were desorbed at 250°C and concentrated on a thermal desorber (Unity[®],

Markes International Limited) at -10°C cold trap for 5 min (helium flow 50 mL min^{-1}) and then were transferred onto the GC/MS system (7890A-GC with 5975C-MS, Agilent Technologies) equipped with a capillary column (Agilent J&W HP-5ms GC Column, 30 m, 0.25 mm, $0.25\text{ }\mu\text{m}$). Helium was used as the carrier gas at a flow rate of 1 mL min^{-1} , injector temperature, 250°C , and the chromatogram was obtained using the following temperature programme: 35°C for 1 min; $10^{\circ}\text{C min}^{-1}$ to 250°C ; and then held at 250°C for 1 min. The National Institute of Standards and Technology (NIST) MS search program (version 2011) was used to identify the compounds based on their MS spectrum.

Chapter 3

**Interaction of methanotrophs with selenium oxyanions and
evaluation of their reducing ability**

3.1 Bacterial response to selenium oxyanions

3.1.1 Minimum inhibitory concentrations of selenium for methanotrophs

Minimum inhibitory concentrations (MICs) for selenate and selenite were determined for *Mc. capsulatus* (Bath) and *Ms. trichosporium* OB3b. Concentrations between 0 - 2500 mg L⁻¹ of selenium (as selenite and selenate) were investigated and the results from the MIC study are shown in Table 3-1

Table 3-1 Minimum inhibition concentrations of selenium for methanotrophs. Data shown from two independent cultures at each selenate or selenite concentration (n=2). Both compared visually to the control media.

	Selenate (mg L ⁻¹)	Selenite (mg L ⁻¹)
<i>Mc. capsulatus</i> (Bath)	2400	70
<i>Ms. trichosporium</i> OB3b	1700	5

As can be seen from Table 3-1, when the selenate concentrations between 1000 to 2500 mg L⁻¹ were investigated, the MICs for selenate for *Mc. capsulatus* (Bath) and *Ms. trichosporium* OB3b were found to be 2400 and 1700 mg L⁻¹, respectively. In contrast, the MICs for selenite were found to be much lower than those of selenate. For *Mc. capsulatus* (Bath), the MIC was found to be 70 mg L⁻¹. Similarly, the MIC was found to be 5 mg L⁻¹ for *Ms. trichosporium* OB3b. Indeed, it is known that MIC is not an absolute constant and that it may vary with several variables such as the nature of the organism being studied, the inoculum size, incubation time, composition of the culture media, and the specific conditions of incubation (e.g., pH, temperature and aeration) (Brock *et al.* 1991). In previous animal studies on the toxicology of selenium and selenium compounds, it has been shown that, selenite in general is the more toxic of the two

selenium oxyanions (Cooper & Glover 1974; Brasher & Ogle 1993; Oehme 1972; Stadtman 1990; Yu *et al.* 1997). Similarly, it is known that selenate is much less toxic than selenite for bacteria (Frankenberger & Engberg 1998; Sarret *et al.* 2005; Zannoni *et al.* 2007). In a study in which the effects of selenite and selenate on growth of *Tetrathibacter kashmirensis* strain CA1 were investigated, Hunter and Manter (2008) reported that selenite was more toxic to the strain than was selenate. Even at concentrations of 8.1 mg L⁻¹, selenate had no clear impact on growth, while selenite slowed growth around 50% when additions to the growth media were 2 mg L⁻¹ or more. These results are consistent with the relative toxicity of selenate and selenite to methanotroph cells.

3.1.2 Bacterial growth under selenite/selenate stress

The growth profile of *Mc. capsulatus* (Bath) and *Ms. trichosporium* OB3b in NMS media in the presence of various concentrations of selenate and selenite was studied based on the MIC measurements. The growth profile in the presence of selenate is shown in Figure 3-1. For *Mc. capsulatus* (Bath), the control (no selenate) exhibited a lag phase of less than 24 hours, followed by faster growth (putative logarithmic growth phase). After 48 hours of growth, the culture entered the stationary phase. A similar growth curve was observed with 100 mg L⁻¹ selenate amended media. In contrast, when 400 and 800 mg L⁻¹ selenate were present, the lag phase was prolonged to around 24 hours, followed by a 48 h long logarithmic growth phase. The stationary phase of the culture treated with 400 or 800 mg L⁻¹ of selenate started at around 72 hours of incubation (Figure 3-1a). For *Ms. trichosporium* OB3b, as shown in Figure 3-1b, the control (0 mg L⁻¹ SeO₄²⁻) exhibited a lag phase at around 24 hours, followed by a steep logarithmic growth phase at around 48 hours. The stationary phase started after around 72 hours

of incubation. A similar growth curves were observed with 100, 200 and 600 mg L⁻¹ selenate amended media.

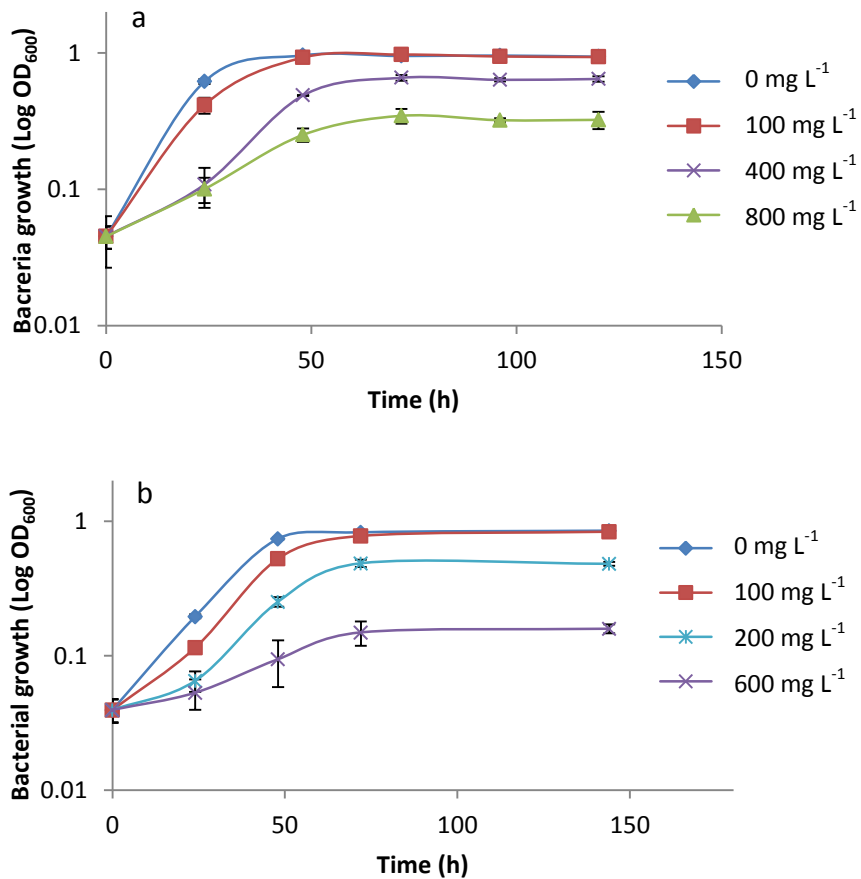


Figure 3-1 Time course of bacterial growth of *Mc. capsulatus* (Bath) (a) and *Ms. trichosporium* OB3b (b) in the presence of various concentrations of sodium selenate. Data shown is from three independent cultures at each selenate concentration. Results plotted as mean \pm 1 standard deviation (n=3).

The presence of selenate at concentrations of 100 mg L⁻¹ did not have a negative impact on the growth curve compared to the control culture. The control and the selenate amended cultures showed a typical sigmoid growth curve. However, at higher selenate concentrations, inhibition of growth was observed. It is worth noting that cultures of *Mc. capsulatus* (Bath) and *Ms. trichosporium* OB3b failed to form reddish cell suspensions, when amended with sodium selenate, indicating that neither strain is able to reduce selenate to red elemental selenium.

In order to determine the toxicity of selenite to the methanotrophs, the growth profile of the bacteria was studied by addition of different concentrations of sodium selenite (0, 10 and 20 mg L⁻¹, and 0, 2 and 4 mg L⁻¹ selenite for *Mc. capsulatus* (Bath) and *Ms. trichosporium* OB3b, respectively) in the cultures. The growth profiles of *Mc. capsulatus* (Bath) and *Ms. trichosporium* OB3b in NMS media in the presence of different concentrations of selenite are shown in Figure 3-2.

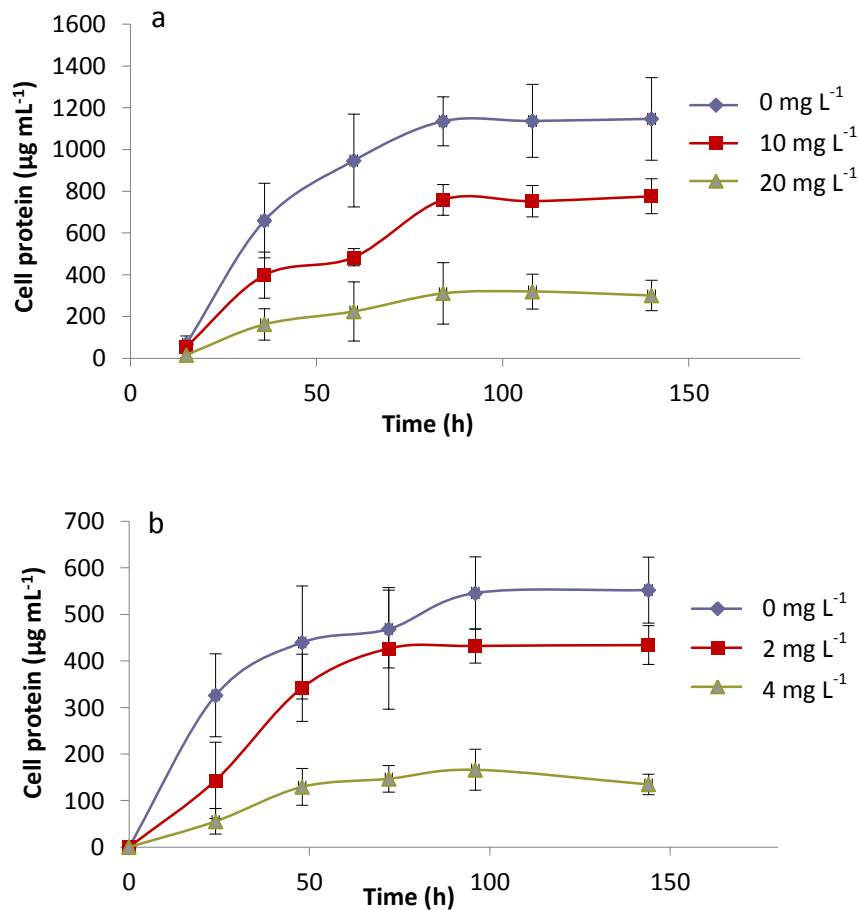


Figure 3-2 Bacterial growth profile of *Mc. capsulatus* (Bath) (a) and *Ms. trichosporium* OB3b (b) under different selenite concentrations. Bacterial growth was measured via the quantification of total cell protein using BCA kit, and expressed as total protein per mL culture. Data shown is from three independent cultures at each selenite concentration. Error bars show ± 1 standard deviation (n=3).

Compared to selenate, the presence of selenite at much lower concentrations elicited a toxic effect and the strains were able to reduce selenite to putative red elemental selenium. The formation of the red precipitate of elemental selenium in the cultures started amended with selenite after 4 and 24 hours for *Mc. capsulatus* [Bath] and *Ms. trichosporium* OB3b, respectively of exposure. Optical density was not used to follow growth of the cultures in these experiments because the presence of Se⁰ particles

would contribute to the OD₆₀₀ consequently the results would not be an accurate measure of growth. Therefore, the total protein content was measured at different time intervals and used as a measure of the growth of the bacterium. When the cultures of *Mc. capsulatus* (Bath) were amended with 10 and 20 mg L⁻¹ selenite, respectively, the cell protein concentrations of the cultures were diminished by 43% and 78%, in the stationary phase relative to the cultures not amended with selenite. Meanwhile, when the cultures of *Ms. trichosporium* OB3b were amended with 2 and 4 mg L⁻¹ selenite, respectively, the cell protein concentrations of the cultures were diminished by 20% and 70% in the stationary phase relative to the cultures not amended with selenite. Whilst selenite reduced the amount of protein produced by the cultures, the timing of the different phases of growth was not affected. Although, selenite was found to be much more toxic than selenate to the methanotrophs, simultaneous protein estimation by BCA method indicated that there was a short time lag period between the growth of the methanotrophs either in the presence or absence of selenite.

Although the precise mechanism of toxicity of selenate and selenite is not known, there is increasing evidence that the toxic character of these compounds is associated with their oxidising capacity; it has been shown that selenite reacts with glutathione or cysteine forming toxic reactive oxygen species (H₂O₂ and O₂⁻) that trigger the production of further oxidative stress enzymes (Kramer & Ames 1988; Bebień *et al.* 2001; Letavayová *et al.* 2006; Lenz & Lens 2009).

3.1.3 Flow cytometric studies

In a study conducted on *Bacillus cereus* (strain CM100B) by Dhanjal and Cameotra (2010), it was shown that there was a gradual decrease in average bacterial cell size grown in the presence of selenite as compared to the control cells which were grown without the addition of the oxyanion as determined by forward scatter in flow cytometric analysis. Under the stressful condition of toxic selenite ions the morphology of the cells is altered resulting in decrease in cell size, which has been attributed to the surface/volume ratio. The authors suggest that the organisms reduce their cell size and increase their relative surface area for better uptake of the nutrients in order to survive under environmental stress conditions. It is also probable that the protein concentration of the cultures decreased in the presence of selenite but the timing of the growth phases is not affected because the smaller cells were dividing with the same kinetics.

To address the hypothesis that selenium oxyanion may affect bacterial cell size of both *Mc. capsulatus* (Bath) and *Ms. trichosporium* OB3b; bacterial cells exposed to toxic selenate or selenite ions were analyzed for difference in their cell size at various time intervals as measured by forward scattering within flow cytometric analysis. Forward scattering analysis of both strains are shown in Figure 3-3 and Figure 3-4. At all time intervals investigated, there was no significant shift in the cell populations tested in comparison to the control cell population, indicating no substantial change in the bacterial cell size. The results indicate that the presence of the selenium oxyanions results in the production of fewer cells of approximately the same size. These results are in agreement with the results of TEM and HAADF imaging detailed in section 4.1.

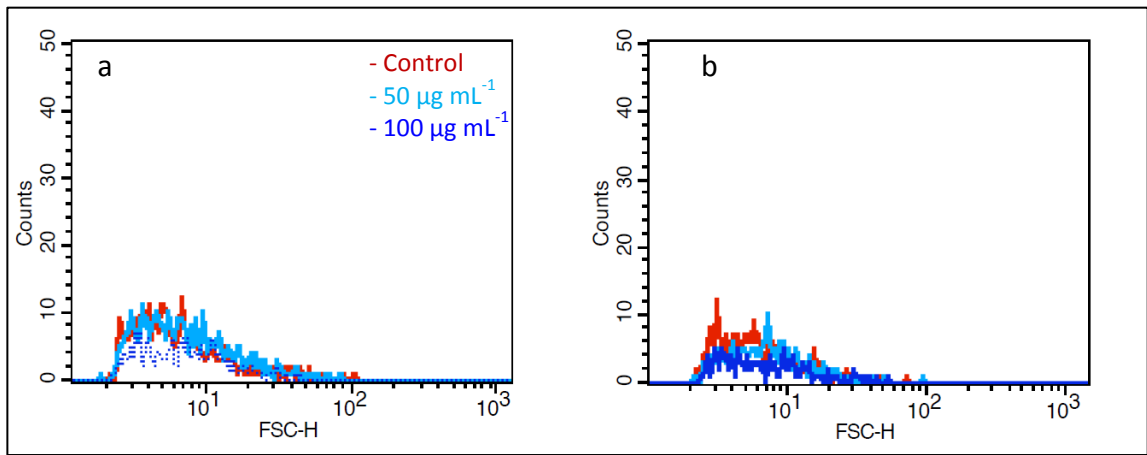


Figure 3-3 Forward scattering analysis of *Mc. capsulatus* (Bath) (a) and *Ms. trichosporium* OB3b (b) grown in the presence of selenate for 48 and 72 h, respectively. Based on visual inspection of the curves, no significant effect on bacterial cell size was observed as measured by flow cytometry, The X-axis is the log scale and the Y-axis indicates the number of bacterial cells (counts in 100). Shift towards left/right on the X-axis indicates decrease/increase in cell size. The measurements were repeated twice with different cultures (n=2).

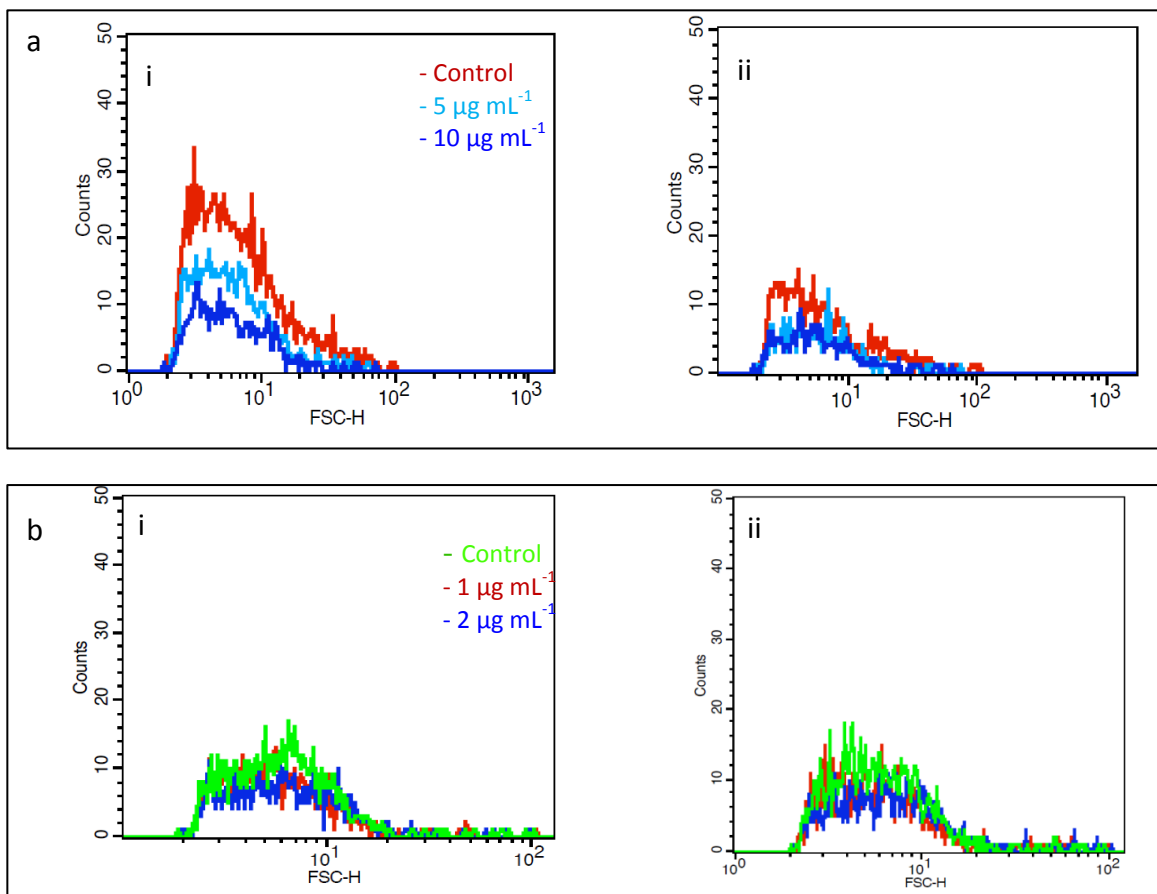


Figure 3-4 Forward scattering analysis of methanotroph cultures grown in the presence of selenite. (a) *Mc. capsulatus* (Bath) after 48 h of bacterial growth (i) and after 72 h of bacterial growth (ii). (b) *Ms. trichosporium* OB3b after 48 h of bacterial growth (i) and after 96 h of bacterial growth (ii). Based on visual inspection of the curves, no significant effect on bacterial cell size was observed as measured by flow cytometry, The X-axis is the log scale and the Y-axis indicates the number of bacterial cells. Shift towards left/right on the X-axis indicates decrease/increase in cell size. The measurements were repeated twice with different cultures (n=2).

3.2 Optimization of the separation and detection conditions of selenium species by HPLC-ICP-MS

High performance liquid chromatography (HPLC) is a chromatographic technique used to separate a mixture of compounds in analytical chemistry and biochemistry with the purpose of identifying, quantifying and purifying the individual components of the mixture. Inductively coupled plasma mass spectrometry (ICP-MS) is capable of detecting metals and several non-metals at concentrations as low as ng L^{-1} . This is achieved by ionizing the sample with inductively coupled plasma and then using a mass spectrometer to separate and quantify the ions according to their size-to-charge ratio. HPLC when coupled with ICP-MS offers the opportunity to carry out elemental speciation studies and high sensitivity and selectivity (Zioła-Frankowska *et al.* 2015). For inorganic selenium species, the hyphenated technique (HPLC–ICP-MS) is the technique of choice for selenium speciation in biological and environmental samples.

In order to separate, detect and quantify different selenium species, namely, selenate, selenite and DL-selenocystine. Simultaneously, in a single analysis, a methodology based on the coupling of HPLC with ICP-MS was developed (see operating conditions in Table 2-1). The chromatogram obtained for a Se standard mixture containing SeO_3^{2-} , SeO_4^{2-} and DL-selenocystine, each at a concentration of $100 \mu\text{g L}^{-1}$ Se is shown in Figure 3-5. As can be seen, baseline separation of both species was achieved in less than 15 minutes. Better detection limits were achieved for ^{78}Se compared to ^{82}Se because of the abundance of Se (23.8% and 8.7% for the two isotopes, respectively). The method was then applied to the selenite and selenate levels in the amended cultures.

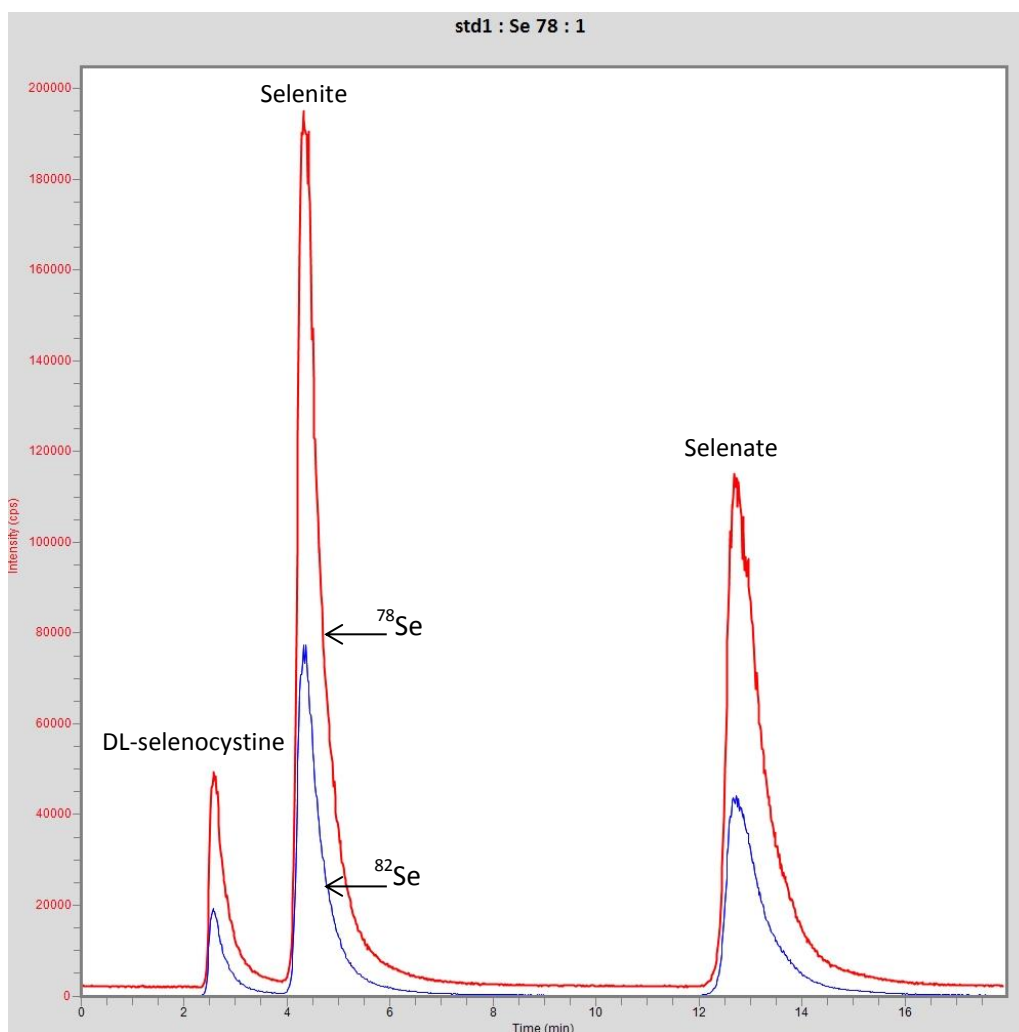


Figure 3-5 Chromatogram of a standard containing of selenite, selenate and DL-selenocystine at $100 \mu\text{g}(\text{Se}) \text{L}^{-1}$. Chromatographic separation of the selenium species was on a Hamilton PRP-X 100 column, ammonium citrate at pH 5.2 and 2% methanol as mobile phase with a flow rate of 1 mL min^{-1} . Chromatogram is representative of more than 8 runs.

3.3 Colour and concentration changes in selenium oxyanion-amended cultures

Each culture, after growth to OD_{600} of 0.5-0.8, was amended separately with selenate or selenite in order to test the ability of the two methanotrophic bacteria

Ms.trichosporium OB3b and *Mc.capsulatus* (Bath) to reduce both selenium oxyanions. Colour changes and the selenate or selenite concentrations in each solution were monitored. The reddish precipitate in the cultures indicates the formation of Se^0 via the reduction of the colourless selenite or selenate. The difference in the colours of the selenite amended solutions and corresponding spectra of the solutions are shown in Figure 3-6. Similar colour change as in the *Ms. trichosporium* OB3b culture (Figure 3-7a) was obtained when *Ms. trichosporium* SMDM (a derivative of *Ms. trichosporium* OB3b in which the genes encoding soluble methane monooxygenase [sMMO] has been deleted) was used in the same experiment. When *Ms. trichosporium* OB3b and *Mc. capsulatus* (Bath) were grown in Cu-free NMS media and amended with 10 mg L^{-1} selenite, the cultures turned red Figure 3-7b. The fact that the sMMO-deleted mutant of *Ms. trichosporium* (SMDM) was unaffected in its ability to transform SeO_3^{2-} indicated that components of sMMO are not needed for this reaction. In addition, both sMMO-positive and sMMO-negative cultures of *Ms. trichosporium* Ob3b (as confirmed via the naphthalene oxidation assay, section 2.2.6) were able to reduce SeO_3^{2-} to red elemental selenium. Changes in concentration with time at different initial selenite concentrations are shown in both Figure 3-8 and Figure 3-9. Also shown in Figure 3-10 is evidence that the presence of methane is essential for the reduction of selenite. No colour or concentration changes were observed in the selenate amended cultures. Results for the determination of the selenate concentrations (10 mg L^{-1}) are shown in Figure 3-11.

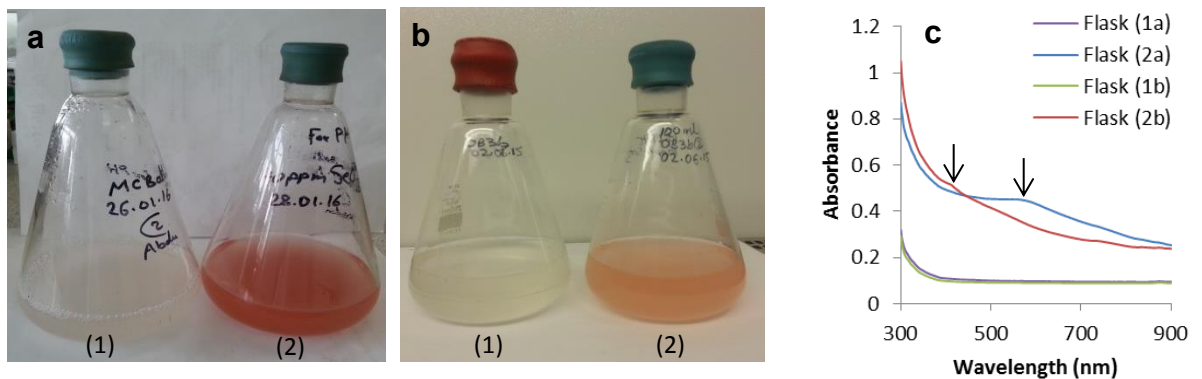


Figure 3-6 Reduction of SeO_3^{2-} to red Se^0 by the methanotrophs *Mc. capsulatus* (a) and *Ms. trichosporium* OB3b (b) at 2 and 3 day incubation respectively. Flask 1 contains no added SeO_3^{2-} ; flask 2, with SeO_3^{2-} added (40 and 20 mg L^{-1} respectively). (c) Absorption spectra of the contents of the four flasks showing the differences in the absorption peak maximum as reflected in the solution colours. The images are representatives of more than 10 replicates of the experiments.

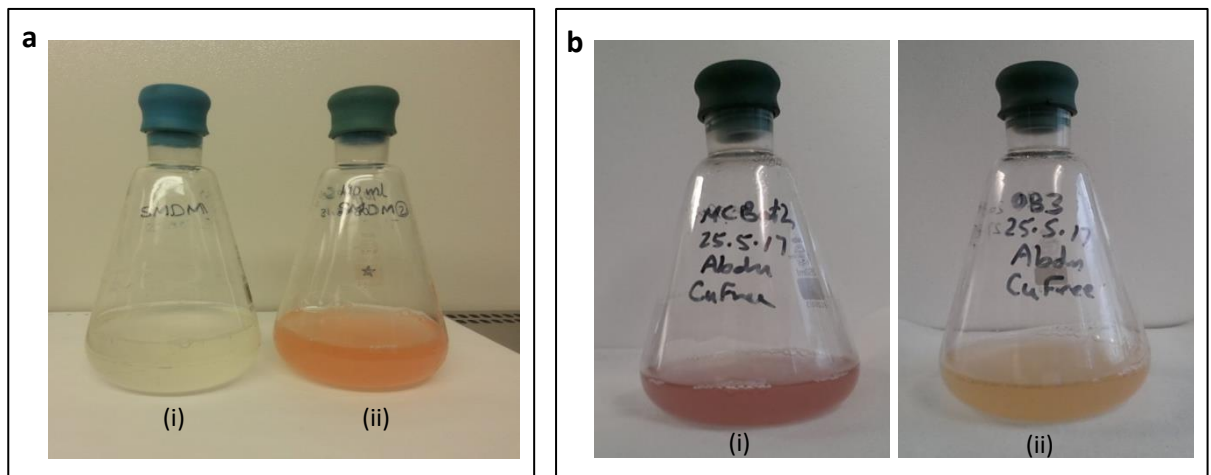


Figure 3-7 Reduction of selenite (10mg L^{-1}) to red Se^0 by sMMO-deleted mutant of *Ms. trichosporium* OB3b (SMDM) (a) without (i) and with (ii) selenite after 48 h incubation times, respectively. Reduction of selenite (b) by and *Mc. capsulatus* (i), *Ms. trichosporium* OB3b (ii), grown in Cu-free NMS media and amended with 10 mg L^{-1} of the oxyanion after 48 h incubation times. The images are representatives of more than 5 replicates of the experiments.

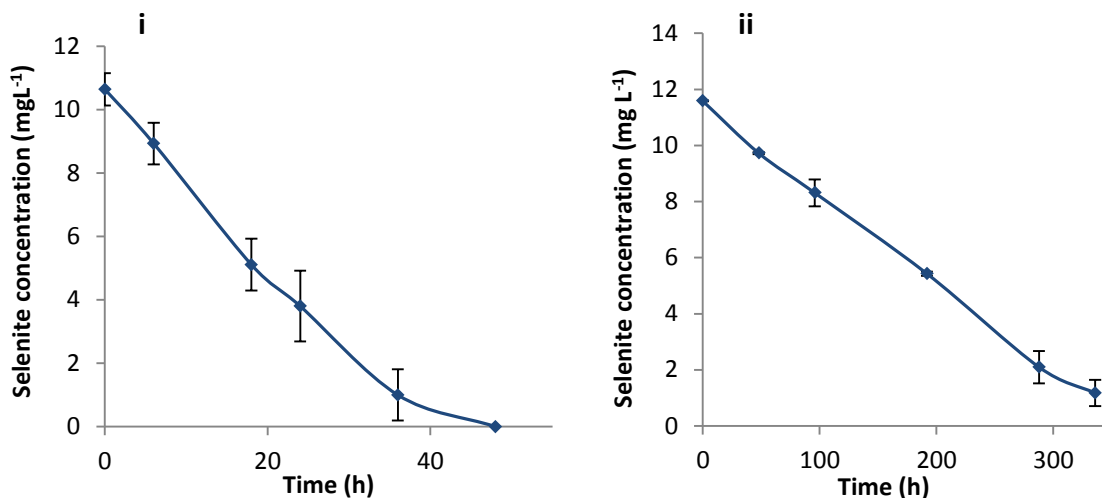


Figure 3-8 Time course of selenite reduction after an initial addition of 10 mg L⁻¹ of the oxyanion to the culture containing *Mc. capsulatus* (Bath) (i) and *Ms trichosporium* OB3b (ii), respectively. The selenite concentrations were monitored with HPLC-ICP-MS system. Values plotted as mean ± 1 standard deviation ($n=3$).

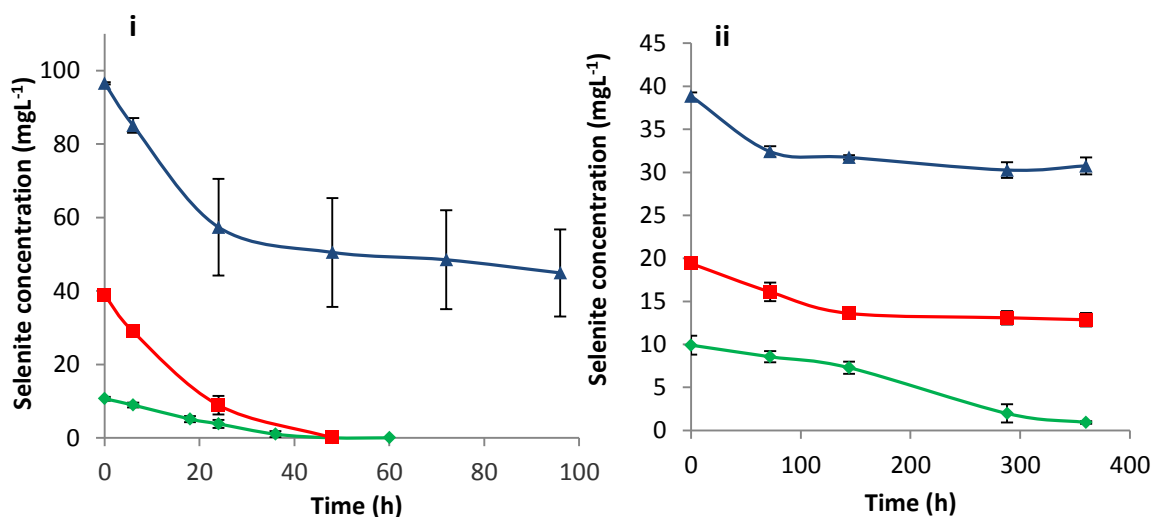


Figure 3-9 The effect on the time course of selenite reduction after an initial addition of 10 (green line), 40 (red line) and 100 (blue line) mg L⁻¹ of the oxyanion to the culture containing *Mc. capsulatus* (Bath) (i), and after an initial addition of 10 (green line), 20 (red line) and 40 (blue line) mg L⁻¹ of the oxyanion to the cultures containing *Ms trichosporium* OB3b (ii), respectively. The selenite concentrations were monitored with HPLC-ICP-MS system. Values plotted as mean ± 1 standard deviation ($n=3$).

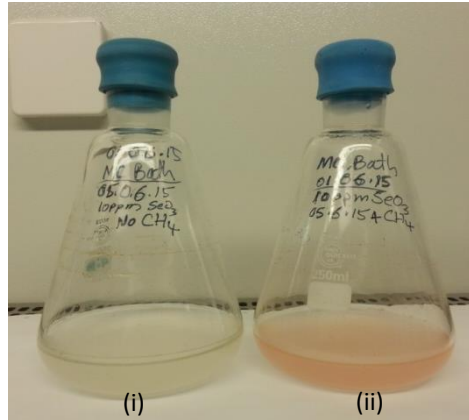


Figure 3-10 Reduction of SeO_3^{2-} (10 mg L^{-1}) to red putative Se^0 by *Mc. capsulatus* (Bath) (b) without (i) and with (ii) methane after 24 h incubation in both cases using the optimum temperature for the growth of each bacterium. Image is representative of 3 replicates of the experiment.

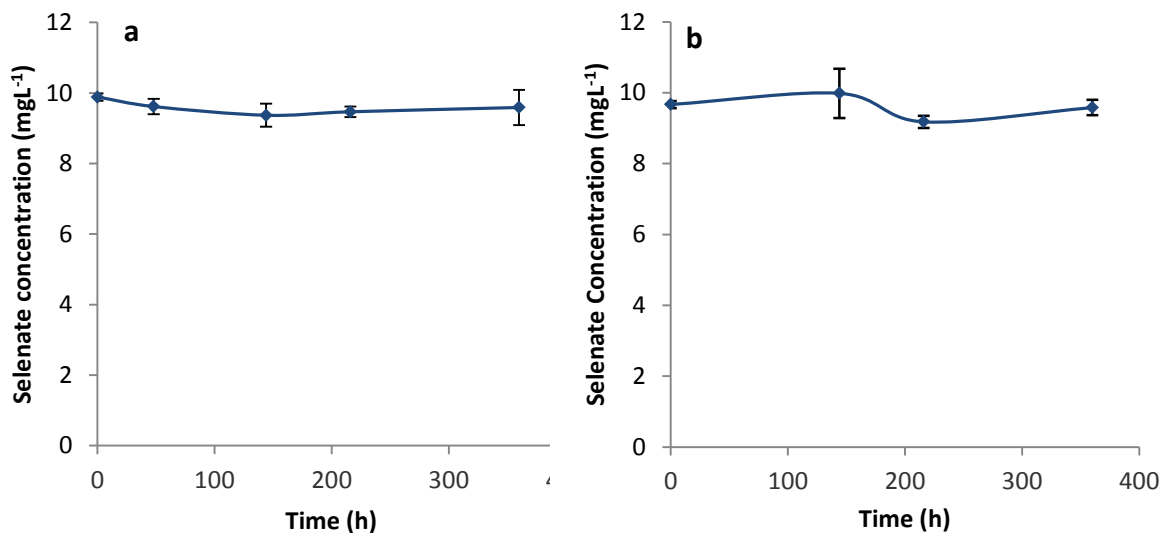


Figure 3-11 The variation of the mean selenate concentrations with time after incubation in the cultures containing *Mc. capsulatus* (Bath) (a) and *Ms trichosporium* OB3b (b), respectively. The selenate concentrations were monitored with HPLC-ICP-MS system. Values plotted as mean \pm 1 standard deviation ($n=3$).

In the selenate amended cultures no colour or selenate concentration changes were observed, which is a strong indication that in the presence of either of these two pure strains of methanotrophs selenate is not bio-transformed into elemental selenium. This finding is in contrast to that of Lai *et al.* (2016b), who used a biofilm microbial community in the presence of methane to show that selenate is reduced to elemental selenium. In our experiments, there were changes in the colour and oxyanion concentration only in the selenite amended solutions. Hence, if the mixed population of methanotrophs in the study of Lai *et al.* had the same selenium-transforming properties as the pure strains analysed here, the overall reaction to convert selenate to elemental selenium may have been accomplished by the combined activities of methanotrophs and other selenate-reducing bacteria. Although there were concentration colour changes in both the *Ms. trichosporium* OB3b and *Mc. capsulatus* (Bath) culture media to which selenite was added the rate at which these occurred was dependant on the type of bacteria used. The slower rate of selenite reduction by the *Ms. trichosporium* OB3b, maybe linked to its slow growth rate compared with the *Mc. capsulatus* (Bath).

The colour change in the cultures containing *Mc. capsulatus* was rapid with perceptible reddish tinge occurring in a matter of hours and developing into an intense reddish hue in less than 24 hours. In contrast, the colour change in the *Ms. trichosporium* OB3b culture was less intense and much slower to develop, appearing after about two days. However, it is noteworthy that the Se^0 may have begun to form long before any perceptible colour change occurs in the solutions as indicated by the reduction in the selenite concentrations at the beginning of the experiments.

3.4 Transformation of selenium oxyanions and elemental selenium content of cultures

Preliminary confirmation that the reddish/yellowish orange suspensions were primarily made-up of putative elemental selenium was obtained by harvesting the particles, and subjecting them to sample pre-treatment followed by selenium determination using UV-vis spectrometry. As shown in Figure 3-12, as the selenite concentrations decreased over time in each culture, the elemental selenium concentrations increased. The decrease in selenite concentrations was monitored with HPLC-ICP-MS system. Values reported are the mean of triplicates reported along with ± 1 standard deviation. It is noteworthy that not all the selenite in solution was converted to elemental selenium as shown by the differences in the initial selenite and the final elemental selenium concentrations for both bacteria. About 75% and 68% on average were transformed into elemental selenium by *Mc. capsulatus* (Bath) and *Ms. trichosporium* OB3b, respectively. Indeed, substantial amounts of selenite had been converted into volatile methyl species of selenium, as will be discussed in Chapter 5. Assimilation into organic selenium compounds might have also occurred beside Se^0 formation. In cultures amended with selenate, no change was observed in the selenate concentration 10 mg L^{-1} during the experiment. This is an indication that neither bacterium is able to reduce selenate to elemental selenium.

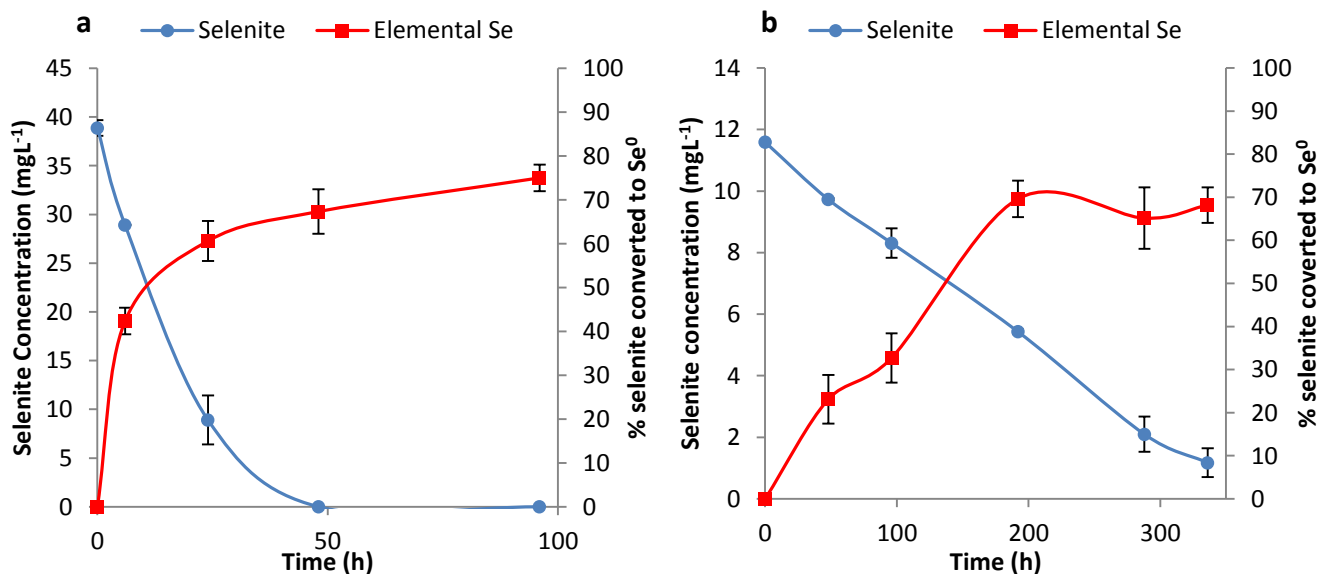


Figure 3-12 Time course of selenite reduction and elemental selenium production by *Mc. capsulatus* (a), and *Ms. trichosporium* OB3b (b). The selenite concentrations were monitored with HPLC-ICP-MS system, and elemental selenium production with UV-vis spectrometry at 500 nm. Values plotted as mean \pm 1 standard deviation ($n=3$).

3.5 Conversion of DL-selenocystine by methanotrophs

In order to find whether some form of selenium other than selenite or selenate could be converted by methanotrophs, selenide in the form of DL-selenocystine (organoselenium species) was investigated. DL-selenocystine has been reported to be about as effective as selenite in stimulating the formation of formate dehydrogenase (FDH) in the metabolism of *Escherichia coli*, whereas DL-selenomethionine was only 1% as effective (Enoch & Lester 1972). Shum and Murphy (1972) reported that selenite was required in a defined medium for the formation of formate dehydrogenase in aerobically as well as anaerobically grown cells of *E. coli*. They also demonstrated that selenocystine could replace the selenite but with selenomethionine only half of the activity was obtained compared with that when selenite was present in the medium.

In the present study, after the growth of *Mc. capsulatus* (Bath) and *Ms. trichosporium* OB3b had reached an OD₆₀₀ of 0.5 - 0.8 (putative stationary phase) under the above mentioned growth conditions, the cultures were amended with 20 mg L⁻¹ DL-selenocystine. Figure 3-13 shows the change in DL-selenocystine content in supernatant from the amended bacterial cultures of two strains, monitored by HPLC-ICP-MS system, as well as the change in total selenium content in the bacterial biomass, measured by ICP-MS. A decrease in the supernatant DL-selenocystine concentration was observed. The cultures caused a fall in the DL-selenocystine concentration of approximately 55% from an initial value of 19.1 mg L⁻¹ over 72 hours, and around 38% from an initial value of 18.9 mg L⁻¹ over 288 hours for *Mc. capsulatus* (Bath) and *Ms. trichosporium* OB3b, respectively. No colour changes were observed in the DL-selenocystine amended cultures, which indicate that the DL-selenocystine has not been converted to red elemental selenium. Interestingly, the longer the incubation time for either bacterium, resulted in an increase in the total selenium content in the bacterial biomass, suggesting that the DL-selenocystine may be assimilated by the methanotrophs into organic selenium compounds. In addition, the HAADF-STEM imaging with EDX maps of the two bacteria showed selenium adsorbed on the cells (see Figure 3-14 and Figure 3-15). The DL-selenocystine depletion in the cultures could not only be attributed to the assimilation into organic selenium compounds but also into selenium volatile selenium species, as will be discussed in Chapter 5.

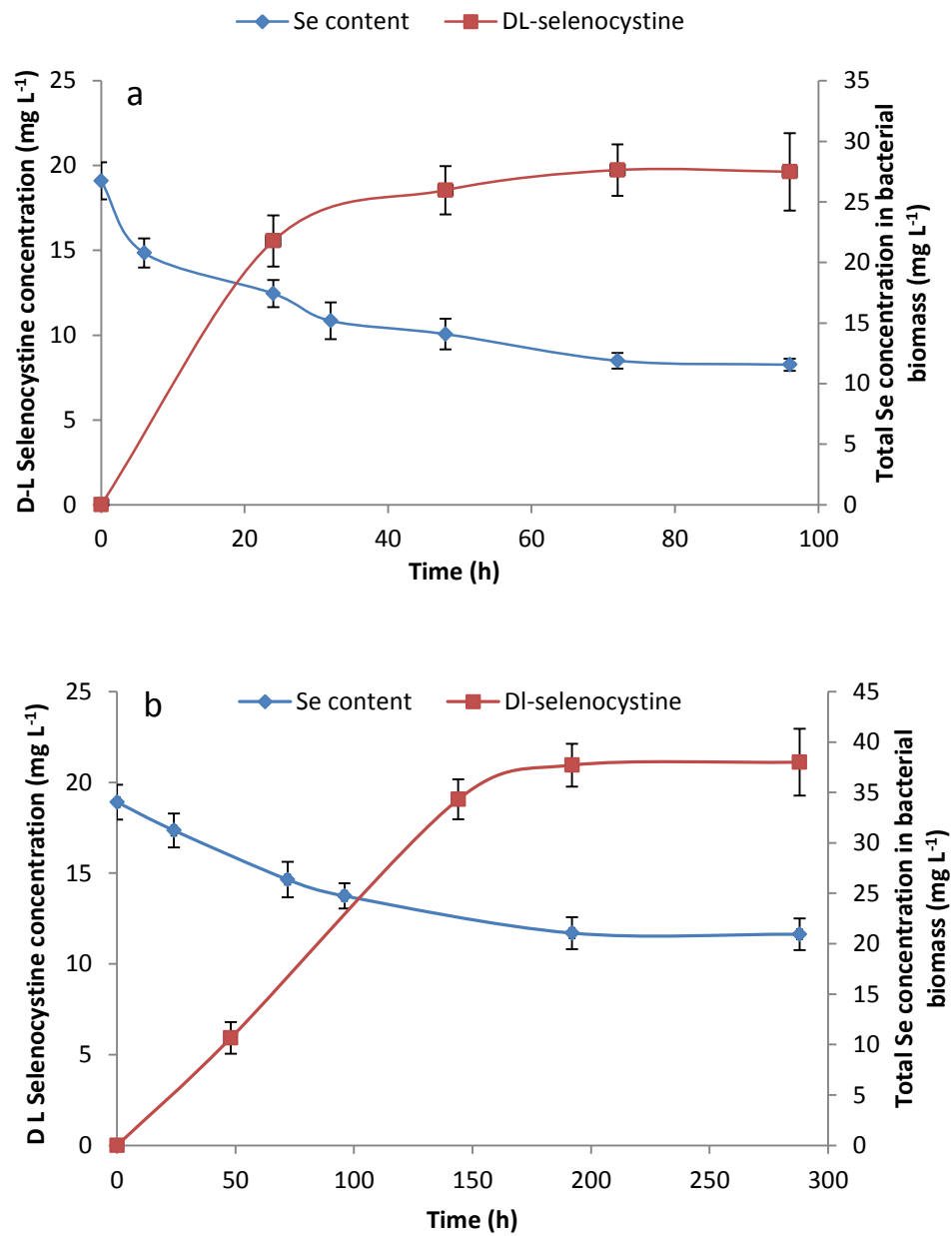


Figure 3-13 Time course of DL-selenocystine change and total selenium content in the bacterial biomass after an addition of 20 mg L⁻¹ of the DL-selenocystine to *Mc. capsulatus* (a) and *Ms. trichosporium* OB3b (b) cultures. The DL-selenocystine concentrations in the amended cultures were determined by using HPLC-ICP-MS, and the total selenium content by the ICP-MS. Results are given as ± 1 standard deviation (n=3).

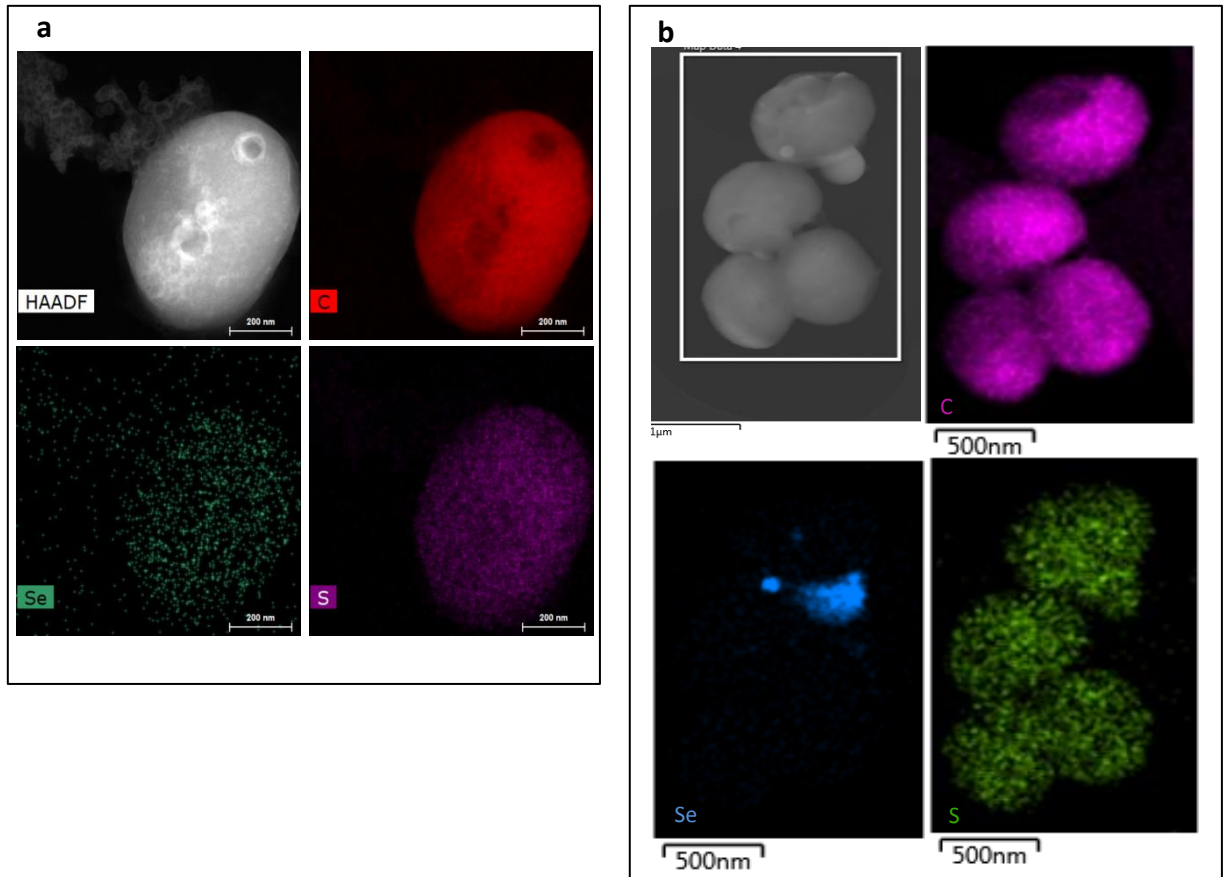


Figure 3-14 HAADF-STEM imaging of *Mc. capsulatus* (Bath) cultures exposed to DL-selenocystine (a) and selenite (b) at 2 day incubation. In the case of DL-selenocystine, the images show selenium adsorbed on the cells with EDX maps (generated from spectra collected from the indicated areas) of relevant elements. The Se from the samples exposed to DL-selenocystine appears to be more evenly distributed, as opposed to the clusters observed in the samples exposed to selenite. This could be attributed to the DL-selenocystine uptake and assimilation into organic selenium compounds. Cells were fixed with 3% glutaraldehyde and 2% OsO₄ immediately before HAADF-STEM. The images are representatives of 4 replicates.

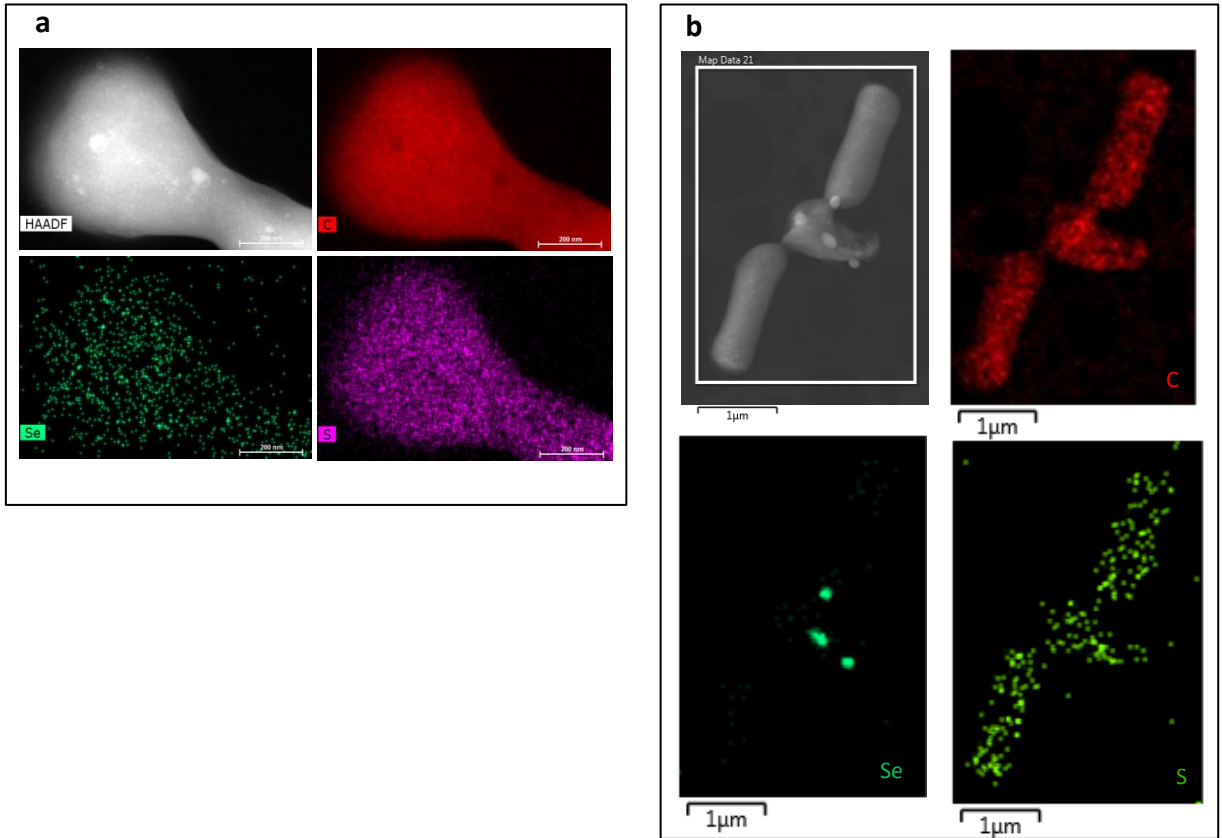


Figure 3-15 HAADF-STEM imaging of *Ms. trichosporium* OB3b cultures exposed to DL-selenocystine (a) and selenite (b) at 4 day incubation. In the case of DL-selenocystine, the images show selenium adsorbed on the cells with EDX maps (generated from spectra collected from the indicated areas) of relevant elements. Cells were fixed with 3% glutaraldehyde and 2% OsO₄ immediately before HAADF-STEM. The images are representatives of 2 replicates.

3.6 EXAFS and XANES measurements

X-ray absorption spectroscopy provides an approach for determining the chemical nature of almost any element without the need for any chemical pretreatment (Pickering *et al.* 1995; Pickering *et al.* 1999). Selenium is a particularly suitable element for this approach, since different chemical forms exhibit significantly different spectra. The XANES of all samples show white-line features typical for red Se as shown at the top of Figure 3-16a. The white line of SeO_3^{2-} shown at the bottom is about 5 eV higher in energy, and coincides with the post-edge minimum of the samples and of red Se^0 , indicating that there are no discernible traces of Se(IV) remaining. The assignment of the spectra as due largely to red elemental selenium is also confirmed by the reconstruction of the EXAFS spectra of all samples by only one principal component, shown as red traces in Figure 3-16a, b. The phase identity of red Se^0 was confirmed by the Fourier transform magnitude (see Figure 3-16c), which shows the two Se-Se peaks typical for the crystalline as well as the amorphous variety of red Se. The EXAFS fit shows the typical local structure, with 2 Se atoms at about 2.35 Å, and an additional Se-Se shell at 3.69 Å; the coordination number of this latter shell was much smaller than expected, as has been observed before for amorphous as well as for crystalline red Se (Scheinost & Charlet 2008; Scheinost *et al.* 2008). The EXAFS fit values also show small variations between the different samples. For strain *Mc. capsulatus*, as well as for *Ms. trichosporium*, the Debye-Waller factors (σ^2) of both bacteria decrease with reaction time, suggesting an increase of structural order with time, (see Table 3-2) synchronous with the particle growth observed by TEM (see “TEM and HAADF-STEM imaging of cell associated selenium” section).

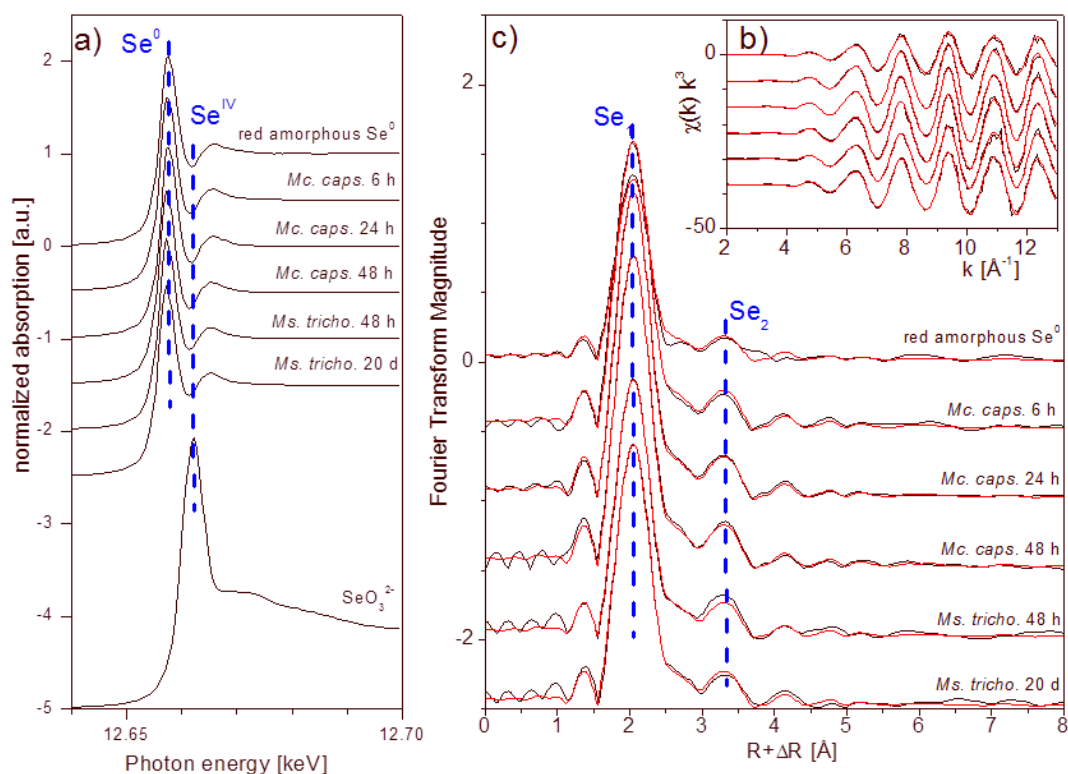


Figure 3-16 K-edge X-ray absorption spectra of cultures of *Mc. capsulatus* and *Ms. trichosporium* and selected references. a) X-ray absorption near-edge structure (XANES) spectra, b) Extended x-ray absorption fine structure (EXAFS) spectra and c) the corresponding Fourier transform magnitude. Experimental data are shown as black traces, the red traces in b) and c) are reconstructions of the experimental data by one principal component. Cells were freeze dried before analysis.

Table 3-2 Se-K edge EXAFS data of Se(IV)-reacted methanotrophs.

Sample	CN	R / \AA	$\sigma^2 / \text{\AA}^2$	CN	R / \AA	$\sigma^2 / \text{\AA}^2$	ΔE_0 (eV)	Xres.
<i>Mc. capsulatus</i> 6 h	2.2 Se	2.35	0.0030	1.0 Se	3.68	0.0063	10.5	4.2
<i>Mc. capsulatus</i> 24 h	2.1 Se	2.35	0.0024	0.9 Se	3.69	0.0047	11.1	2.8
<i>Mc. capsulatus</i> 48 h	2.0 Se	2.35	0.0022	0.6 Se	3.69	0.0010	10.8	4.1
<i>Ms. trichosporium</i> OB3b 48 h	1.9 Se	2.35	0.0027	0.8 Se	3.69	0.0034	11.0	2.5
<i>Ms. trichosporium</i> OB3b 480 h	2.1 Se	2.35	0.0032	0.6 Se	3.70	0.0027	11.5	3.8

3.7 Confirmation of the site of selenite reduction and role of methane

In order to confirm the site of selenite reduction and to test the hypothesis that methane gas acts as the source of electrons for the bio-reduction of the selenium oxyanions, control experiments were performed with both strains from which methane was omitted, and no red colour was formed in the presence of selenite indicating that the presence of the carbon and energy source methane is needed for reduction of the selenite (see Figure 3-10). In order to determine the cellular location of the selenite-reducing activity, experiments were performed with cell fractions: cell wall, cell membrane and cytoplasm fractions were separately amended with selenite and monitored visually (see Figure 3-17). The results showed that the red colour of elemental selenium was detected in the cell wall fraction, and a weak red tinge in the cell membrane fraction probably due to the traces of reductase enzyme(s) contamination, which may have diffused from the cell wall to the cell membrane (Dhanjal & Cameotra 2010). By contrast, no reduction activity was observed in the cytoplasmic fraction for both strains, suggesting that this fraction possess no selenite-reducing ability.

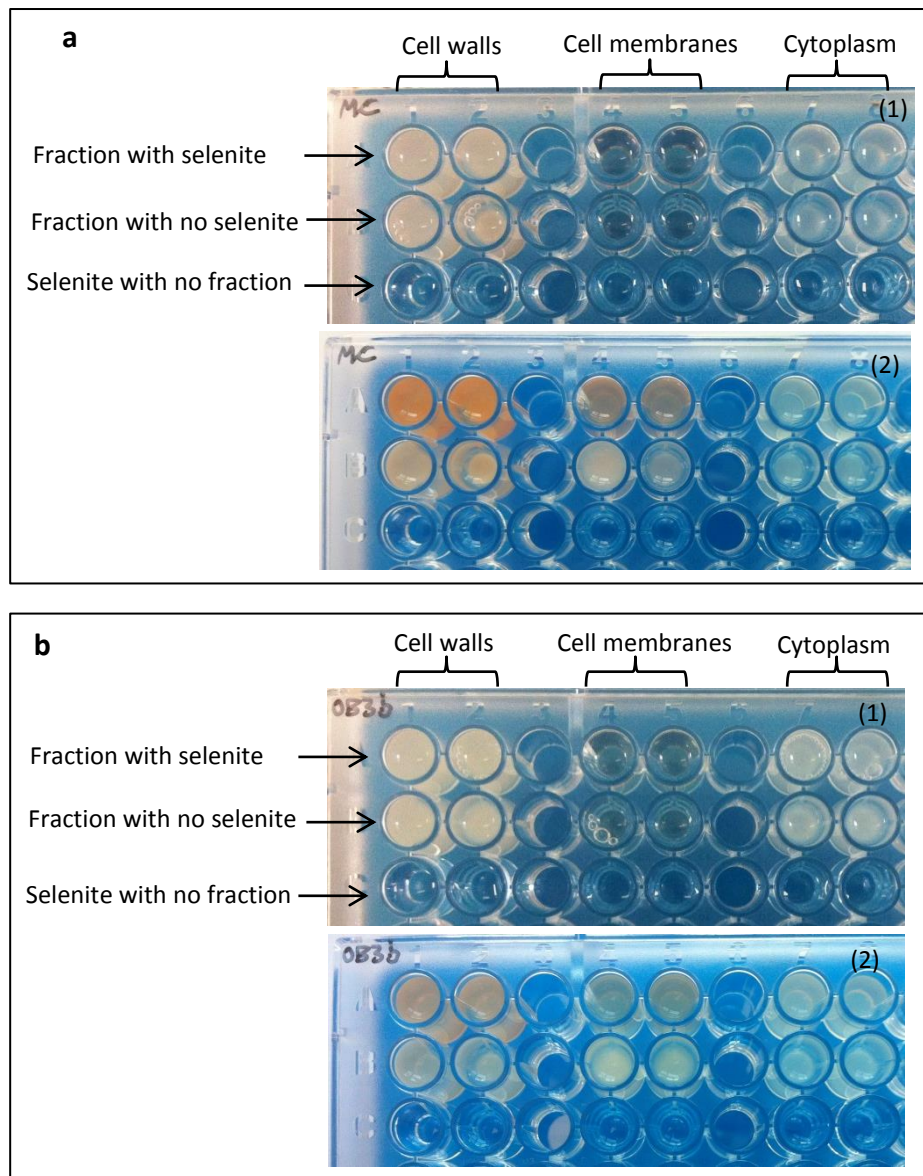


Figure 3-17 Results of experiments showing selenite reduction after an initial addition of 100 mg L^{-1} of the oxyanion incubated in the reaction mixture without methane in the presence of different cell fractions: cell walls, cell membrane and cytoplasm of *Mc. capsulatus* (Bath) (a) and *Ms trichosporium* OB3b (b) immediately after the addition of the oxyanion (1) and after 72 hours (2), respectively. The Images are representatives of more than 8 replicates of the experiments.

The results of the experiments with the cell fractions show that the reduction occurs on the cell wall fraction of both bacteria, which is consistent with the likely extracellular location of the selenium particles that are formed. Reduction of selenite

by the cell wall fractions occurred in the absence of methane. Also, since the sMMO-deleted mutant of *Ms. trichosporium* OB3b (SMDM) formed nanoparticles indistinguishable from the wildtype strain, it appears that the components of the sMMO enzyme system (including its NAD(P)H-dependent reductase) are not essential for the reduction of selenite. Since the cell wall fraction of the cells is capable of reducing selenite in the absence of added reducing agents, although the cultures as a whole require methane to perform the reaction, it seems that methane (activated either by sMMO or the particulate methane monooxygenase system) is likely the ultimate source of reducing agents, though other mediator(s) are involved in transferring the electrons to selenite (Smith & Murrell 2011). However, boiling the wall fraction and membrane fraction samples resulted in a complete loss of reduction activity (Figure 3-18), indicating that the reduction process was an enzymatic reaction and mediated by cell wall-associated proteins.

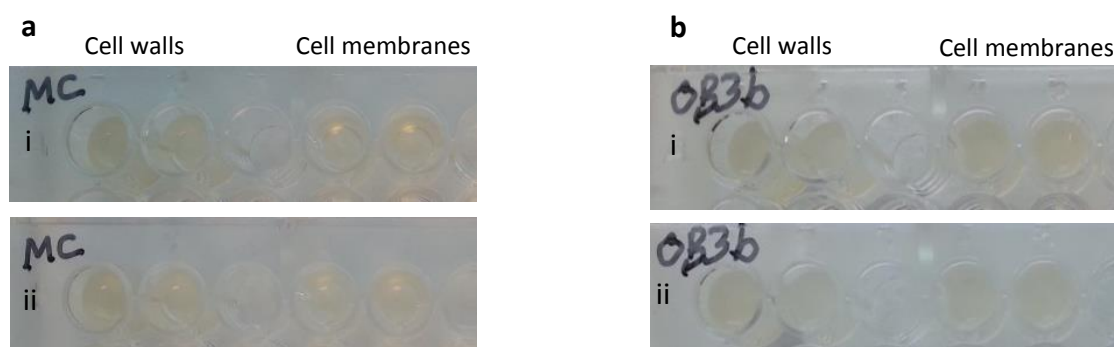


Figure 3-18 Results of experiments showing loss of selenite reduction after an initial addition of 100 mg L^{-1} of the oxyanion incubated in the reaction mixture without methane in the presence of boiled cell wall and cell membrane fractions of *Mc. capsulatus* (Bath) (a) and *Ms. trichosporium* OB3b (b) immediately after the addition of the oxyanion and after 72 hours, respectively. The images are representatives of 3 replicates of the experiments.

3.8 Search for enzymes with possible selenite reductase activity in *Mc. capsulatus* (Bath) and *Ms. trichosporium* OB3b contains genome

To identify enzymes that could be involved in reduction of selenite by *Mc. capsulatus* (Bath) and *Ms. trichosporium* OB3b, the database of translated open reading frames from the complete genome sequence (i.e., all the known and potential proteins of the organism) was searched using BLAST (<http://www.ncbi.nlm.nih.gov/BLAST/>) in order to find homologues of known classes of selenite reductases from other bacteria. Selenite reductases from other bacteria were used as queries to screen potential homologues in the methanotrophs studied.

Initially old-yellow-enzyme NADH:flavin oxidoreductase from *Sinorhizobium medicae* (Hunter 2014b; accession no. YP_001326930), which was reported to act as aerobic selenite reductase was used as query to screen potential homologues in *Mc. capsulatus* (Bath) and *Ms. trichosporium* OB3b. The results of the protein-protein BLAST search indicated that the enzyme is similar to a single protein from each of the two methanotrophs studied (accession no. WP_010959983, $E = 2 \times 10^{-130}$ and accession no. WP_003609730, 6×10^{-30} for *Mc. capsulatus* and *Ms. trichosporium* OB3b, respectively). Glutathione reductase (GR) from *Pseudomonas seleniipraecipitans* (Hunter 2014a; accession no. YP_791214), which shows selenite-reductase-activity (reduces SeO_3^{2-} to Se^0), has a significant homologue in *Mc. capsulatus* (accession no. WP_010962191, $E = 1 \times 10^{-55}$) and *Ms. trichosporium* OB3b (accession no. WP_003611917, $E = 7 \times 10^{-156}$). The *Pseudomonas mendocina* thioredoxin reductase (Hunter & Manter 2009; accession no. YP_001187877), which also reduces selenite, has two significant homologues in *Mc. capsulatus* (accession no. WP_010960952, $E =$

0.0 and WP_010960098, $E = 2 \times 10^{-3}$), and one significant homologue in *Ms. trichosporium* OB3b (accession no. WP_003609996, $E = 4 \times 10^{-126}$)

The fumarate reductase of *Shewanella oneidensis* MR-1, (accession no. WP_011070758, Li Bao 2014), a flavoprotein capable of mediating selenite reduction and sulfite reductase of *Clostridium pasteurianum* (Harrison *et al.* 1984; accession no. OMH22246), did not have any significant homologues in the two strains. The nitrate reductase of *Thauera selenatis* (DeMoll-Decker & Macy 1993; accession no. AAL86933), which may catalyse the reduction of selenite to elemental selenium, also did not have any significant matches in the genome of *Mc. capsulatus* or *Ms. trichosporium* OB3b.

These results identify five candidate selenite-reducing enzymes in the two methanotrophs studied and are consistent with a similar mechanism of selenite reduction in *Mc. capsulatus* (Bath) and *Ms. trichosporium* OB3b. These findings suggest that the methanotroph homologues of an enzyme may be responsible for selenite reductase.

3.9 The role of methanobactin in the reduction of selenium oxyanions

In addressing the hypothesis that methanobactin may play a role in the reduction of selenium oxyanions, experiments were performed by mixing various concentration of methanobactin (50, 100 and 200 mg L⁻¹) with Se(IV) or Se(VI) solutions (to a final concentration of 100 mg L⁻¹) in a 96-well microtitre plates. No colour change was observed as the mixtures in the wells were assessed visually during the incubation time (96 hours, at room temperature and 30°C). This finding indicates that methanobactin is not essential for the reduction of selenium oxyanions.

3.10 Conclusions

Selenite is the more toxic of the two selenium oxyanions and, as would be expected, it was more toxic to the two strains than was selenate. The minimum inhibitory concentrations (MICs) for selenite were 70 and 5 mg L⁻¹ for *Mc. capsulatus* (Bath) and *Ms. trichosporium* OB3b, respectively. Meanwhile, the MICs for selenate were 2400 and 1700 mg L⁻¹ for *Mc. capsulatus* (Bath) and *Ms. trichosporium* OB3b, respectively. Unlike selenate, bacterial growth in the presence of selenite was accompanied by the production of red Se⁰. Although the two strains tolerate high levels of selenate, cell growth was negatively affected by the increase of both selenate and selenite concentrations. When the bacterial cells are exposed to selenate or selenite, no substantial change in the bacterial cell size was observed as measured by flow cytometry (forward scatter plots). *Mc. capsulatus* (Bath) and *Ms. trichosporium* OB3b are both able to reduce the toxic selenite but not selenate to extracellular red spherical nanoparticulate elemental selenium. This could be attributed to the absence reductases that catalyse selenate reduction. The presence of elemental selenium is confirmed by X-ray absorption near-edge structure and extended X-ray absorption fine structure. Selenite reduction activity was observed mainly in the cell wall fraction. The reduction process was an enzymatic reaction and mediated by cell wall-associated proteins. Neither particulate monooxygenase (pMMO) nor soluble monooxygenase (sMMO) was essential for selenite reduction. No indication that methanobactin is involved in selenite reduction. These results provide the bases for understanding the growth characteristics of this group of bacteria in the presence of toxic selenium oxyanions. Information that is useful in the design of bioremediation strategies for the treatment of selenium-contaminated soil, sediments, and wastewater.

Chapter 4

Characterization of elemental selenium produced by methanotrophs

4.1 TEM and HAADF-STEM imaging of cell-associated selenium

Electron micrographs with corresponding EDX spectra of the cells of the two species of bacteria amended with selenite are shown in Figure 4-1. The EDX analysis of the electron dense particles shows that they contain selenium, a trace of sulfur and phosphorus in addition to copper from the grid and possibly from the medium, and osmium from the cell fixing agent. The nanoparticles were spherical and in a variety of sizes. It was found that the mean elemental selenium particle sizes formed in the *Mc. capsulatus* cultures were in the main larger than those produced by *Ms. trichosporium* OB3b. This is borne out in the difference in colour intensity of the selenite-amended cultures, and confirmation in the differences in the two peak maximum obtained in the spectra of the two solutions. The more intense reddish colour was found in the *Mc. capsulatus* solutions with the larger elemental selenium particles in contrast to the yellowish orange observed in the *Ms. trichosporium* OB3b cultures. The mean particle sizes in the *Mc. capsulatus* cultures was about 387 nm compared to 221 nm for *Ms. trichosporium* OB3b cultures after 48 and 288 hours incubation, respectively.

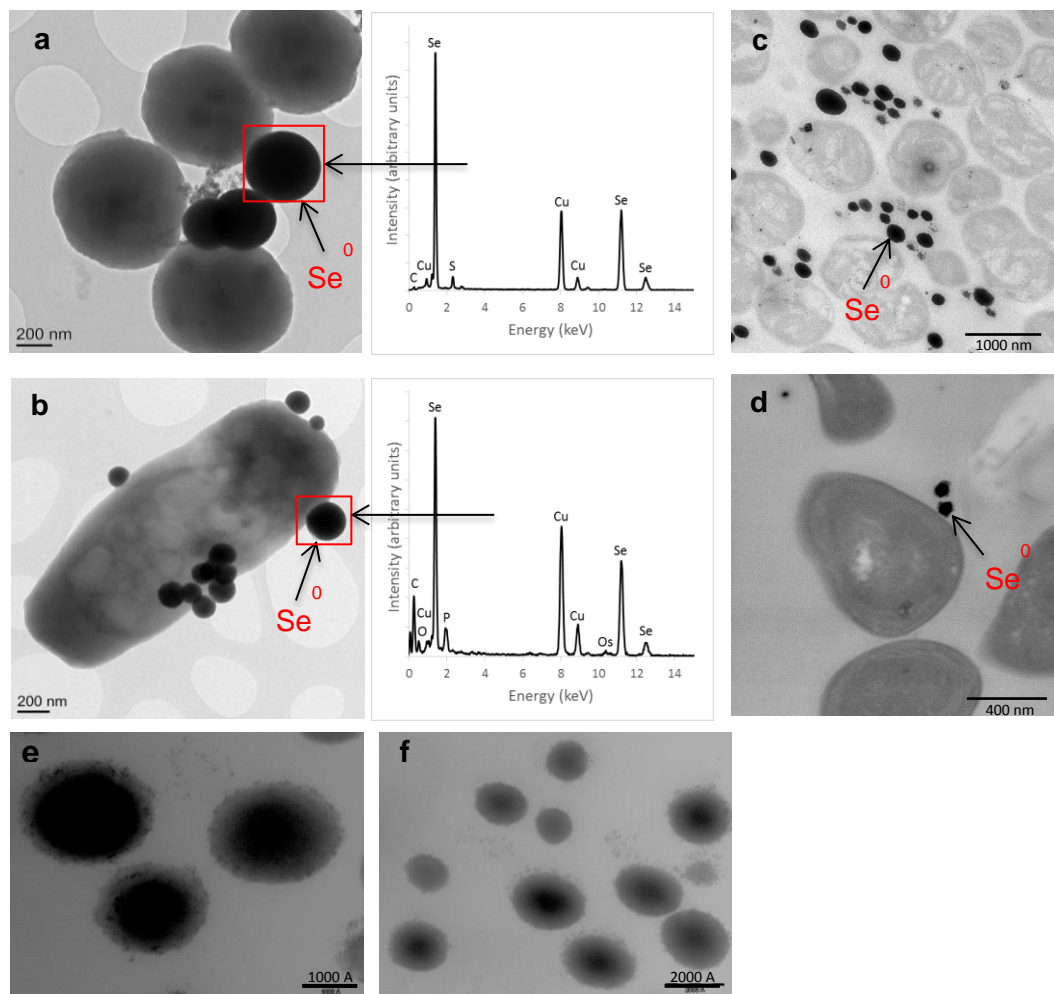


Figure 4-1 TEM of *Mc. capsulatus* (a) and *Ms. trichosporium* OB3b (b) cultures exposed to SeO_3^{2-} (20 mg L^{-1}), and EDX analysis within the electron dense regions (Se^0 nanospheres). c and d TEM thin-section micrographs of *Mc. capsulatus* (c) and *Ms. trichosporium* OB3b (d), showing the locations of the Se^0 nanospheres (extracellular). The images are representatives of more than 10 replicates of the experiments. (e) and (f) HRTEM of SeNPs of *Mc. capsulatus* and *Ms. trichosporium* OB3b, respectively, showing cloud like layer surrounding the selenium nanoparticles. Cells were fixed with 3% glutaraldehyde and 2% OsO_4 immediately before TEM. The images are representatives of 4 replicates.

The electron micrographs suggest that the elemental selenium nanoparticles are in extracellular space and attached to the surface of the cells suggesting that extracellular selenite reduction is followed by subsequent growth. The HAADF-STEM imaging with EDX maps of the two bacteria are shown in Figure 4-2. The electron micrograph image (delimited by white square) of *Mc capsulatus* (Bath) shows the bacteria and a selenium

nanoparticle. The distribution of the elements, C, O and P map to the bacteria, and that of Se and S overlap in the area corresponding to the nanoparticle. Similar image and mapping of the same elements for *Ms trichosporium* OB3b show that C, P and O map well to the bacteria, and S and Se overlap but this time the nanoparticles are distributed all over the bacteria. In addition, HRTEM-EDX images showed that the SeNPs of both *Mc capsulatus* (Bath) and *Ms trichosporium* OB3b are surrounded by a cloud like layer (Figure 4-1e and f), suggesting the presence of organic material on the BioSeNPs such as extracellular polymeric substances EPS, which has been previously reported (Jain *et al.* 2015b).

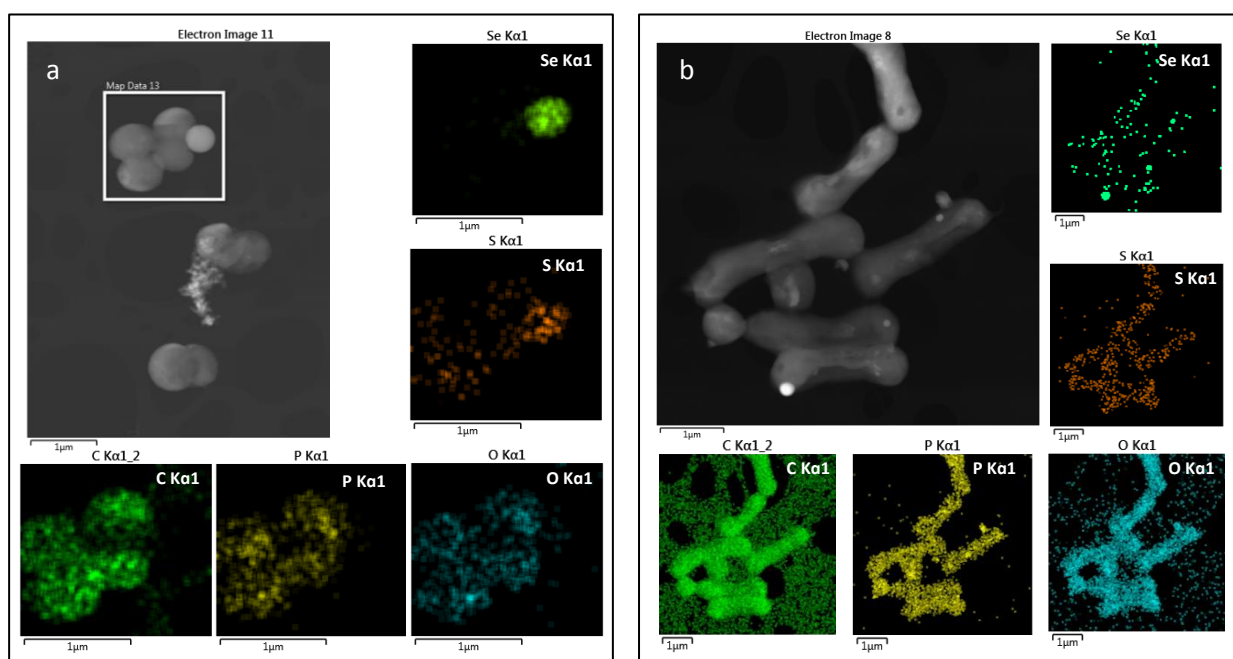
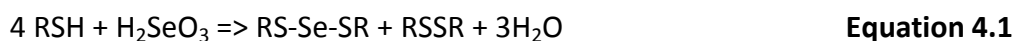


Figure 4-2 HAADF-STEM imaging of *Mc capsulatus* (a) and *Ms trichosporium* OB3b (b) showing Se nanospheres attached to the cells with EDX maps (generated from spectra collected from the indicated areas) of relevant elements. Cells were fixed with 3% glutaraldehyde and 2% OsO₄ immediately before HAADF-STEM. The images are representatives of more than 10 replicates of the experiments.

A more detailed examination of the particles with the aid of HAADF-STEM imaging and EDX mapping provided evidence that the maps of selenium and sulphur overlap, which

would suggest that both elements are present in a single structure. This is hardly surprising since the initial reactions in the previously proposed pathways for the biological reduction of selenium involve a variety of thiol group containing compounds (Painter 1941), which react as shown in Equation 4.1,



Thiol groups react with selenite producing disulfide (RSSR) and an unstable intermediate, selenotrisulfides (RS-Se-SR), which subsequently may decompose to elemental selenium.

The close Se and S mapping the EDX images of the cultures would indicate that the pathways involving the reaction of the intermediate RS-Se-SR is likely to result in the co-precipitation of both elements. Of relevance is the observation that both sulfur and selenium are co-precipitated in the presence of sulfate-reducing bacteria (Zannoni *et al.* 2007). This is further evidence to indicate that there may be reactions common to the biological transformation of both elements. Abiotic and biotic reactions could together account for the co-precipitation of both elements. One example of a possible abiotic reduction reaction involving both selenium and sulfur is given in Equation 4.2,



The reaction as given in this equation predicts a 1:2 ratio in the formation of elemental Se and S. Proposed by Hockin and Gadd (2003).

4.2 Time course experiments for the formation of elemental selenium nanoparticles

Time course experiments to show the formation of elemental selenium nanoparticles in each selenite-amended culture were performed in order to establish whether the

particle sizes changed with incubation time. As shown in Figure 4-3, the longer the incubation time for either bacterium, resulted in an increase in the mean selenium nanoparticle sizes, obtained by measuring one hundred and forty particles at random at the selected time. Histograms of the distribution of 170 nanoparticles obtained using the two strains of bacteria are shown in Figure 4-4. The nanoparticles sizes were measured from the TEM data using the freely available ImageJ programme (version 1.48v). TEM images taken at three different times show the growth of the particles (Figure 4-5). The results of the time course experiments (Figure 4-3) provide evidence that the initial particles act as nuclei for further growth. In addition, it is indicative that both of these bacteria can be used to produce nanoparticles of a variety of sizes provided there is timely intervention to stop further nanoparticle growth.

Indeed, in the scheme proposed by Jain *et al* (2015b) the synthesis of biogenic elemental selenium (BioSeNPs) by an anaerobic granular sludge and wastewater occurs in two steps: initial reduction of selenite to elemental selenium particles either intracellularly or extracellularly followed by growth of the nanoparticles. Intracellularly produced elemental selenium nanoparticles are first coated with protein before they are expelled into extracellular space. Irrespective of the origin of the elemental selenium particles, they are invariably capped and stabilized with extracellular polymeric substances (EPS) (Jain *et al.* 2015b).

It can be seen from these experiments that for the production of nanoparticles of sizes less than 100 nm, the slower reacting *Ms. trichosporium* OB3b is to be preferred over the faster *Mc. capsulatus*. Further examination of the particles produced by both bacteria for diffraction patterns did not show evidence of any crystalline structure.

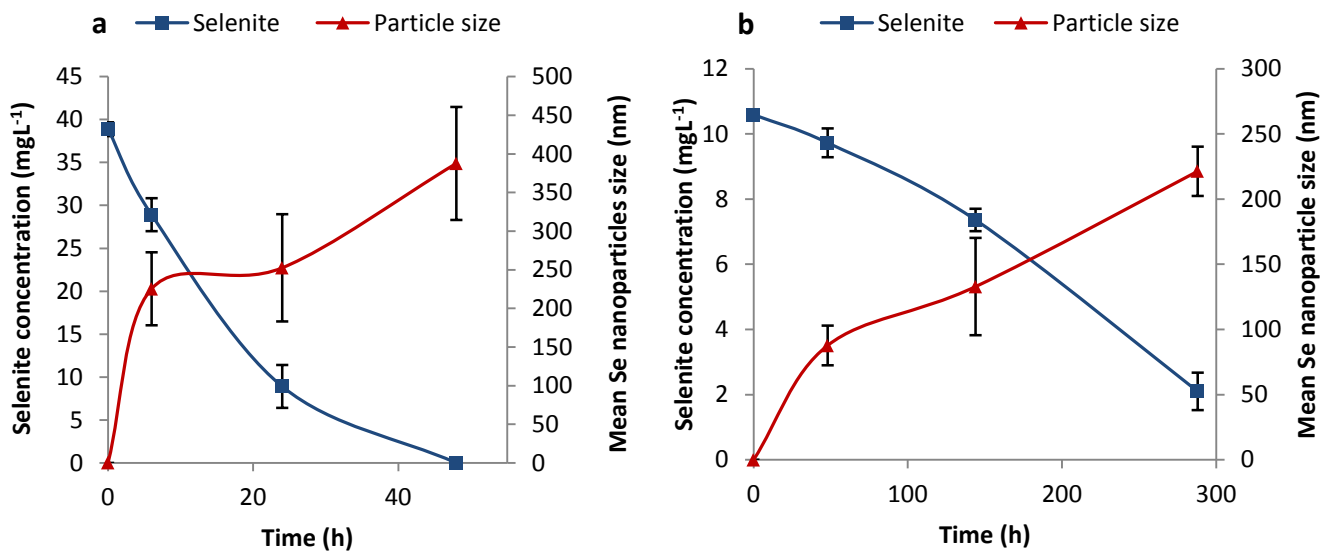


Figure 4-3 Time course of Se nanospheres growth and SeO₃²⁻ reduction by *Mc. capsulatus* (a) and *Ms. trichosporium* OB3b (b). The mean selenium nanoparticle size ± 1 standard deviation (n=140) was measured by TEM.

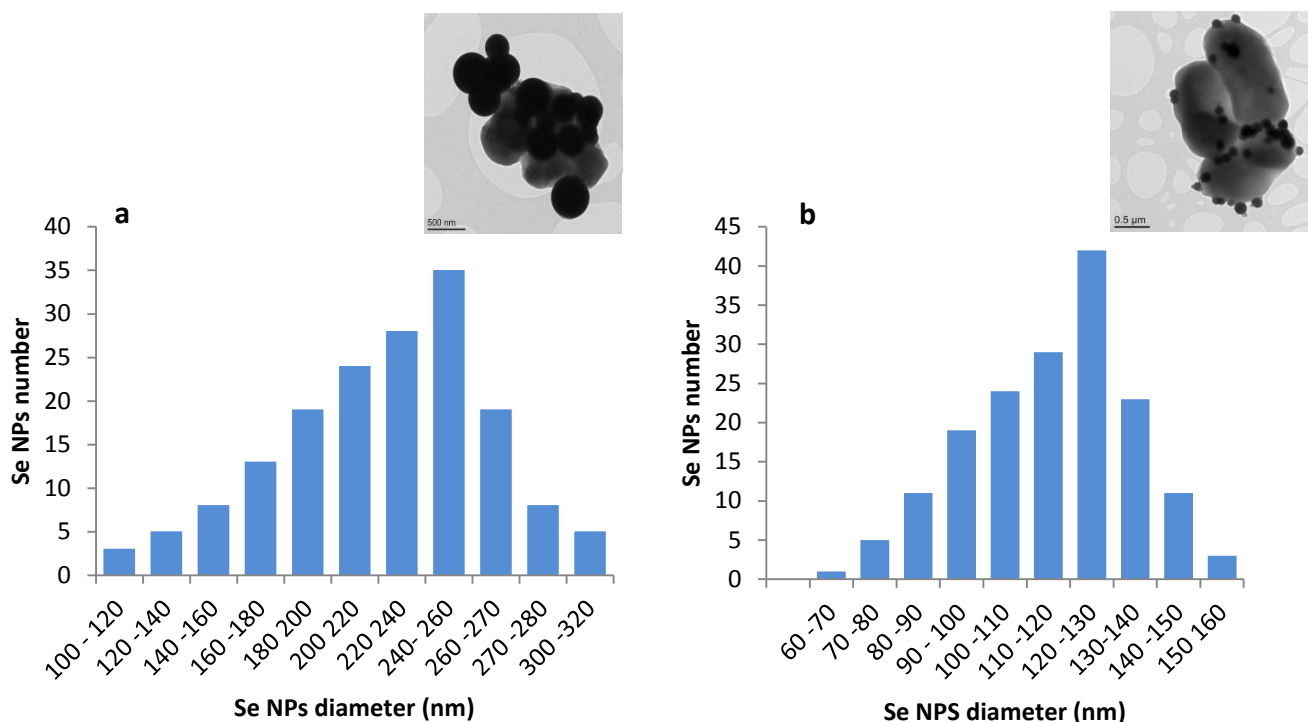


Figure 4-4 The frequency distribution histogram of the selenium nanoparticles produced from the TEM images after the formation in the cultures containing the methanotrophs *Mc. capsulatus* (Bath) (a) and *Ms. trichosporium* OB3b (b), at incubation times of 24 h and 144 h, respectively. Histograms are representatives of 170 nanoparticles for each strain.

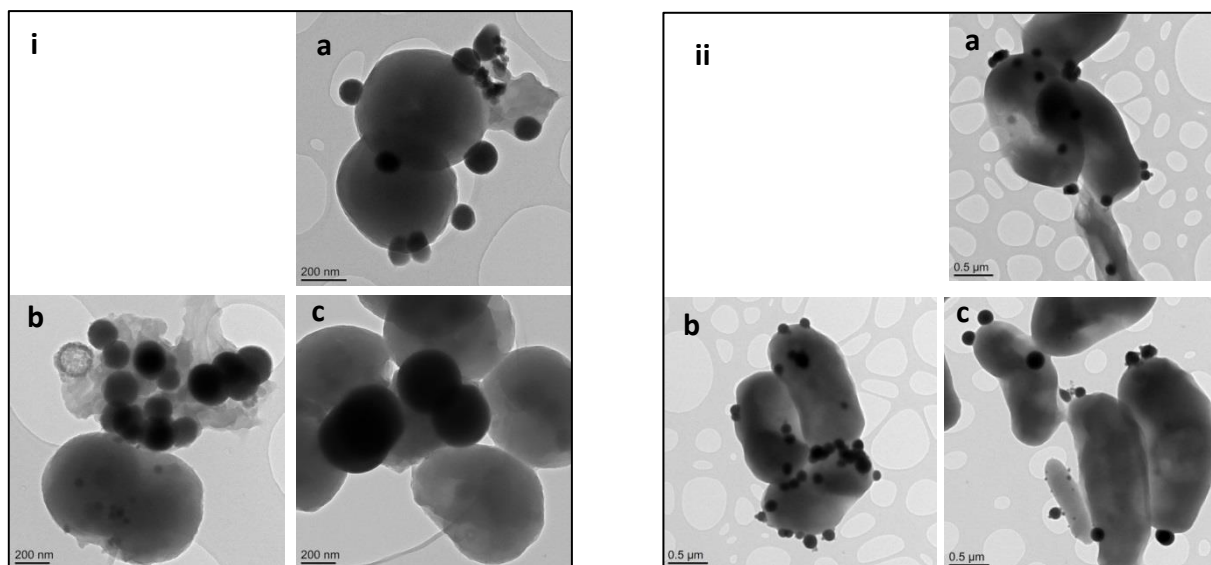


Figure 4-5 TEM micrographs of the cells and selenium nanoparticles at different incubation times 6, 24 and 48 h in the cultures containing *Mc. capsulatus* (Bath)(i), and at incubation times of 48, 144 and 288 h in the cultures containing *Ms. trichosporium* OB3b(ii), respectively. The images are representatives of more than 10 replicates of the experiments.

4.3 Extraction and purification of SeNPs

The BioSeNPs were collected by lysing the cells using lysozyme and French press, cleaned by successive washes with 1.5M Tris-HCl buffer (pH 8.3) containing 1% SDS and finally separated from insoluble debris by two-phase water-octanol extraction (Figure 4-6a). Purified SeNPs (Figure 4-6b) were kept for further characterization by SDS-PAGE; transmission electron microscope (TEM)-energy dispersive X-ray (EDX); high-angle annular dark-field imaging (HAADF)-STEM; X-ray photoelectron spectroscopy (XPS); Raman analysis and zeta potential.

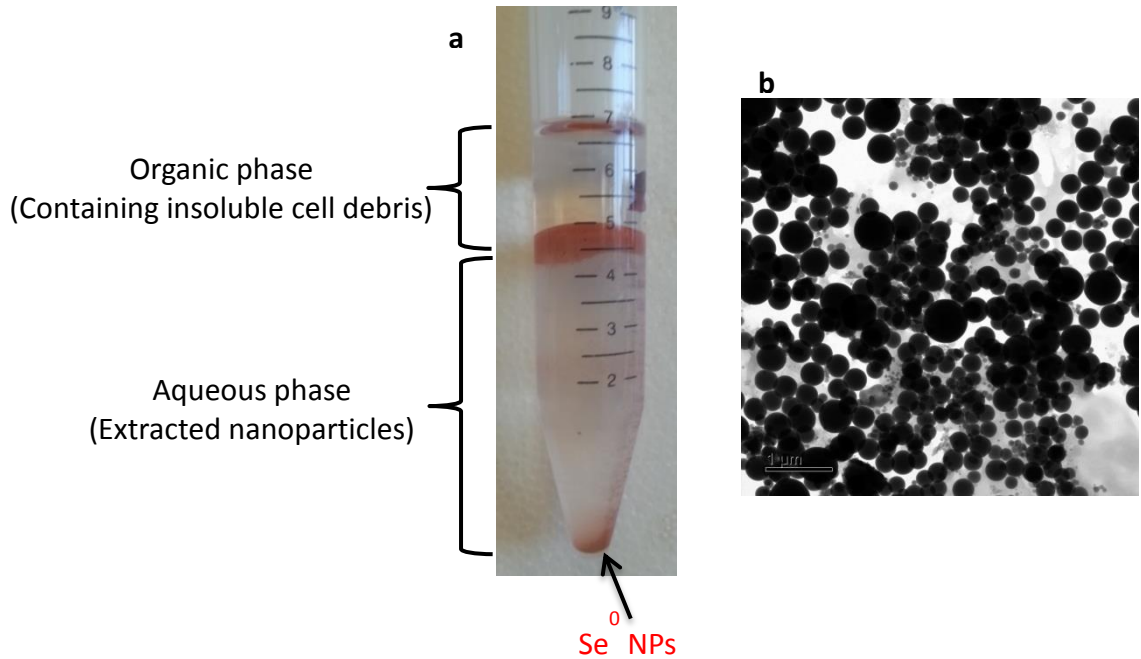


Figure 4-6 Extraction of purified SeNPs by a two-phase water-octanol extraction system (a). TEM image of the purified SeNPs produced by methanotrophs (b). The images are representatives of more than 5 replicates of the experiments.

4.4 SDS-PAGE analyses of selenium nanoparticles

Biogenic selenium nanoparticles (BioSeNPs) are known to be associated with protein (Lenz *et al.* 2011; Dobias *et al.* 2011; Jain *et al.* 2015b; Tugarova & Kamnev 2017). In addressing this hypothesis, SDS-PAGE analyses was performed for SeNPs produced by both *Mc. capsulatus* (Bath) and *M. trichosporium* OB3b. As shown in Figure 4-7, SDS-PAGE results showed that the particles were associated with proteins in support of our hypothesis. Silver staining revealed a number of protein bands for SeNPs produced by the two strains. Protein bands were found to be most abundant at apparent molecular masses of around 18 kDa (shown in the red boxes).

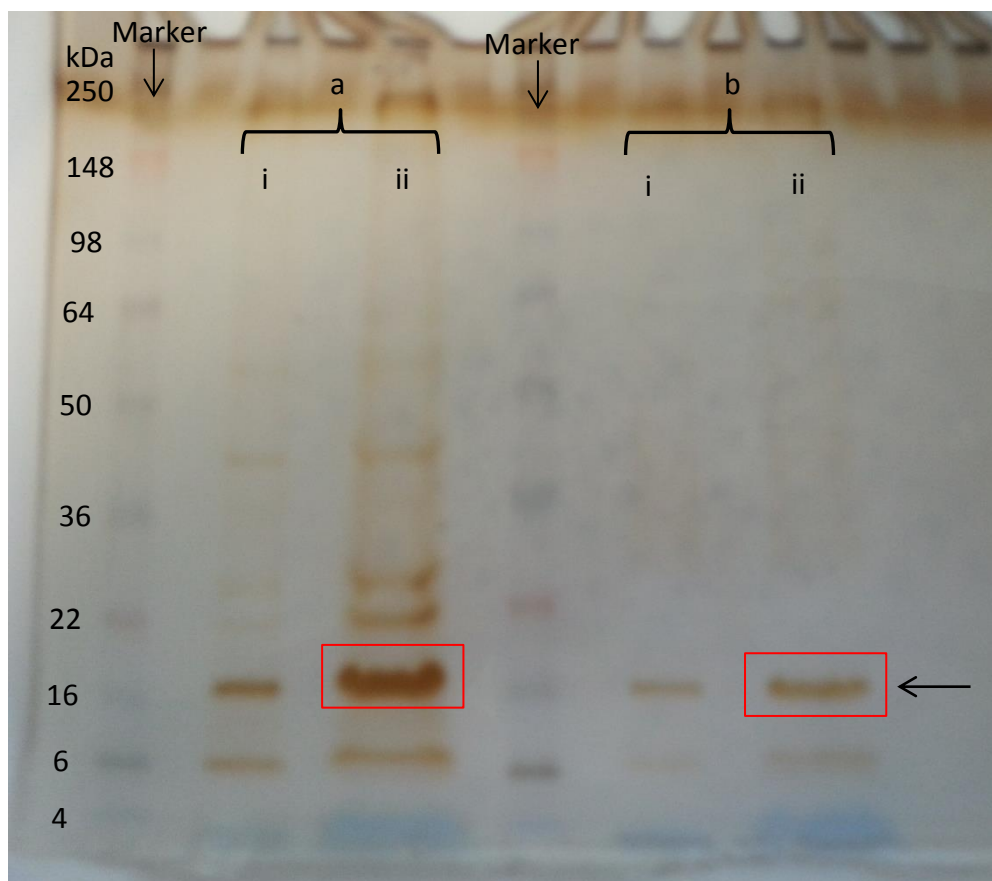


Figure 4-7 SDS-PAGE gel images of SeNPs of proteins associated with biogenic selenium nanoparticles produced by *Mc. capsulatus* (Bath) (a) and *Ms. trichosporium* OB3b (b) with loading volumes of 5 (lane i) and 15 (lane ii) μ l. Protein bands of \sim 18 kDa (indicated by red rectangle boxes) represent key proteins. The image is representative of more than 5 replicates of experiments.

4.5 X-ray photoelectron spectroscopy analysis

X-ray photoelectron spectroscopy (XPS) is an analysis technique used to obtain chemical information about the surfaces of a wide range of materials. Both composition and the chemical state of surface elements can be measured by XPS. The XPS measurements were performed to further investigate the composition and functional groups on the surface of the BioSeNPs. Regarding the SeNPs produced by *Mc. capsulatus* (Bath), the wide scan XPS spectra are shown in Figure 4-8a while high

resolution spectra for Se 3d, C 1s, O 1s and N 1s are shown in Figure 4-8b, c, d and e, respectively. The data processing and deconvolution of photoelectron peaks were obtained using a commercial software package (Casa XPS v2.3.16PR1, Casa Software Ltd., UK). Elemental selenium is generally observed between 54.9 and 56.3 eV, whereas selenite is generally found at 58.2 eV (Naveau, 2007). In our case, the deconvolution of high-resolution Se 3d spectra, which exists in a weak doublet showed two prominent peaks of Se 3d_{5/2} at binding energy of 55.9 and 55.1 eV, respectively. The two peaks correspond to elemental selenium, no oxidized selenium species was detected on the SeNPs. This finding is consistent with the results found in the EXAFS and XANES measurements, which indicated that there were no discernible traces of Se(IV) on the SeNPs.

Figure 4-8c shows strong emission due to C 1s. Several species of C 1s from different functional groups constitute this strong emission. The XPS peak for C 1s at binding energy of 285.0 eV can be assigned to C-C or C-H in lipids or amino acid side chains (Song *et al.* 2014). The XPS peak at binding energy of 286.34 eV is attributed to C-O or C-N from alcohol, ether amine, or amide (Yuan *et al.* 2010). While the peak at 288.19 eV assigned to C=O or O-C-C in carbonyl, amide or hemiacetal (Sun *et al.* 2009). The O 1s spectra were deconvoluted into two component peaks. The O 1s peak at 532.91 eV is attributed to the alcohols, hemiacetal, or acetal groups (Yuan *et al.* 2010). The second O 1s peak at 531.37 eV is mainly attributed to the O double bonded to C (O=C), as in carboxylate, carbonyl, ester, or amide. N 1s produces a peak at 400.1 eV due to associated amine groups, which is commonly found in amino acids and aminosugars (Kaur *et al.* 2009).

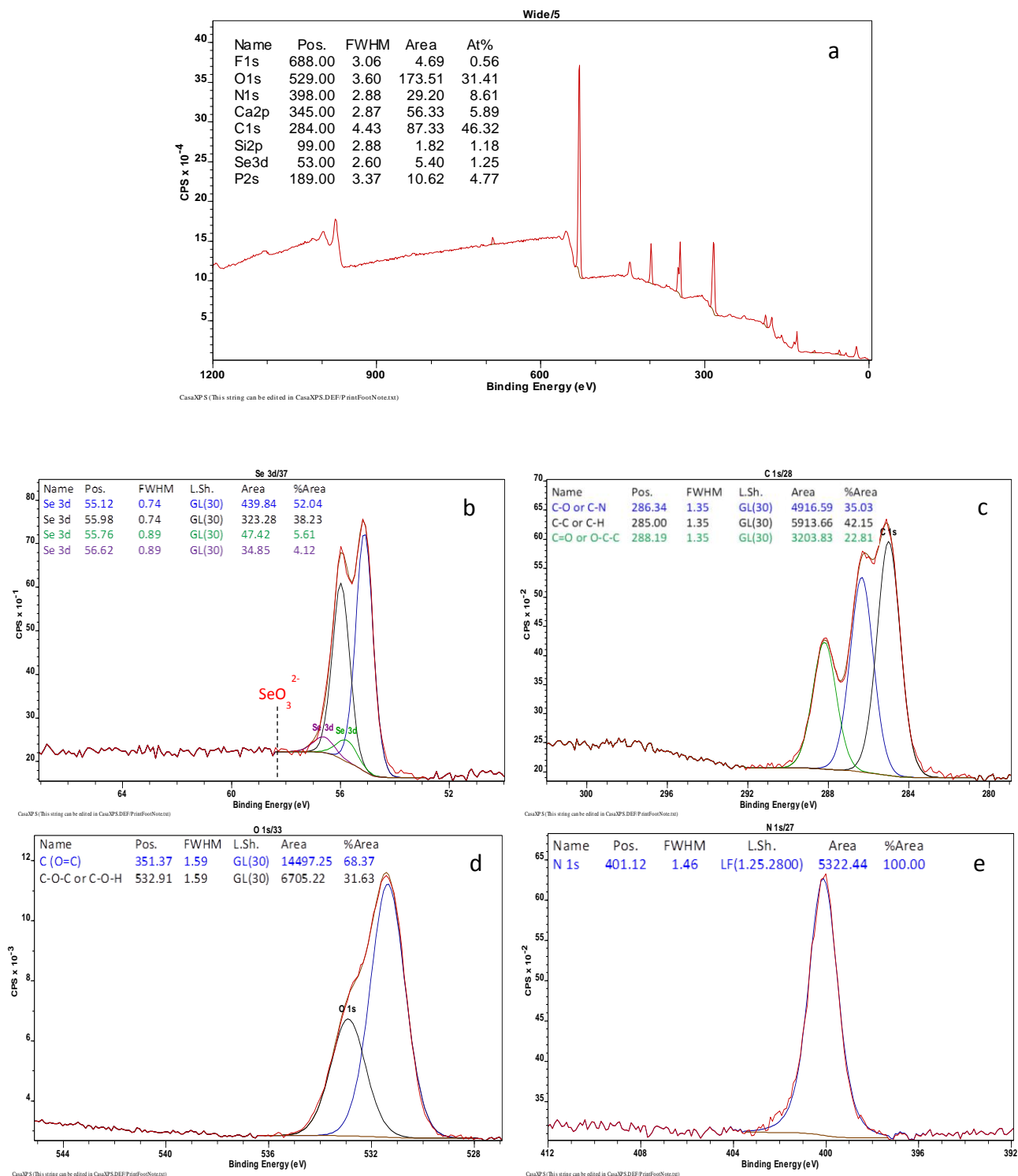


Figure 4-8 Wide scan X-ray photoelectron spectra of the SeNPs produced by *Mc. capsulatus* (a) and high resolution spectra for Se 3d, C 1s, O 1s and N 1s are shown in b, c, d and e, respectively. The spectra are representatives of 2 runs of the experiments.

The XPS peak for S was not observed in the wide scan spectra or on the high resolution S 2p and S 2s spectra of SeNPs produced by *Mc. capsulatus* (Bath) although S was clearly observed in the HAADF-STEM measurements. Both the S 2p and S 2s transition are overlapped by selenium peaks, by the Se 3p and Se 3s peaks, respectively. The relative peak intensities for all these features seen in the spectra collected and shown here can be compared to what would be expected for selenium and for sulphur samples. For example, for sulphur the S 2s and S 2p peaks are of similar heights, but the Se 3p peaks is nearly three times as intense as the Se 3s peak. Based on this comparison, the wide scans have all been fitted on the assumption that there is no sulphur present, only selenium, as this seemed most likely given the relative intensities of the peaks at these positions in the spectra associated with these samples. However, this is an assumption; there may be some sulphur present.

Similarly, the SeNPs of *Ms. trichosporium* OB3b, the wide scan XPS spectra are shown in Figure 4-9a, while high resolution spectra for Se 3d, C 1s, O 1s and N 1s are shown in Figure 4-9b, c, d and e, respectively. The deconvolution of the Se 3d peak gives two prominent peaks of Se 3d at binding energy of 56.02 and 55.16 eV that refer to the elemental selenium. The C 1s signal was characterized by three components, localized at binding energy 285.0 eV, 286.41 eV and 288.12 eV and assigned to C–C/C–H (in lipids or amino acid side chains), C–O/C–N (from alcohol, ether amine, or amide) and –COO groups (in carbonyl, amide or hemiacetal), respectively. The O 1s peak is decomposed into two peaks. The peak at 532.84 eV is attributed to the alcohols, hemiacetal, or acetal groups, and the other peak at 531.58 eV is attributed to C (O=C), as in carboxylate, carbonyl, ester, or amide (Yuan *et al.* 2010). N 1s peak at binding energy of 400.1 eV was assigned to the amine group. Although the peak for S was not

observed in the XPS spectra due to the overlap of Se on the S peaks in the spectra, the element seems to be absent since the element was not observed in the HAADF-STEM measurements.

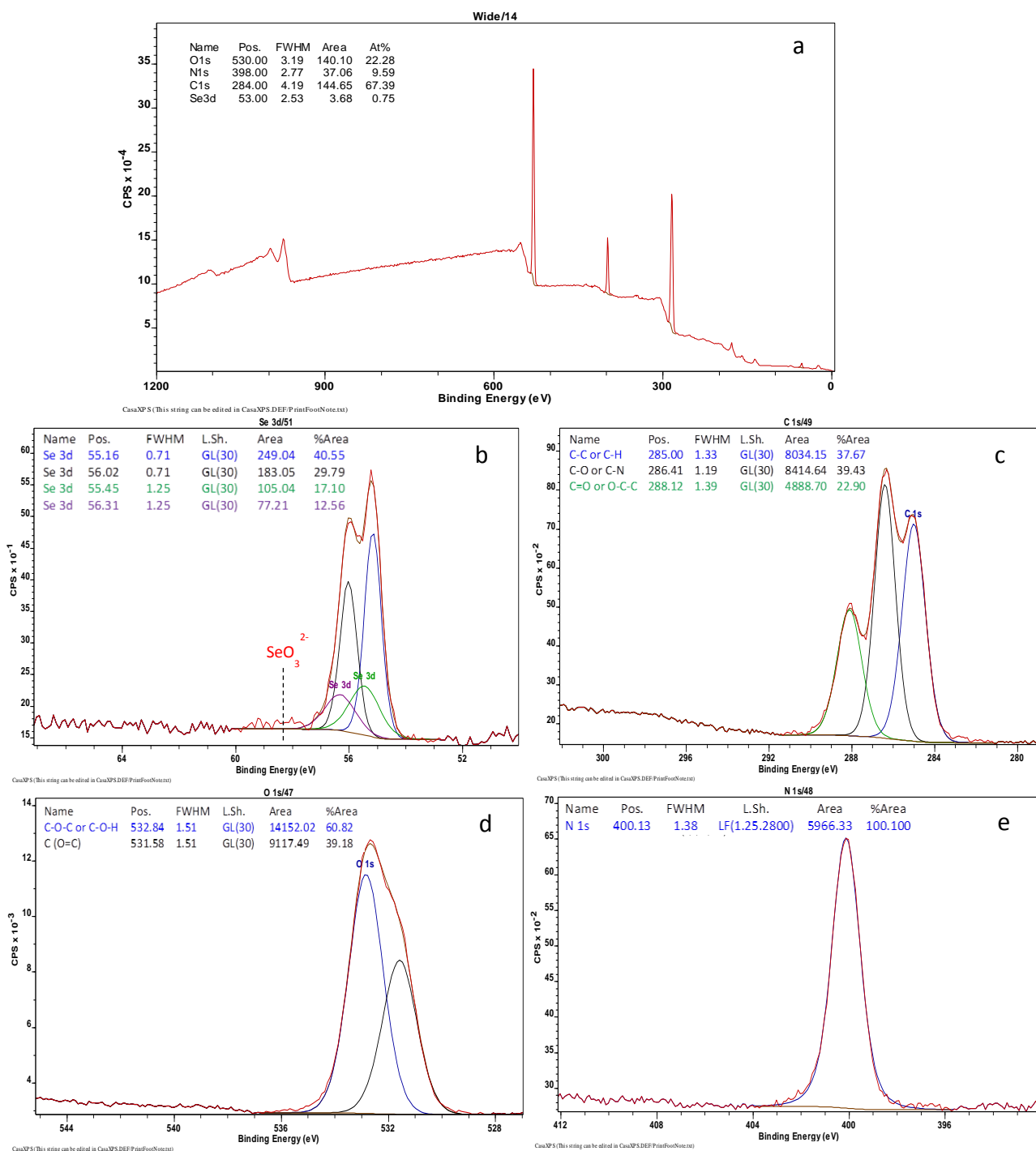


Figure 4-9 Wide scan x-ray photoelectron spectra of the SeNPs produced by *Ms. trichosporium* OB3b (a) and high resolution spectra for Se 3d, C 1s, O 1s and N 1s are shown in b, c, d and e, respectively. The spectra are representatives of 2 runs of the experiments.

In general, the BioSeNPs of both *Mc. capsulatus* and *Ms. trichosporium* OB3b are mainly composed of Se C, O, N and/or S (see Tables 4-2 to 4-5), indicating that Se nanoparticles are coated with organic materials probably proteins and extracellular polymeric substances (EPS). The latter material has been shown to be present as the capping compounds in the bioproduction of selenium nanoparticles (Jain *et al.* 2015b). This is in good agreement with SDS-PAGE analyses of the SeNPs, which showed that the particles were associated with proteins. This would suggest that proteins are responsible for both the formation and the stabilization of Bio-SeNPs as described previously (Debieux *et al.* 2011; Zhang *et al.* 2011; Ramya *et al.* 2015; Kora & Rastogi 2016; Lampis *et al.* 2017; Kamnev *et al.* 2017).

Table 4-1 Results of curve-fitting Se 3d spectra

Sample	Se3d5/2		Se3d3/2		Se3d5/2		Se3d3/2	
	B.E.(eV)	%Area	B.E.(eV)	%Area	B.E.(eV)	%Area	B.E.(eV)	%Area
SeNPs of <i>Mc. capsulatus</i>	55.1	52.0	55.8	5.6	56.0	38.2	56.6	4.1
SeNPs of <i>Ms. trichosporium</i> OB3b	55.2	40.6	55.5	17.1	56.0	29.8	56.3	12.6

Table 4-2 Results of curve-fitting C 1s spectra

Sample	B.E. (eV)	%Area	B.E. (eV)	%Area	B.E. (eV)	%Area
SeNPs of <i>Mc. capsulatus</i>	285.0	42.2	286.3	35.0	288.2	22.8
SeNPs of <i>Ms. trichosporium</i> OB3b	285.0	37.7	286.4	39.4	288.1	22.9

Table 4-3 Results of curve-fitting O1s spectra

Sample	B.E. (eV)	%Area	B.E. (eV)	%Area
SeNPs of <i>Mc. capsulatus</i>	531.4	68.4	532.9	31.6
SeNPs of <i>Ms. trichosporium</i> OB3b	531.6	39.2	532.8	60.8

Table 4-4 Results of curve-fitting N 1s spectra

Sample	B.E. (eV)	%Area
SeNPs of <i>Mc. capsulatus</i>	400.1	100.0
SeNPs of <i>Ms. trichosporium</i> OB3b	400.1	100.0

4.6 Fourier transform infrared (FTIR) analysis

FTIR spectroscopy is a well-established highly informative analytical technique which has been successfully used in microbiology (Beekes *et al.* 2007; Kamnev 2008; Ojeda *et al.* 2008; Alvarez-Ordóñez *et al.* 2011; Ojeda & Dittrich 2012; Saulou *et al.* 2013; Skotti *et al.* 2014; Ferreira *et al.* 2016; Tugarova *et al.* 2017; Kamnev *et al.* 2017). FTIR spectroscopy can provide useful semiquantitative information on the presence of bioorganic components of nanoparticles' capping layers and their relative contents featured by vibration modes of their typical functional groups. Particularly for proteins of the SeNPs 'capping layer', their secondary structure can differ from that of natural cellular proteins, as featured by the positions of various spectral components of the amide I band (typically within the region 1620–1680 cm^{-1}) (Kora & Rastogi 2016; Kamnev *et al.* 2017).

In this study, the nature of the organic components of microbially produced SeNPs was further analyzed by FTIR spectroscopy. The FTIR spectra of the SeNPs produced by both *Mc. capsulatus* and *Ms. trichosporium* OB3b, samples of biomass of the two strains (controls), as well as the Chem-SeNPs were recorded in order to identify the functional groups capping the synthesized SeNPs. The FTIR spectra (registered in transmission mode) are shown in Figure 4-10. Wavenumbers of the maxima for the main bands in the FTIR spectra are summarised in Table 4-5. together with their tentative assignment (Naumann *et al.* 1995; Beekes *et al.* 2007; Burattini *et al.* 2008; Kamnev 2008; Alvarez-Ordóñez *et al.* 2011; Ojeda & Dittrich 2012; Kamnev *et al.* 2017).

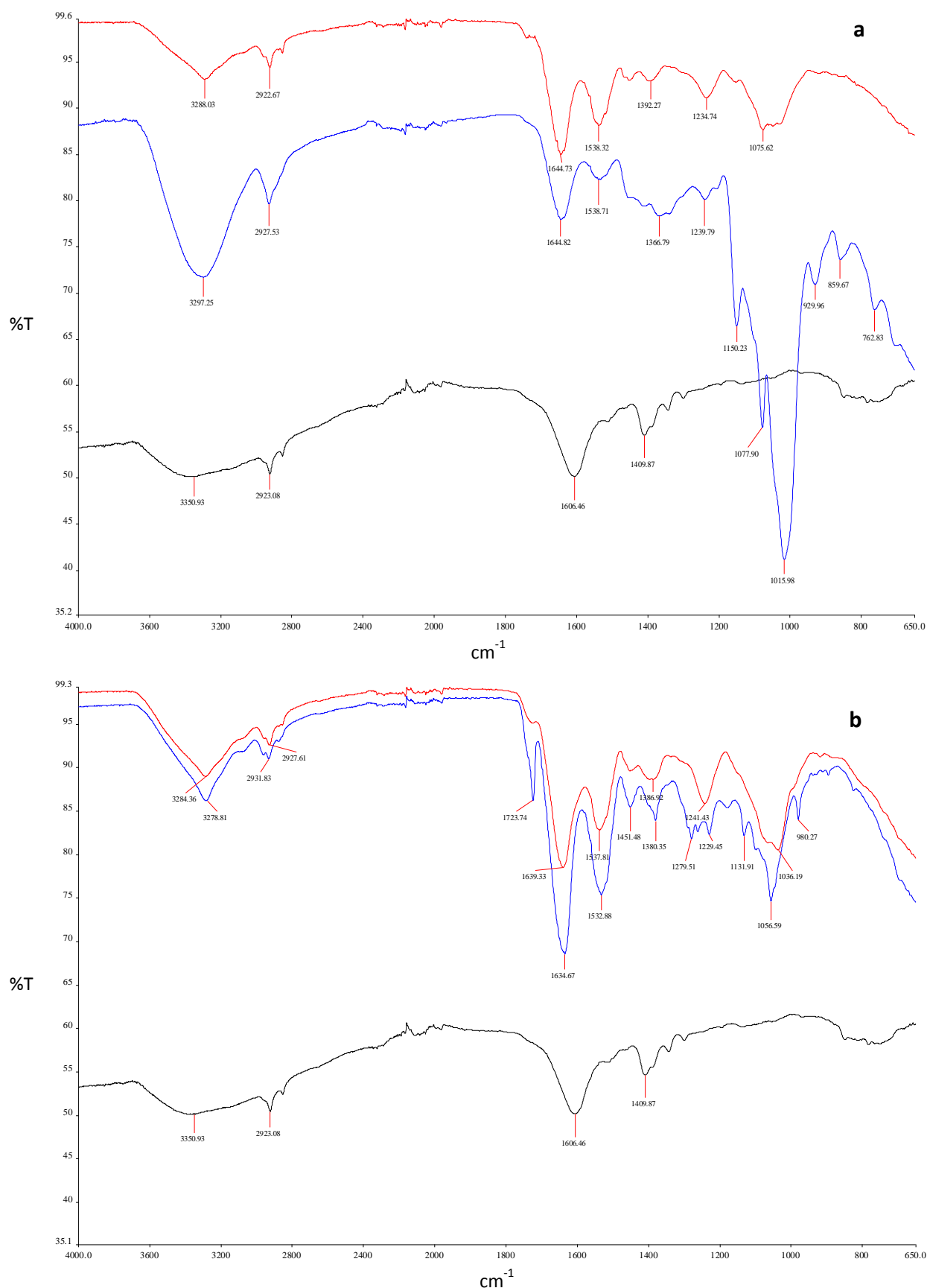


Figure 4-10 The FTIR spectra of freeze dried Bio-SeNPs (blue lines) and bacterial biomass (red lines) of *Mc. capsulatus* (a) and *Ms. trichosporium* OB3b (b) harvested at $\text{OD}_{600} \sim 0.7$, separated by centrifugation, washed with phosphate buffered saline pH 7.2 and freeze dried; as well as Chem-SeNPs (black lines) obtained through reaction of Na_2SeO_3 with L-cysteine. The spectra are representatives of more than 5 runs of the experiments.

Table 4-5 Tentative assignments of main bands to the relevant functional groups (wavenumber, cm^{-1}) (Naumann *et al.* 1995; Beekes *et al.* 2007; Burattini *et al.* 2008; Kamnev 2008; Alvarez-Ordóñez *et al.* 2011; Ojeda & Dittrich 2012; Kamnev *et al.* 2017).

Sample	O—H; N—H (amide I) in proteins, ν	C—H in $>\text{CH}_2$, ν_{as}	C=O (ester moiety), ν	Amide I (in proteins)	Carboxyl COO^- , ν_{as}	Amide II (in proteins)	$-\text{CH}_2/-\text{CH}_3$ δ (in proteins, lipids, polyesters, etc.)	C=O of COO^- , ν_s	C—O—C/C—C—O ν (in ester moieties)	Amide III / O—P=O ν_{as}	C—O, C—C, C—H, C—O—C δ in polysaccharides, and polyesters	Phosphoryl groups, ν_s	"fingerprint region"
Cell biomass of <i>Mc. capsulatus</i>	3288	2922		1644		1538		1392		1234	1075		
SeNPs produced by <i>Mc. capsulatus</i>	3297	2927		1644		1538		1366		1239	1150 1077 1015	919	859 762
Cell biomass of <i>Ms. trichosporium</i>	3284	2927		1639		1537		1386		1241	1036		
SeNPs produced by <i>Ms. trichosporium</i>	3278	2931	1723	1634		1532	1451	1380	1279	1229	1131 1056	980	
Chem-SeNPs		2923				1606		1409					

For the SeNPs produced by *Mc. capsulatus*, the peak centred at 3297 cm^{-1} correspond to the —OH and —NH stretching vibrations of the amine and carboxylic groups. Peaks at 2927 cm^{-1} corresponded to the aliphatic saturated C—H stretching modes (Naumann *et al.* 1995; Kamnev *et al.* 2017). The peaks at 1644 , 1538 , and 1239 cm^{-1} are characteristic of amide I, amide II, and amide III bands of the proteins, respectively (Alvarez-Ordóñez *et al.* 2011; Ojeda & Dittrich 2012). The symmetrical stretch of carboxylate group can be attributed to the bands observed at 1366 cm^{-1} . The peaks at 1150 , 1077 and 1015 cm^{-1} corresponded to the C—O stretching vibrations of ether groups (Naumann *et al.* 1995; Beekes *et al.* 2007). The presence of phosphoryl groups was confirmed by the peak at 919 cm^{-1} . Additionally, peaks at 859 and 762 cm^{-1} (fingerprint region) could be mainly attributed to aromatic ring vibrations of aromatic amino acids (tyrosine, tryptophan, phenylalanine) and nucleotides (Burattini *et al.* 2008; Kamnev 2008).

Meanwhile, the SeNPs of *Ms. trichosporium* OB3b had a peak at 3278 cm^{-1} ; corresponding to the $-\text{OH}$ and $-\text{NH}$ stretching vibrations of the amine and carboxylic groups; and the band at 2931 cm^{-1} corresponded to the aliphatic saturated C–H stretching modes (Naumann *et al.* 1995; Kamnev *et al.* 2017). The peaks at 1634, 1532, and 1229 cm^{-1} corresponded to amide I, amide II, and amide III of the proteins, respectively (Alvarez-Ordóñez *et al.* 2011; Ojeda & Dittrich 2012). The peaks at 1131 and 1056 cm^{-1} are assigned to the C–O stretching, which reveals the occurrence of carbohydrates and polysaccharides. The peak at 980 cm^{-1} reveals the presence of phosphoryl groups (Burattini *et al.* 2008; Kamnev *et al.* 2017). Indeed, the peaks of SeNPs of *Ms. trichosporium* OB3b resembled that of SeNPs produced by *Mc. capsulatus*. However, unlike the SeNPs of *Mc. capsulatus*, SeNPs of *Ms. trichosporium* OB3b exhibited two peaks at 1723, and 1451 cm^{-1} . The peak recorded at 1723 cm^{-1} is assigned to C=O stretching in lipid esters, while that at 1451 cm^{-1} corresponds to various CH_2/CH_3 bending vibrations in lipids and proteins.

The FTIR spectra of SeNPs of both *Mc. capsulatus* and *Ms. trichosporium* OB3b differ from those of the bacterial biomass (controls) and the Chem-SeNPs. The main difference between the spectra is that the Bio-SeNPs exhibit more peaks in the polysaccharide vibration region, indicating the presence of proteins and polysaccharides in the biomacromolecules capping the SeNPs (Shirsat *et al.* 2015; Jain *et al.* 2015b; Wadhvani *et al.* 2016; Kamnev *et al.* 2017; Tugarova & Kamnev 2017). This finding is consistent with the results found in the SDS-PAGE and XPS analyses, which demonstrated the presence of proteins and organic material on the nanoparticles.

By contrast, Chem-SeNPs obtained through reaction of Na_2SeO_3 with L-cysteine displayed a broad absorption band around 3350 cm^{-1} and absorption band at 2923 cm^{-1} that are assigned to O–H vibrations of the absorbed H_2O and C–H vibration in the alkyl chain of L-cys, respectively. The peak at 1606 cm^{-1} can be mainly attributed to C=O vibrations. It is noteworthy that the presence of organic residues such as carbohydrates, lipids, and proteins on the surface of biogenic SeNPs were completely absent in Chem-SeNPs (see Figure 4-10). FTIR spectra of SeNPs separated from bacterial cells showed bands typical of proteins, polysaccharides and lipids associated with the particles (in line with their TEM images showing a thin layer over the particles), in addition to strong carboxylate bands, which evidently stabilise the SeNPs structure and morphology.

4.7 Raman spectroscopy

Raman spectroscopy permits the observation of vibrational, rotational, and other low-frequency modes in a sample, and it provides useful information on the structure, morphology and chemical composition of materials (Yang *et al.* 2007). Raman spectroscopic technique was used to monitor molecular-level changes in the structure and composition of cellular macrocomponents that accompanied metabolic responses of different strains of the ubiquitous rhizobacterium *Azospirillum brasilense* (Pereg *et al.* 2016; Cassán & Diaz-Zorita 2016) (which showed different adaptation capabilities and often different ecological behaviour) to various stress conditions. This vibrational spectroscopic technique can also be useful in studying microbially synthesised selenium nanoparticles (Tugarova *et al.* 2017; Tugarova & Kamnev 2017).

In the present study, Raman was used in order to identify the vibrational mode of the produced SeNPs. Figure 4-11 shows the measured Raman spectra of Se nanoparticles produced by *Mc. capsulatus* (a) and *Ms. trichosporium* OB3b (b). The spectra were recorded in the range 50 to 500 cm^{-1} excited using the 532 nm line of argon ion laser.

The spectra show prominent peaks at 251.6 cm^{-1} and 247.9 cm^{-1} (for SeNPs of *Mc. capsulatus* and *Ms. trichosporium* OB3b, respectively). The two peaks, which correspond to the Se–Se covalent bond, are a characteristic stretching mode of amorphous selenium (a-Se) (Lucovsky *et al.* 1967; Okano *et al.* 2007; Scopigno *et al.* 2011; Van Overschelde *et al.* 2013). In a study on photoinduced structural changes in amorphous selenium, Lukács *et al.* (2010) reported a Raman spectra peaks around 250 cm^{-1} wavenumbers correspond to 2.35 Å Se–Se covalent bond vibrational modes in amorphous selenium. This finding is in a good agreement with Raman and X-ray absorption spectroscopy data of the present study. The latter showed two Se-Se peaks typical of amorphous red selenium, and a typical local structure with two Se atoms at about 2.35 Å. Meanwhile, the bands for trigonal selenium (t-Se) at about 234 cm^{-1} (Quintana *et al.* 2002) and the monoclinic Se (m-Se) at about 264 cm^{-1} (Rajalakshmi & Arora 1999; Kuzmin *et al.* 2012) are not observed in Figure 4-11a and b.

The Raman scattering spectra provided further evidence that the selenium nanoparticles are in the amorphous state. The band at 359.1 cm^{-1} for SeNPs of *Mc. capsulatus* can be assigned to the S–Se stretching vibrations (Eysel & Sunder 1979; Vogel *et al.* 2017). In comparison with the Raman spectra published by Eysel and Sunder who studied a homologous series of various $\text{Se}_n\text{S}_{8-n}$ mixed crystal compounds, the spectrum is a close match that of Se_6S_2 species. Similar to the results in the literature, the spectrum is only characterized by the stretching vibration of Se–Se and

S–Se interactions. Unlike SeNPs of *Mc. capsulatus*, the band of S–Se stretching vibrations was not observed for SeNPs of *Ms. trichosporium* OB3b. This finding is consistent with the results found in the HAADF-STEM and XPS measurements, which suggested the absence of S in the SeNPs.

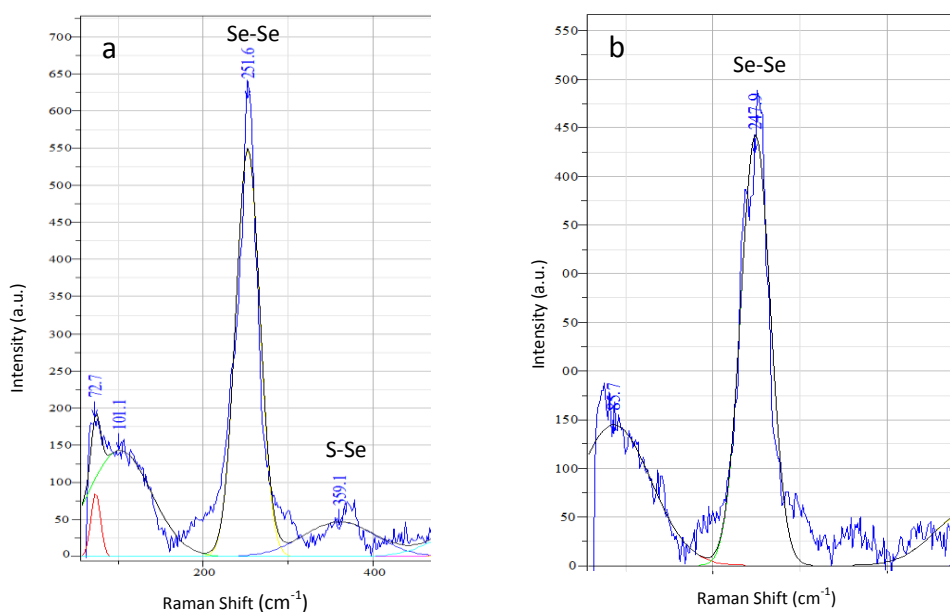


Figure 4-11 The Raman spectra of purified Se nanospheres from *Mc. capsulatus* (a) and *Ms. trichosporium* OB3b (b). The spectra are representatives of more than 3 runs of the experiments. a.u., stands for arbitrary units.

4.8 Zeta potential and average particle size values of selenium nanoparticles

Zeta potential analysis is a technique for the determination of the surface charge on NPs in colloidal solution by measuring the effective electrical charge associated with the surface of particle/molecules in the medium (Hunter 2013). In the present study, zeta potential and average particle size analyses were performed in order to establish whether the surface charge of the generated SeNPs changed with incubation time. The

zeta potential of the SeNPs was measured using a Zetasizer Nano ZS particle analyzer (Malvern Instruments Limited, Malvern, UK), and the size distribution was measured by dynamic light scattering method (DLS) with the same instrument.

Zeta potential and average particle size of the SeNPs are presented in Table 4-6. The longer the incubation time for either bacteria, resulted in an increase in the mean selenium nanoparticle sizes, obtained with the DLS measurements, which is in good agreement with the TEM results presented in Figure 4-3. Zeta potential measurements indicate a slightly negative charge on the selenium nanoparticles (around -16.5 and -9.82 for *Mc. capsulatus* (Bath) and *Ms. trichosporium* OB3b, respectively). Similar negative zeta potential values were reported for BioSeNPs formed at ambient temperature by bacterial cultures of *Bacillus cereus* (Dhanjal & Cameotra 2010), *Bacillus selenatarsenatis* (Buchs *et al.* 2013) and *Azospirillum brasilense* (Vogel *et al.* 2017). Jain *et al.* (2015b) reported that the zeta potential for BioSeNPs produced by anaerobic granular sludge was -17.5 ± 0.9 mV at pH 7.0 and 100 mM NaCl.

In the present study, it is worth noting that no significant change was observed in the zeta potential over time, indicating that the nanoparticles grow gradually with the same surface chemical composition. If all the particles in suspension have a negative or positive zeta potential, then they will tend to repel each other and there is little tendency for the particles to aggregate. However, if the particles have low zeta potential values then there is a propensity for the particles to come together and form aggregates (Dhanjal & Cameotra 2010). The slightly negative charge on Se^0 particles probably accounts for the stability of the selenium nanoparticles without the formation of aggregates.

Table 4-6 Time course of growth and Zeta potential of Se nanoparticles produced by *Mc. capsulatus* and *Ms. trichosporium* OB3b.

Sample	Time	Size (nm)	Zeta potential (mV) in 10% NaCl
SeNPs of <i>Mc. capsulatus</i> (Bath)	6 hours	225 ± 24	-16.5 ± 1.6
	16 hours	233 ± 31	-16.1 ± 1.3
	48 hours	364 ± 36	-15.3 ± 1.1
SeNPs of <i>Ms. trichosporium</i> OB3b	48 hours	77 ± 16	-9.82 ± 0.9
	144 hours	123 ± 19	-8.93 ± 1.2
	240 hours	156 ± 31	-8.27 ± 0.8

4.9 Application of SeNPs

Synthesis of selenium nanoparticles has been the subject of many studies due to its important commercial and therapeutic applications (Shoeibi & Mashreghi 2017). Selenium nanoparticles are known to exhibit diverse biological properties including antibacterial (Tran & Webster 2011), antifungal, anti-protozoan, antitapeworm (Bartůněk *et al.* 2015), antioxidant (Rezvanfar *et al.* 2013; Kong *et al.* 2014; Forootanfar *et al.* 2014), antitumor (Ren *et al.* 2013; Kumar *et al.* 2015), antibiofilm (Shakibaie *et al.* 2015; Khiralla & El-Deeb 2015), anti-inflammatory (Wang *et al.* 2014), antiviral, wound healing (Ramya *et al.* 2015), chemopreventive, chemotherapeutic (Chen *et al.* 2008), mercury sequestration (Fellowes *et al.* 2011; Jiang *et al.* 2012) and metal adsorption activities (Jain *et al.* 2015a).

SeNPs can be synthesized using either biological or chemical methods. Several chemical methods have been reported for the synthesis of SeNPs of desired size and polydispersity index. The chemical synthesis methods may include reduction of sodium selenite by glutathione (GSH, glutamyl cysteinyl glycine) (Johnson *et al.* 2008; Ramos & Webster 2012) or glucose (Chen *et al.* 2010), by reaction of an ionic liquid with sodium selenosulfate (Langi *et al.* 2010), by reduction of selenious acid with glutathione in the

presence of sodium alginate (Vekariya *et al.* 2012), and reaction of acetone with selenium dioxide (Shah *et al.* 2010). However, these methods are environmentally hazardous, expensive and in many cases, require specialized equipment. In contrast, the biosynthesis of selenium nanoparticles under ambient temperature and pressure at neutral pH utilizing bacteria has gained much attention as an alternative approach due to the natural abundance of diverse bacteria (e. g. methane-oxidizing bacteria), fast growth rate, high productivity, low cost, ease of culturing, downstream processing, handling and genetic manipulation (Wang *et al.* 2010; Srivastava & Mukhopadhyay 2013; Li *et al.* 2014a). The degree of control over the size and shape of SeNPs is extremely high in the case of chemical synthesis, whereas in the case of microbial synthesis of SeNPs, most of the reported microorganisms resulted in the synthesis of spherical SeNPs and in rare cases nanowires. All of the microorganisms studied so far have synthesized only polydisperse nanoparticles with sizes ranging from 50 nm to 500 nm, with the average size being 100 nm (Dhanjal & Cameotra 2010; Kuroda *et al.* 2011; Prakash *et al.* 2009). The major challenges in the biogenic production method are deprived product quality, i.e., higher polydispersity index and larger size along with the need for meticulous postproduction treatment (Shirsat *et al.* 2015). Nevertheless, literature gives us enough indications suggesting that the challenges can be addressed by understanding the mechanism of action involved in the biogenic production of SeNPs.

Specific properties of biogenic SeNPs which differ from those obtained chemically have been outlined in a study by Oremland *et al.* (2004) who compared features of biologically and chemically produced selenium nanoparticles. The authors showed that monoclinic crystalline structures of selenium nanoparticles produced by selenium

oxyanion respiring bacteria were compact, uniform, stable and their size ranged from 200 to 400 nm. In contrast, the size of selenium nanoparticles produced by auto oxidation of H₂Se gas and chemical reduction of selenite with ascorbate ranged between 10 nm to 50 nm. Moreover, all the three different microbial species *Sulfurospirillum barnesii*, *Bacillus selenitireducens* and *Selenihalanaerobacter shriftii* used in their study, showed unique and different spectral (UV-visible and Raman spectra) properties. The band gap energy, the energy required to excite a valence electron to the conduction band, was lower for all three biologically synthesized nanospheres compared to chemically synthesized nanospheres. The band gap calculated for the chemically synthesized nanospheres was 2.1 eV, which was considerably higher than the band gaps for selenium nanospheres derived from *S. barnesii* (1.62 eV), *S. shriftii* (1.52 eV), and *B. selenitireducens* (1.67 eV). The microbial synthesis of SeNPs results in unique, complex, compacted nanostructural arrangements of Se atoms. These arrangements probably reflect a diversity of enzymes involved in the dissimilatory reduction that are subtly different in different microbes. Remarkably, these conditions cannot be achieved by current methods of chemical synthesis reported (Yadav *et al.* 2008). Recent report by Vogel *et al.* (2017), *Azospirillum brasilense* was shown to be capable of producing selenium particles containing a certain amount of sulfur Figure 4-12. The particles were homogeneous and stable Se_{8-n}S_n structured spheres with an average size of 400 nm and negative surface charge of -18 mV at neutral pH range.



Figure 4-12 Structure of selenium-sulfur nanoparticles produced by *Azospirillum brasilense*. The particles were homogeneous and stable Se₈-nS_n structured spheres. Reprinted with permission from (Vogel *et al.* 2017).

In addition, biogenic SeNPs are stable because of the natural coating of the organic molecules and do not aggregate with time, whereas external addition of stabilizing agents is required when chemical synthesis is used (Nancharaiah & Lens 2015b). In a study on proteins associated with SeNPs, Dobias *et al.* (2011) compared SeNPs produced by *E. coli* to chemically synthesized SeNPs. They identified four proteins with different functions: propanol-preferring alcohol dehydrogenase (AdhP), isocitrate dehydrogenase [NADP] (Idh), Outer membrane protein C precursor (Porin ompC, OmpC) and isocitrate lyase (AceA) that bound specifically to SeNPs and observed a narrower size distribution as well as more spherical morphology when the particles were synthesized chemically in the presence of proteins. The authors also demonstrated that when the chemical synthesis of selenium nanoparticles occurs in the presence of alcohol dehydrogenase, the size of the produced nanoparticles was three-fold smaller (122 ± 24 nm) than the size of chemically synthesized selenium nanoparticles in the absence of *E. coli* AdhP (319 ± 57 nm). These results support the assertion that a protein sheath may be important in the industrial-scale synthesis of SeNPs of uniform size and properties.

There are a variety of applications of SeNPs in industry, the growth of some crops, prevention and treatment of certain diseases including cancer, as well as antifungal

activities (Shirsat *et al.* 2015). The most prominent feature of the SeNPs is reducing oxidative stress through antioxidant actions which are useful in the treatment of cancers and heart diseases (Chen *et al.* 2008; Flohé 2011; El-Batal *et al.* 2012). Orally administered SeNPs-enriched *Lactobacillus brevis* to mice with breast cancer was found to highly stimulate the immune responses (Yazdi *et al.* 2013). In addition, selenium encapsulation in non-viral carriers such as chitosan acts as a proteinase inhibitor and increases the immune response in the treatment of colorectal cancer and fibrosarcoma (Shakibaie *et al.* 2010). In addition to the numerous reports that show anticarcinogenic activity of SeNPs against several types of cancers, selenium nanoparticles also have antibacterial properties, especially in biofilm-forming bacteria (Tran & Webster 2011; Shoeibi & Mashreghi 2017). Study of these antibacterial properties has demonstrated that elemental selenium-enriched probiotics have antibacterial effects *in vitro* and *in vivo* against *Escherichia coli*. Furthermore, studies have demonstrated that selenium nanoparticles reduce *S. aureus* adhesion and proliferation on commercial endotracheal tubes by over 99% (Ramos 2012). In addition to therapeutic uses, SeNPs have been used in detector devices and quantum dot (QD) for medical and environmental diagnostics. SeNPs can form the core of the nanocrystals in QD engineering (Prasad 2009; Tian *et al.* 2012). They are also good biosensors for the detection of toxic compounds such as H₂O₂ in food, pharmaceutical, clinical, industrial and environmental analyses (Wang *et al.* 2010) as well as the detection of the toxic dinitrobutylphenol (DNBP), which is released into wastewater, causing environmental pollution, and a SeNPs-based chemiluminescence system is, so far, the best method for its detection (Iranifam *et al.* 2013). Future perspective of biological synthesis of SeNPs process should move towards a controlled manipulation of the microorganisms to produce the desired shape and size of nanoparticles.

4.10 Conclusions

In conclusion, the pure strains of the methanotrophic bacteria *Mc. capsulatus* and *Ms. trichosporium* OB3b are able to reduce the toxic selenite form to nontoxic nanoparticulate Se^0 . The produced SeNPs were characterized by TEM-EDX, HAADF-STEM, SDS-PAGE, XPS, FTIR, Raman and Zeta potential. The nanoparticles were extracellular, spherical and in a variety of sizes. The longer incubation time for either bacterium, resulted in an increase in the mean selenium nanoparticle sizes. The nanoparticles grow gradually with the same surface chemical composition as no significant change was observed in the negative surface charge over time. The elemental red selenium nanoparticles formed during selenite reduction were found to be amorphous containing a certain amount of sulfur. The SDS- PAGE results showed that the purified selenium nanoparticles were associated with proteins. The mean elemental selenium particle sizes formed in the *Mc. capsulatus* cultures were in the main larger than those produced by *Ms. trichosporium* OB3b. The potential uses of biogenic SeNPs in the field of nanobiotechnology, is indicative that methanotrophs represents a very valuable biological resource. In fact, whilst being exploited for the bioremediation of selenite-polluted environments, it could be used concomitantly for the production of new biomaterials of nano-technological value.

Chapter 5

Detection and identification of volatile selenium species

5.1 Volatile selenium species of selenite-amended cultures

In order to detect volatile selenium species for selenite-amended cultures, the headspace of the incubation flask was sampled using a syringe and injected into a GC-MS after sample preconcentration through a sorption tube. Each test was performed in triplicate (from three independent cultures). It was observed in preliminary experiments with selenite-amended culture medium solutions that the colour of the suspensions tended to fade with time, an indication that Se^0 was probably being transformed into other selenium species. Indeed, separate experiments with harvested nanoparticles from both bacteria revealed that volatile selenium species were formed in the headspace of the flasks. Interestingly, the distribution profile of the methylated species was different compared to those formed when selenite was added to the culture medium. In the former solutions, two species dimethyl diselenide and dimethyl selenenyl sulphide, were detected in the headspace of both bacteria. It has been suggested by a number of investigators (Chau *et al.* 1976; Doran & Alexander 1977; McCarthy *et al.* 1993; Michalke *et al.* 2000; Chasteen & Bentley 2003; Kagami *et al.* 2013) that diverse microbes are capable of transforming selenite into volatile selenium species.

In the selenite-amended cultures of both bacteria, it was observed that the volatile selenium species were detected as the red elemental selenium colour was developing. The headspace of the culture medium of both bacteria with and without selenite addition and standards were sampled and analysed for volatile selenium-containing species. GC-MS chromatograms of all the samples analysed are shown in Figure 5-1 and Figure 5-2, showing a variety of volatile methylated selenium and mixed selenium-sulphur species produced by both organisms. In addition to the two previously

identified methylated species (DMSeS and DMDSe), methylselenol (MeSeH), dimethyl selenide and methylselenoacetate were detected in the *Mc. capsulatus* (Bath) headspace. Table 5-1 presents a summary of the volatile selenium-containing species produced when each bacterium culture is amended with selenite, biogenic selenium produced by the bacterium and commercial amorphous red selenium, respectively.

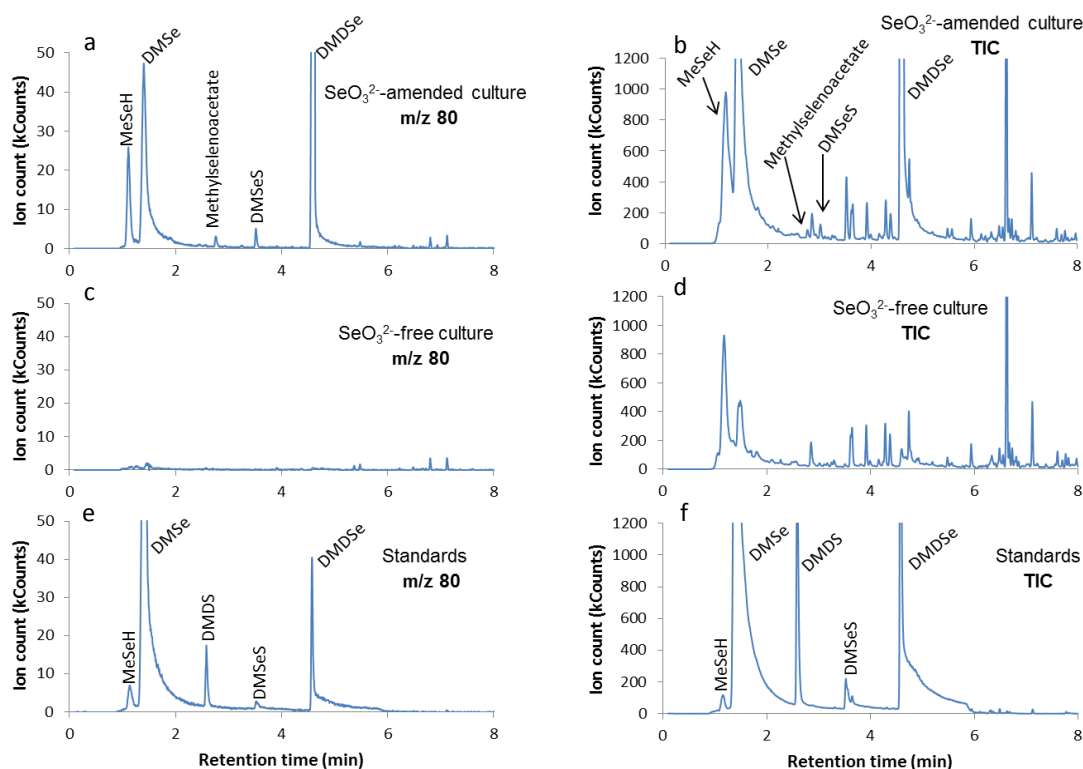


Figure 5-1 GC-MS chromatograms of the headspace gas of the *Mc. capsulatus* (Bath) cultures amended with (40 mg L^{-1}) (a & b) and without selenite (c & d) at 24 hours, and that of mixed standards containing MeSeH, DMSe, dimethyl disulphide (DMDS), DMSeS and DMDSe (e and f). Chromatograms are representatives of at least triplicate runs.

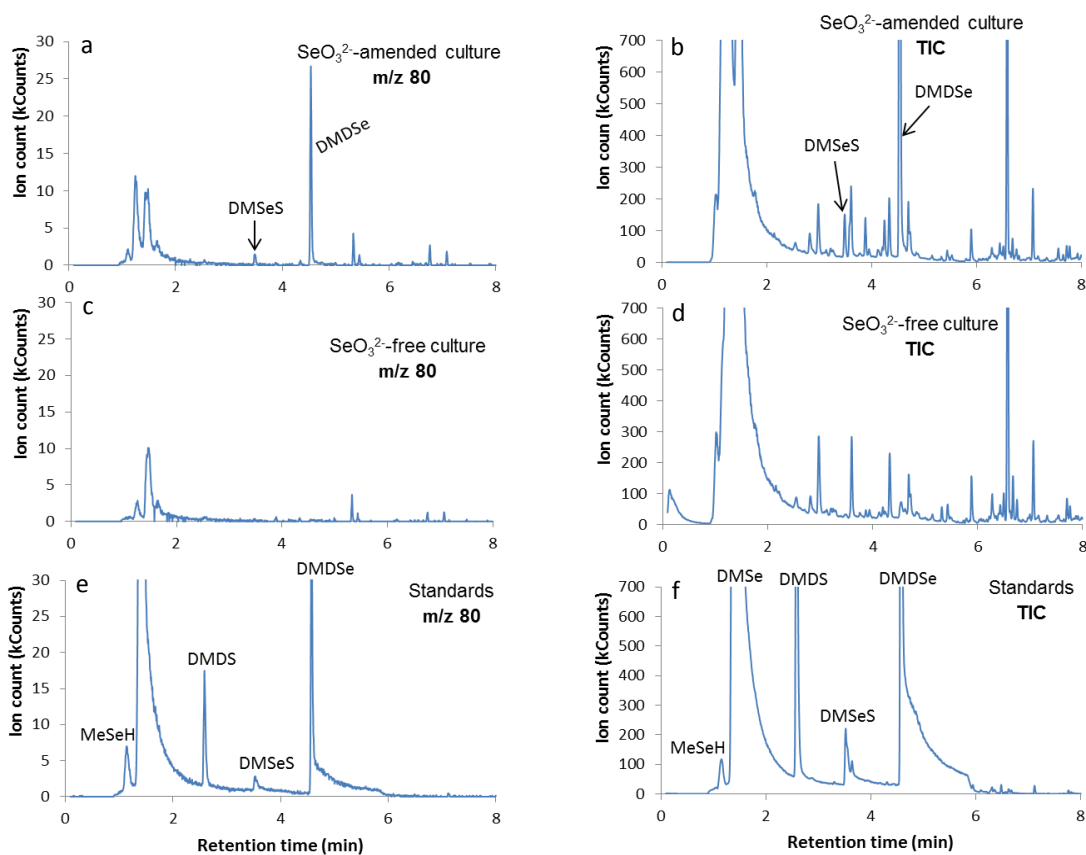


Figure 5-2 GC-MS chromatograms of the headspace gas of the *Ms. trichosporium* OB3b cultures amended with (20 mg L^{-1}) (a & b) and without selenite (c & d) at 24 hours and that of mixed standards containing MSeH, DMSe, dimethyl disulphide (DMDS), DMSes and DMDSe (e & f). Chromatograms are representatives of at least triplicate runs.

Table 5-1 Volatile selenium species produced by methanotrophs from different selenium-containing substrates.

Strain	Substrate	Product				
		DMSe	DMDSe	DMSes	methyl selenol	methylselenoacetate
<i>Mc. capsulatus</i> (Bath)	selenite	+	+	+	+	+
	Bio- Se^0	+	+	+	-	-
	Che- Se^0	+	+	+	-	-
<i>Ms. trichosporium</i> OB3b	selenite	-	+	+	-	-
	Bio- Se^0	+	+	-	-	-
	Che- Se^0	+	-	-	-	-

Identification of the selenium-containing species in the headspace of the cultures was achieved by matching the retention times of the standards together with mass spectra information stored in the instrument NIST library database. Using this approach, it was possible to detect methylselenol (CH_3SeH , MSeH), methylselenoacetate ($\text{C}_3\text{H}_6\text{OSe}$), dimethyl selenide (CH_3SeCH_3 , DMSe), dimethyl diselenide ($\text{CH}_3\text{SeSeCH}_3$, DMDS₂) and dimethyl selenenyl sulphide ($\text{CH}_3\text{SeSCH}_3$, DMSeS) in the headspace of selenite-amended *Mc. capsulatus* culture medium. In contrast, only two volatile selenium-containing species, DMDS₂ and DMSeS, were detected in the headspace of the selenite-amended *Ms. trichosporium* culture.

It is noteworthy that with both culture media, these selenium species were detected soon after selenite addition (4 and 20 hours for *Mc. capsulatus* and *Ms. trichosporium* OB3b, respectively). Results of experiments with the harvested nanoparticles clearly show that these are required for the formation of volatile selenium species, but also, other species are directly formed through other possible pathways as suggested by Challenger (1945) and Reamer and Zoller (1980). The manner in which the methylation of selenium may link to the one-carbon central metabolism of the methanotrophs remains to be established. The ability of *Mc. capsulatus* (Bath) and *Ms. trichosporium* OB3b to produce DMSe from SeO_3^{2-} may support Doran's (1982) hypothesis that SeO_3^{2-} is reduced via elemental selenium to a selenide form before it is methylated to form methylselenol and finally DMSe. The presence of methylselenol in the headspace of *Mc. capsulatus* (Bath) cultures could be a proof of its existence as an intermediate.

The results presented above clearly indicate that the pure strains of the methanotrophic bacteria *Mc. capsulatus* and *Ms. trichosporium* OB3b are able to reduce selenite to produce elemental selenium and volatile selenium species. The formation of elemental selenium appears to be mainly an extracellular process, probably accomplished indirectly with electrons derived from methane. It is probable that reducing agents containing sulfhydryl groups on the cell wall plays a key role in the bioreduction process of selenite. This opens up the possibility that methanotrophs (which are widespread across diverse environments) may play a significant role in the global selenium cycle. The results also suggest that these bacteria may be useful in preparing selenium nanoparticles of a range of sizes for biotechnological applications. Much remains to be determined about the pathway of selenium biotransformations in methanotrophs, though it appears that elemental selenium may not necessarily be an intermediate on the pathway to the formation of all volatile selenium species.

5.2 Volatile selenium species of selenate-amended cultures

Similar to the test with selenite, the production of volatile selenium species for selenate-amended cultures was investigated at various concentrations of selenate (ranging from 10 to 800 mg L⁻¹). For the headspace of *Mc. capsulatus* (Bath) cultures, no volatile selenium species were detected when the cultures were amended with 10 or 20 mg L⁻¹ selenate. However, at higher selenate concentrations (ranging from 50 to 800 mg L⁻¹), three methylated selenium species, DMSe, DMDS_e, and DMS_eS were detected. As shown in Figure 5-3, DMSe, DMDS_e, and DMS_eS were identified as

volatile selenium species in the headspace above cultures amended with 600 mg L^{-1} selenate at 24 hours. Since selenite and elemental selenium were not detected in the *Mc. capsulatus* (Bath) cultures, it thus appears that a distinct process, which does not require reduction to elemental selenium, is likely to be involved. This methylation process could be volatilizing selenium directly into DMSe, DMDSe, and DMSeS from selenate.

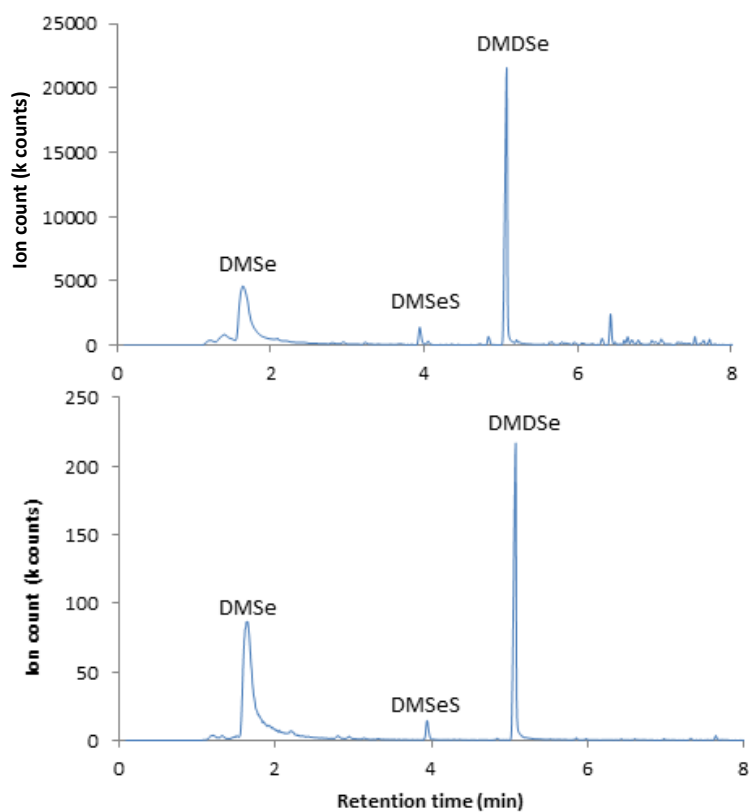


Figure 5-3 GC-MS chromatograms of the headspace gas of the *Mc. capsulatus* (Bath) cultures amended with selenate (600 mg L^{-1}) at 24 hours. The upper chromatograms were obtained by monitoring total ion current (TIC), and the lower chromatograms by selecting the 80 m/z ion. Chromatograms are representatives of at least triplicate runs.

In contrast, no methylated selenium species were detected in the headspace gas above the cultures of *Ms. trichosporium* OB3b amended with different concentrations of selenate (ranging from 10 - 500 mg L⁻¹), indicating that the strain is not able to transform selenate to methylated selenium species.

5.3 Volatile selenium species of DL-selenocystine-amended cultures

To identify the volatile selenium species produced by the strains, the headspace gas above the DL-selenocystine-amended (20 mg L⁻¹) cultures were analyzed by GC-MS system. For the *Mc. capsulatus* (Bath), as shown in Figure 5-4, DMSe, DMSeS, and DMDS_e were identified as methylated selenium species in the head space at all time intervals investigated. Identification of these species was achieved by matching the retention times of the standards together with mass spectra data stored in the NIST database. As can be seen from the Figure 5-4, there is a gradual increase in the concentration of the three species with the time, as there is an increase in their peak heights/areas. It is noteworthy that as the DMSe, DMSeS, and DMDS_e concentrations increased over time in the headspace gas above the cultures, the DL-selenocystine concentrations decreased in the cultures (see Figure 3-13a).

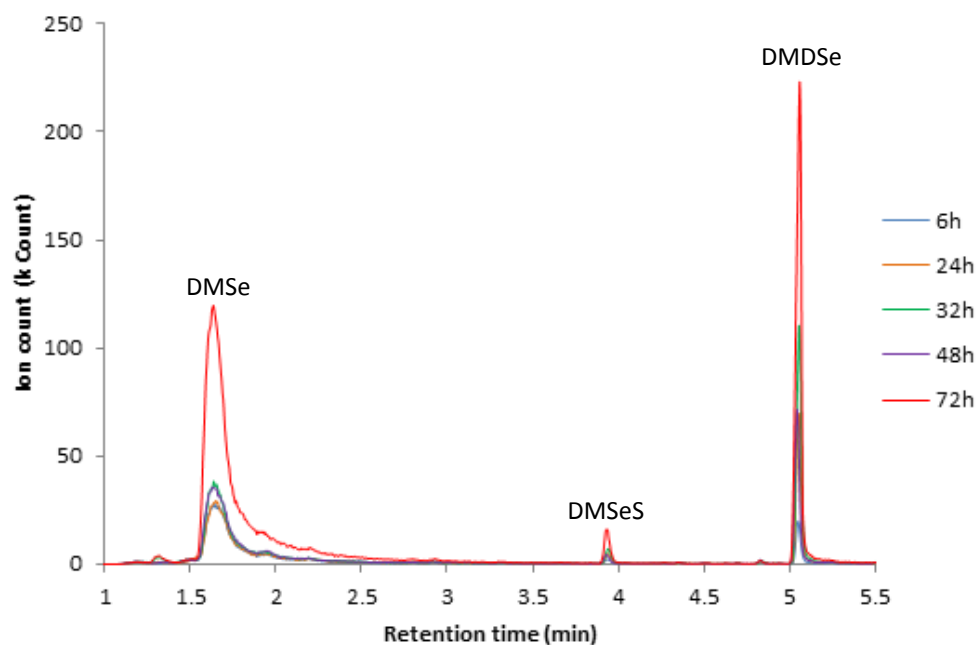


Figure 5-4 Mass chromatograms of the headspace gas of the *Mc. capsulatus* (Bath) cultures amended with DL-selenocystine (20 mg L^{-1}) at different time intervals. The chromatograms were obtained by selecting the 80 m/z ion by using GC-MS system. Chromatograms are representatives of at least triplicate runs.

In contrast, no methylated selenium species were detected in the headspace gas above the cultures of *Ms. trichosporium* OB3b amended with DL-selenocystine (20 mg L^{-1}), indicating that the strain is not able to transform DL-selenocystine to methylated selenium species.

5.4 Conclusions

Mc. capsulatus (Bath) and *Ms. trichosporium* OB3b are both able to convert selenite to methylated selenium species. The methylation of inorganic oxyanions by the two strains could be occurring through (i) several possible pathways as postulated by Challenger (1945), Reamer and Zoller (1980) and Doran (1982), in which selenite is first reduced to Se^0 before it can be methylated, (ii) methylated species are directly formed through other possible pathways. *Mc. capsulatus* (Bath), but not *Ms. trichosporium* OB3b is capable of considerable volatilization of selenate and DL-selenocystine. The bacterium transformed these compounds into DMSe, DMDS_e, and DMSeS. The mechanisms for the reduction and methylation of selenite by *Mc. capsulatus* (Bath) and *Ms. trichosporium* OB3b are not clearly understood. A detoxification mechanism seems likely because the products are 500 to 700 times less toxic than selenite. It is also unclear why *Ms. trichosporium* OB3b was not able to methylate selenate and DL-selenocystine. Further investigations are required to determine the nature of the intermediates that are formed during the selenium methylation processes. From a biotechnological standpoint, these methylation processes might be effectively exploited for the remediation of selenite-contaminated environments. Although the biological significance of Se methylation is not clearly understood, once the selenium volatilized as methyl derivatives is released and dispersed to the atmosphere, Se has lost its hazardous potential by dilution.

Chapter 6

General discussion and future directions

6.1 General discussion

Although a considerable number of studies have been conducted on the microbial transformation of selenium in the environments, no attention has been paid to the role of methane-oxidizing bacteria in transforming selenium species. The overall aim of the studies reported in this thesis was to investigate the microbial transformation of selenium using methanotrophs for developing and implementing successful methanotrophic bioremediation of selenium. The major achievement of this research is that for the first time, it has been shown that the methanotrophs, a major group of microorganisms with a critical role in the global methane cycle, can be used for the biotransformation of selenium oxyanions pollution. In the presence of methane as a sole carbon source, the commonly used laboratory model strains of methane-oxidizing bacteria *Mc. capsulatus* (Bath) and *Ms. trichosporium* OB3b, were shown to transform selenium oxyanions to elemental selenium and volatile selenium species.

Results reported in Chapter 3 have shed light on the interaction of methane-oxidizing bacteria with selenium oxyanions and their reducing ability. *Mc. capsulatus* (Bath) and *Ms. trichosporium* OB3b can grow aerobically in the presence of both selenite and selenate but exhibits different growth patterns. While the presence of selenate does not appear to have a negative impact on the growth curve compared to the control treatment, the presence of selenite elicits a toxic effect. Minimum inhibitory concentrations (MIC) assay showed that selenite is the more toxic of the two selenium oxyanions (selenate and selenite). Although, *Mc. capsulatus* (Bath) and *Ms. trichosporium* OB3b exhibited high tolerance to selenate compared to selenite, the strains were both able to reduce selenite but not selenate to red elemental selenium.

The reduction of selenite by methanotrophs perhaps a detoxification mechanism in order to diminish toxic potential of the oxyanion.

Flow cytometry (forward scatter plots) measurements clearly indicate that no substantial change in the bacterial cell size when the bacterial cells are exposed to selenate or selenite. This is in contrast with results reported by Dhanjal and Cameotra (2010), who found that there was a significant decrease in average bacterial cell size of *Bacillus cereus* (strain CM100B) which was grown in the presence of selenite. Possibly, the changes in cell morphology could be explained by the surface/volume ratio. The organisms reduce their cell size and increase their relative surface area for better uptake of the nutrients for survival under environmental stress conditions.

Unlike selenite, only a limited number of bacterial species have been shown to reduce selenate to red elemental selenium under aerobic conditions [reviewed in Kuroda *et al.* (2011)]. *Enterobacter cloacae* strain SLD1a-1 was reported to reduce selenate to elemental selenium under aerobic cultivation (Losi & Frankenberger 1997). Indeed, selenate reduction by this strain was observed only after oxygen depletion from the nutrient medium, suggesting that selenate reduction occurs during anaerobic respiration. This is consistent with the results of a genetic study into this strain which revealed that selenate reduction is related to the transcription factor FNR (Yee *et al.* 2007), which generally activates global expression of genes for anaerobic growth when oxygen levels are depleted (Unden *et al.* 1995). However, the use of *E. cloacae* SLD1a-1 in the bio-treatment of industrial wastewater may be limited because a longer lag time is required for selenate reduction at higher concentrations (Losi & Frankenberger 1997). In addition, the reduction of selenate at concentrations over 1 mM by this bacterium has not been reported to date. Therefore, further studies are required in

order to determine whether *E. cloacae* SLD1a-1 can be applied to the treatment of high concentrations of selenate. *Stenotrophomonas maltophilia* was reported to reduce selenate and selenite under microaerobic conditions (Dungan *et al.* 2003).

Visual observations of *Mc. capsulatus* and *Ms. trichosporium* OB3b cultures amended with selenate and selenite indicated that reduction of selenite leads to the production of red elemental selenium in the growth medium, whereas selenate had no visible effect on the cultures. TEM analysis of the *Mc. capsulatus* and *Ms. trichosporium* OB3b cultures amended with selenite demonstrated the formation of spherical nanospheres adhering to bacterial biomass (extracellular). EDX spectra of these nanospheres clearly indicated the presence of selenium, as the specific absorption peaks at 1.4, 11.22, and 12.5 keV were recorded. This observation is in contrast to the mainly intracellular Se^0 particles seen by Tugarova *et al.* (Tugarova *et al.* 2013; Tugarova *et al.* 2014) after the reduction of selenite by *Azospirillum brasilense*. Cell lysis can be an explanation for occurrence of extracellular particles (Tugarova *et al.* 2014).

In the current study particles were not detected inside the cells and the observed number of extracellular particles and intact cells gives rise to the assumption that enzymatic reactions were occurring on the cell surface are involved in the reduction of selenite. In order to determine the cellular location of the selenite-reducing activity, experiments were performed with cell fractions: cell wall, cell membrane and cytoplasm fractions were separately amended with selenite and monitored visually. The results showed that the red colour of elemental selenium was detected in the cell wall fraction, and a weak red tinge in the cell membrane fraction was probably due to the traces of reductase enzyme(s) contamination, which may have diffused from the cell wall to the cell membrane (Dhanjal & Cameotra 2010). By contrast, no reduction

activity was observed in the cytoplasmic fraction for both strains, suggesting that this fraction possess no selenite-reducing ability. Therefore, It can be ruled out that selenite reduction starts inside the cells followed by secretion of small particles which then grow further outside the cells as described for *S.maltophilia* (Lampis *et al.* 2017).

The cell-associated selenium nanospheres were not composed entirely of selenium, and signals of other elements such as carbon, oxygen, sulfur and phosphorus were also detected in the TEM-EDX spectra and STEM-HAADF-EDX maps, suggesting that some bioactive compounds excreted by bacteria might be associated with the selenium nanospheres. In order to establish the oxidation state of selenium in the red particles formed by methanotrophic reduction of selenite in the growth medium, XAS was performed. An X-ray Absorption Near-Edge Structure (XANES) edge energy of 11,919 eV as well as the overall shape of the white line and post white line features confirm the zero-valent oxidation state of the cell-associated selenium nanoparticle samples. The phase identity of red Se^0 was confirmed by the Fourier transform magnitude, which shows the two Se-Se peaks typical for amorphous red Se^0 .

The formed selenium nanoparticles were separated from the biomass and purified for further characterization. The isolated selenium nanoparticles were characterized by a combination of techniques including ICP-MS, Transmission electron microscopy (TEM) energy dispersive X-ray (EDX) spectrometry, high-angle annular dark-field (HAADF) scanning TEM (STEM), X-ray photoelectron spectroscopy (XPS), Fourier-transform infrared spectroscopy (FTIR), zeta potential and Raman spectroscopy techniques (Chapter 4). The mean selenium content of the isolated selenium nanoparticles was 70% and 67 % (n=2) for *Mc. capsulatus* and *Ms. trichosporium* OB3b, respectively as measured by ICP-MS. Thus, the data further supports results obtained from the TEM-

EDX spectra and STEM-HAADF-EDX maps, which indicated that the cell-associated selenium nanospheres were not composed entirely of selenium.

XPS and FTIR were applied to provide further information about the composition and functional groups on the surface of the selenium nanoparticles. The XPS and FTIR analyses indicated the presence of an organic outer coating, as previously reported in the bioproduction of selenium nanoparticles by *E. coli* (Jain *et al.* 2015b), which is likely to keep the particles in solution in aqueous solvents. In this respect, there is a significant knowledge gap in understanding the mechanism of bioformation of selenium NPs so as to preclude, at the present research stage, mass production on an industrial scale using bacterially based nano-manufacturing (Borghese *et al.* 2017). In addition to the XPS and FTIR analyses, SDS-PAGE results obtained from this study confirmed the presence of proteins in the isolated selenium nanoparticles.

Bacterial synthesis of NPs is generally achieved by a reduction step followed by a precipitation step with the latter composed of two parts: nucleation and crystal growth (Pearce *et al.* 2008). To date, only the reduction step has been studied extensively (Zannoni *et al.* 2007; Turner *et al.* 2012) whereas the biological processes responsible for nucleation and crystal growth are not fully understood although there is some evidence that proteins might play a key role in the nucleation and crystal growth of bacteriogenic metallic NPs (Dobias *et al.* 2011; Jain *et al.* 2015b). A bacterial protein – cytochrome c3 – was found to reduce selenate in aqueous solution leading to the formation of one-dimensional chain like aggregates of selenium nanoparticles (Abdelouas *et al.* 2000). Single proteins (Mms6 and BSA) were shown to be able to control the shape of the final selenium nanoparticles (Kaur *et al.* 2009). In a study by Pearce *et al.* (2009), the mechanisms of selenite reduction to elemental selenium

nanospheres and then selenide were compared between *V. atypica* and the subsurface metal-reducing bacteria *G. sulfurreducens* and *S. oneidensis*. In the same study, the potentially important role of extracellular proteins in stabilizing the Se-based nanoparticles was addressed. A topic that has also been studied in *E. coli* in an investigation by Dobias *et al.* (2011) where four proteins (AdhP, Idh, OmpC and AceA) were shown to play a critical role in controlling particle size and morphology.

Selenium nanoparticles produced by *S. barnesii*, *S. shriftii* and *B. selenitireducens* exhibit Raman spectra with different peaks (Oremland *et al.* 2004). Selenium nanospheres produced by *S. barnesii* and *B. selenitireducens* formed Se₆ conformation (*i.e.* chains of 6 Se atoms), while *S. shriftii* nanoparticles had a Se₈ (*i.e.* chain of 8 Se atoms). The Raman spectra of selenium nanoparticles produced by *S. shriftii* displayed a peak at 260 cm⁻¹ that indicates a single chain of Se while a peak at 234 cm⁻¹ indicates Se polymer formation, thus further confirming the bimodal distribution. Selenium nanospheres formed by *S. barnesii* and *B. selenitireducens* had a Se₆ structure, but their vibrational spectra differ from each others. This is indicative that they differed in the configuration of the Se₆ chains. For selenium nanospheres produced by *B. selenitireducens*, Se₆ vibrational modes A_{1g} and E_g were dominated in the stable D_{3d} (chair) structure as compared to those in the unstable C_{2v} (boat) structure of selenium nanospheres formed by *S. barnesii*.

In the present study, Raman spectra showed a peak at 251.6 cm⁻¹ and 247.9 cm⁻¹ (for SeNPs of *Mc. capsulatus* (Bath) and *Ms. trichosporium* OB3b, respectively). These two peaks are characteristics of amorphous selenium (Okano *et al.* 2007; Van Overschelde *et al.* 2013). In addition to these peaks, the spectrum SeNPs of *Mc. capsulatus* showed a peak at 359.1 cm⁻¹ corresponds to the S–Se stretching vibrations (Eysel & Sunder

1979). This finding is consistent with data obtained in the very recent report by Vogel *et al.* (2017) who reported *Azospirillum brasilense* was shown to be capable of producing mixed Se–S extracellular particles with the composition close to Se_6S_2 . The isolated particles gave a strong broadened Raman Se–Se stretching band centred at 257 cm^{-1} and a weak but noticeable broadened band at 356 cm^{-1} ascribed to S–Se stretching vibrations. Therefore, the Raman data obtained from the present study further supports results of the HAADF-STEM mapping, which showed high levels of sulfur are associated with the nanoparticulate Se^0 of *Mc. capsulatus* (Bath).

In order to establish whether the surface charge of the generated SeNPs changed with incubation time, zeta potential analyses were performed. It is worth noting that no significant change was observed in the zeta potential over time, indicating that the nanoparticles grow gradually with the same surface chemical composition. Zeta potential measurements demonstrate a slightly negative charge on the selenium nanoparticles (around -16.5 and -9.82 for *Mc. capsulatus* (Bath) and *Ms. trichosporium* OB3b, respectively). Similar negative zeta potential values were reported for BioSeNPs formed at ambient temperature by bacterial cultures of *Bacillus cereus* (Dhanjal & Cameotra 2010), *Bacillus selenatarsenatis* (Buchs *et al.* 2013) and *Azospirillum brasilense* (Vogel *et al.* 2017). Jain *et al.* (2015b) reported that the zeta potential for BioSeNPs produced by anaerobic granular sludge was $-17.5 \pm 0.9\text{ mV}$.

In the biological system, certain elements are transformed into a variety of volatile methylated forms. In the case of selenium, two dominant species i.e. dimethylselenide and dimethyldiselenide have been reported. These species are volatile and the microorganism may get rid of toxic effects of selenium through the transformation of the excess of this element to its volatile forms followed by its removal from the micro/macro ecosystems. Several investigations have been carried out to develop a detailed understanding of the mechanism/pathways of biomethylation and transformation of selenium (Challenger 1945; Reamer & Zoller 1980; Doran 1982; Chasteen 1993). In general, methylation of inorganic selenium involves a reduction and a methylation step, but the exact order in which these reactions occur is yet to be fully elucidated.

In the present study, *Mc. capsulatus* (Bath) and *Ms. trichosporium* OB3b were investigated for their volatilization potential. Substantial amount of the toxic selenite was volatilized by the two strains; however, *Mc. capsulatus* (Bath) but not *Ms. trichosporium* OB3b volatilized both selenate and DL-selenocystine. For selenite reduction, results of experiments with the harvested nanoparticles clearly show that these are required for the formation of volatile selenium species, but also, other species are directly formed through other possible pathways as suggested by Challenger (1945), Reamer and Zoller (1980) and Doran (1982). For selenate-amended cultures of *Mc. capsulatus* (Bath), since selenite and elemental selenium were not detected in the cultures, it thus appears that a distinct process, which does not require reduction, is likely to be involved. This methylation process could be volatilizing selenium directly into DMSe, DMDS_e, and DMSeS from selenate.

Methylation and volatilization of selenium has been shown to be mainly a biotic process and is primarily thought to be a protective mechanism used by microorganisms to detoxify their surrounding environment (Dungan & Frankenberger 1999). This may explain therefore the ability of the cultures of *Mc. capsulatus* (Bath) and *Ms. trichosporium* OB3b to convert selenium oxyanions to volatile species. The biotransformation of selenium to volatile selenium compounds is considered a major process in the movement of selenium in the environment (Haygarth 1994). Although biological significance of selenium methylation is yet to be elucidated, once volatile selenium compounds are released to the atmosphere, selenium lose its hazardous potential it precipitates through rain. Therefore, microbial transformation of selenium to less toxic volatile forms may ultimately prove to be an effective approach to remediate seleniferous environments (Gupta *et al.* 2012).

In an experiment a constructed wetland was shown to effectively remove selenium from selenite contaminated oil refinery wastewater. Almost 89% of the selenium entering the constructed wetland was removed (Hansen *et al.* 1998). A large proportion of the Se removed by the wetland was accumulated in plant tissues and sediments, and it was estimated that 10% to 30% of the removed Se was volatilized. Rhizospheric bacteria associated with Indian mustard plants were observed to enhance selenium reduction and volatilization by several folds (de Souza *et al.* 1999). Climatic conditions such as precipitation and temperature significantly affect the selenium volatilization in the constructed wetland. Volatilization within a surface flow wetland has been observed to vary from approximately 9% in the winter to over 50% in the summer months in the constructed wetland in California (Terry *et al.* 1992; Johnson *et al.* 2009). At molecular level over-expression of bacterial thiopurine methyl

transferease (bTPMT) gene conferred resistance in *E. coli* towards selenium oxyanions along with methylation of inorganic and organic selenium into dimethylselenide (DMSe) and dimethyldiselenide (DMDS_e) (Ranjard *et al.* 2002). This enzyme could become a key in the remediation of anthropogenically or naturally Se-contaminated sites. A novel genes encoding COQ5 methyltransferease (BoCOQ5-2) in ubiquinone biosynthetic pathway has been isolated and found to specifically promote selenium volatilization in both bacteria and plants. Transgenic bacteria expressing *BoCOQ5-2* produced an over 160-fold increase in volatile selenium compounds when they were exposed to selenate in addition to enhanced tolerance to selenate and selenite (Zhou *et al.* 2009). The successful demonstration of alteration of ubiquinone biosynthesis in stimulating selenium volatilization through enhanced oxidative stress tolerance has opened a new perspective for the study of Se metabolism as well as genetic engineering of microorganisms and/or Se accumulators for the remediation of selenium-contaminated environments.

6.2 Future directions

The transformation of selenium oxyanions by methane-oxidizing bacteria to elemental selenium/volatile selenium species were studied in this thesis. The results obtained from this study provide the bases for understanding the growth characteristics of this group of bacteria in the presence of toxic selenium oxyanions. This study has extended our understanding of the formation of selenium nanoparticles and methylation of selenium by this group of bacteria.

There are still many areas identified in this study that needs to be explored. An area of potential interest is the identification of enzyme(s) responsible for selenite reduction, since the results reported in this study showed that the reduction of selenite by methane-oxidizing bacteria is enzymatic. Identification of the enzyme(s) may prove useful in the design of remediation strategies. The results from this study indicated also that the produced selenium nanoparticles are coated with organic materials probably proteins and extracellular polymeric substances (EPS). The role these play in the formation and stabilisation of selenium colloidal solutions needs to be explored. For selenium methylation, further investigations are required to determine the nature of the intermediates that are formed during the selenium methylation processes.

Over 100 new strains of methane-oxidizing bacteria have been cultivated, of which only two have been tested for selenium oxyanions transformation during the work reported in this thesis. In order to find new and useful organism for bioremediation of selenium, it can be proposed that the interaction between Se oxyanions and other methanotroph species should be investigated.

The results presented in this study suggest that this work should be repeated using a field scale investigation, rather than small scale (under laboratory conditions), to determine whether the observed bioremediation of selenium can be scaled up to a practical process of industrial use. The potential uses of biogenic SeNPs in the field of nanobiotechnology, is indicative that methanotrophs represents a very valuable biological resource. In fact, whilst being exploited for the bioremediation of selenite-polluted environments, it could be used concomitantly for the production of new biomaterials of nano-technological value.

It is hoped the results presented in this thesis, together with the results of the additional work proposed in this section, will allow widespread implementation of methane-oxidizing bacteria for the remediation of selenium pollution as well as the production of SeNPs for technological applications.

References

- Abdelouas, A., Gong, W., Lutze, W., Shelnutt, J., Franco, R. & Moura, I.** 2000. Using cytochrome c 3 to make selenium nanowires. *Chemistry of Materials*, **12**, 1510-1512.
- Abell, G. C., Stralis-Pavese, N., Sessitsch, A. & Bodrossy, L.** 2009. Grazing affects methanotroph activity and diversity in an alpine meadow soil. *Environmental Microbiology Reports*, **1**, 457-465.
- Afkar, E., Lisak, J., Saltikov, C., Basu, P., Oremland, R. S. & Stolz, J. F.** 2003. The respiratory arsenate reductase from *Bacillus selenitireducens* strain MLS10. *FEMS Microbiology Letters*, **226**, 107-112.
- Al Hasin, A., Gurman, S. J., Murphy, L. M., Perry, A., Smith, T. J. & Gardiner, P. H.** 2009. Remediation of chromium (VI) by a methane-oxidizing bacterium. *Environmental Science & Technology*, **44**, 400-405.
- Alvarez-Ordóñez, A., Mouwen, D. J. M., López, M. & Prieto, M.** 2011. Fourier transform infrared spectroscopy as a tool to characterize molecular composition and stress response in foodborne pathogenic bacteria. *Journal of Microbiological Methods*, **84**, 369-378.
- Ankudinov, A. L. & Rehr, J.** 1997. Relativistic calculations of spin-dependent X-ray-absorption spectra. *Physical Review B*, **56**, R1712.
- Antony, C. P., Kumaresan, D., Ferrando, L., Boden, R., Moussard, H., Scavino, A. F., Shouche, Y. S. & Murrell, J. C.** 2010. Active methylootrophs in the sediments of Lonar Lake, a saline and alkaline ecosystem formed by meteor impact. *The ISME Journal*, **4**, 1470-1480.
- Astratinei, V., Van Hullebusch, E. & Lens, P.** 2006. Bioconversion of selenate in methanogenic anaerobic granular sludge. *Journal of Environmental Quality*, **35**, 1873-1883.
- Ayano, H., Miyake, M., Terasawa, K., Kuroda, M., Soda, S., Sakaguchi, T. & Ike, M.** 2014. Isolation of a selenite-reducing and cadmium-resistant bacterium *Pseudomonas* sp. strain RB for microbial synthesis of CdSe nanoparticles. *Journal of Bioscience and Bioengineering*, **117**, 576-581.
- Bacon, M. & Ingledew, W. J.** 1989. The reductive reactions of *Thiobacillus ferrooxidans* on sulphur and selenium. *FEMS microbiology Letters*, **58**, 189-194.
- Bajaj, M., Schmidt, S. & Winter, J.** 2012. Formation of Se (0) nanoparticles by *Duganella* sp. and *Agrobacterium* sp. isolated from Se-laden soil of North-East Punjab, India. *Microbial Cell Factories*, **11**, 64.
- Bandow, N.** 2014. Isolation and binding properties of methanobactin from the facultative methanotroph *Methylocystis* strain SB2. (Doctoral dissertation, Iowa State University).

- Bandow, N., Gilles, V. S., Freesmeier, B., Semrau, J. D., Krentz, B., Gallagher, W., McEllistrem, M. T., Hartsel, S. C., Choi, D. W. & Hargrove, M. S.** 2012. Spectral and copper binding properties of methanobactin from the facultative methanotroph *Methylocystis* strain SB2. *Journal of Inorganic Biochemistry*, **110**, 72-82.
- Barkes, L. & Fleming, R. W.** 1974. Production of dimethylselenide gas from inorganic selenium by eleven soil fungi. *Bulletin of Environmental Contamination and Toxicology*, **12**, 308-311.
- Barlow, J., Gozzi, K., Kelley, C. P., Geilich, B. M., Webster, T. J., Chai, Y., Sridhar, S. & van de Ven, Anne L.** 2017. High throughput microencapsulation of *Bacillus subtilis* in semi-permeable biodegradable polymersomes for selenium remediation. *Applied Microbiology and Biotechnology*, **101**, 455-464.
- Barton, L.** 2005. Structural and functional relationships in prokaryotes. Springer Science & Business Media. Inc., New York, N.Y.
- Bartůněk, V., Junková, J., Šuman, J., Kolářová, K., Rimpelová, S., Ulbrich, P. & Sofer, Z.** 2015. Preparation of amorphous antimicrobial selenium nanoparticles stabilized by odor suppressing surfactant polysorbate 20. *Materials Letters*, **152**, 207-209.
- Bebien, M., Chauvin, J. P., Adriano, J. M., Grosse, S. & Vermeiglio, A.** 2001. Effect of selenite on growth and protein synthesis in the phototrophic bacterium *Rhodobacter sphaeroides*. *Applied and Environmental Microbiology*, **67**, 4440-4447.
- Beekes, M., Lasch, P. & Naumann, D.** 2007. Analytical applications of Fourier transform-infrared (FT-IR) spectroscopy in microbiology and prion research. *Veterinary Microbiology*, **123**, 305-319.
- Behling, L. A., Hartsel, S. C., Lewis, D. E., DiSpirito, A. A., Choi, D. W., Masterson, L. R., Veglia, G. & Gallagher, W. H.** 2008. NMR, mass spectrometry and chemical evidence reveal a different chemical structure for methanobactin that contains oxazolone rings. *Journal of the American Chemical Society*, **130**, 12604-12605.
- Bird, M. L. & Challenger, F.** 1942. Studies in biological methylation. Part IX. The action of *Scopulariopsis brevicaulis* and certain Penicillia on salts of aliphatic seleninic and selenonic acids. *Journal of the Chemical Society (Resumed)*, 574-577.
- Bird, M. L. & Challenger, F.** 1939. The formation of organo-metalloidal and similar compounds by micro-organisms. Part VII. Dimethyl telluride. *Journal of the Chemical Society (Resumed)*, 163-168.
- Birringer, M., Pilawa, S. & Flohé, L.** 2002. Trends in selenium biochemistry. *Natural Product Reports*, **19**, 693-718.
- Bissett, A., Abell, G. C., Bodrossy, L., Richardson, A. E. & Thrall, P. H.** 2012. Methanotrophic communities in Australian woodland soils of varying salinity. *FEMS Microbiology Ecology*, **80**, 685-695.

- Biswas, K. C., Barton, L. L., Tsui, W. L., Shuman, K., Gillespie, J. & Eze, C. S.** 2011. A novel method for the measurement of elemental selenium produced by bacterial reduction of selenite. *Journal of Microbiological Methods*, **86**, 140-144.
- Boden, R. & Murrell, J. C.** 2011. Response to mercury (II) ions in *Methylococcus capsulatus* (Bath). *FEMS microbiology Letters*, **324**, 106-110.
- Borghese, R., Brucale, M., Fortunato, G., Lanzi, M., Mezzi, A., Valle, F., Cavallini, M. & Zannoni, D.** 2017. Reprint of "Extracellular production of tellurium nanoparticles by the photosynthetic bacterium *Rhodobacter capsulatus*". *Journal of Hazardous Materials*, **324**, 31-38.
- Borodina, E., Nichol, T., Dumont, M. G., Smith, T. J., Murrell, J. C.** 2007. Mutagenesis of the "leucine gate" to explore the basis of catalytic versatility in soluble methane monooxygenase. *Applied and Environmental Microbiology* **73**:6460–6467
- Brasher, A. M. & Ogle, R. S.** 1993. Comparative toxicity of selenite and selenate to the amphipod *Hyaella azteca*. *Archives of Environmental Contamination and Toxicology*, **24**, 182-186.
- Bremer, J. & Natori, Y.** 1960. Behavior of some selenium compounds in transmethylation. *Biochimica et Biophysica Acta*, **44**, 367-370.
- Brock, T., Madigan, M., Martinko, J. & Parker, J.** 1991. *Biology of microorganisms*. 6th.
- Brusseau, G. A., Tsien, H., Hanson, R. S. & Wackett, L. P.** 1990. Optimization of trichloroethylene oxidation by methanotrophs and the use of a colorimetric assay to detect soluble methane monooxygenase activity. *Biodegradation*, **1**, 19-29.
- Buchs, B., Evangelou, M. W., Winkel, L. H. & Lenz, M.** 2013. Colloidal properties of nanoparticulate biogenic selenium govern environmental fate and bioremediation effectiveness. *Environmental Science & Technology*, **47**, 2401-2407.
- Burattini, E., Cavagna, M., Dell'Anna, R., Campeggi, F. M., Monti, F., Rossi, F. & Torriani, S.** 2008. A FTIR microspectroscopy study of autolysis in cells of the wine yeast *Saccharomyces cerevisiae*. *Vibrational Spectroscopy*, **47**, 139-147.
- Burra, R., Pradenas, G. A., Montes, R. A., Vásquez, C. C. & Chasteen, T. G.** 2010. Production of dimethyl triselenide and dimethyl diselenenyl sulfide in the headspace of metalloid-resistant bacillus species grown in the presence of selenium oxyanions. *Analytical Biochemistry*, **396**, 217-222.
- Cantafio, A. W., Hagen, K. D., Lewis, G. E., Bledsoe, T. L., Nunan, K. M. & Macy, J. M.** 1996. Pilot-scale selenium bioremediation of San Joaquin drainage water with *Thauera selenatis*. *Applied and Environmental Microbiology*, **62**, 3298-3303.
- Cassán, F. & Diaz-Zorita, M.** 2016. *Azospirillum* sp. in current agriculture: From the laboratory to the field. *Soil Biology and Biochemistry*, **103**, 117-130.

- Challenger, F.** 1945. Biological methylation. *Chemical Reviews*, **36**, 315-361.
- Challenger, F. & North, H. E.** 1934. The production of organo-metalloidal compounds by micro-organisms. Part II. Dimethyl selenide. *Journal of the Chemical Society (Resumed)*, 68-71.
- Chasteen, T., Silver, G., Birks, J. & Fall, R.** 1990. Fluorine-induced chemiluminescence detection of biologically methylated tellurium, selenium, and sulfur compounds. *Chromatographia*, **30**, 181-185.
- Chasteen, T. G.** 1993. Confusion between dimethyl selenenyl sulfide and dimethyl selenone released by bacteria. *Applied Organometallic Chemistry*, **7**, 335-342.
- Chasteen, T. G. & Bentley, R.** 2003. Biomethylation of selenium and tellurium: microorganisms and plants. *Chemical Reviews*, **103**, 1-26.
- Chau, Y. K., Wong, P. T., Silverberg, B. A., Luxon, P. L. & Bengert, G. A.** 1976. Methylation of selenium in the aquatic environment. *Science (New York, N.Y.)*, **192**, 1130-1131.
- Chen, H., Shin, D., Nam, J., Kwon, K. & Yoo, J.** 2010. Selenium nanowires and nanotubes synthesized via a facile template-free solution method. *Materials Research Bulletin*, **45**, 699-704.
- Chen, T., Wong, Y., Zheng, W., Bai, Y. & Huang, L.** 2008. Selenium nanoparticles fabricated in *Undaria pinnatifida* polysaccharide solutions induce mitochondria-mediated apoptosis in A375 human melanoma cells. *Colloids and Surfaces B: Biointerfaces*, **67**, 26-31.
- Chen, X., Yang, G., Chen, J., Chen, X., Wen, Z. & Ge, K.** 1980. Studies on the relations of selenium and Keshan disease. *Biological Trace Element Research*, **2**, 91-107.
- Chung, J., Nerenberg, R. & Rittmann, B. E.** 2006. Bioreduction of selenate using a hydrogen-based membrane biofilm reactor. *Environmental Science & Technology*, **40**, 1664-1671.
- Clark, L. C., Combs, G. F., Turnbull, B. W., Slate, E. H., Chalker, D. K., Chow, J., Davis, L. S., Glover, R. A., Graham, G. F. & Gross, E. G.** 1996. Effects of selenium supplementation for cancer prevention in patients with carcinoma of the skin: a randomized controlled trial. *Jama*, **276**, 1957-1963.
- Cooper, W. & Glover, J.** 1974. The toxicology of selenium and its compounds. *Selenium*, 664-674.
- Cox, D. & Alexander, M.** 1974. Factors affecting trimethylarsine and dimethylselenide formation by *Candida humicola*. *Microbial Ecology*, **1**, 136-144.
- Dalton, H.** 1980. Oxidation of hydrocarbons by methane monooxygenases from a variety of microbes. *Advances in Applied Microbiology*, **26**, 71-87.

- Dassama, L. M., Kenney, G. E. & Rosenzweig, A. C.** 2017. Methanobactins: from genome to function. *Metallomics*, **9**, 7-20.
- de Souza, M. P., Chu, D., Zhao, M., Zayed, A. M., Ruzin, S. E., Schichnes, D. & Terry, N.** 1999. Rhizosphere bacteria enhance selenium accumulation and volatilization by Indian mustard. *Plant Physiology*, **119**, 565-574.
- Debieux, C. M., Dridge, E. J., Mueller, C. M., Splatt, P., Paszkiewicz, K., Knight, I., Florance, H., Love, J., Titball, R. W., Lewis, R. J., Richardson, D. J. & Butler, C. S.** 2011. A bacterial process for selenium nanosphere assembly. *Proceedings of the National Academy of Sciences of the United States of America*, **108**, 13480-13485.
- DeMoll-Decker, H. & Macy, J. M.** 1993. The periplasmic nitrite reductase of *Thauera selenatis* may catalyze the reduction of selenite to elemental selenium. *Archives of Microbiology*, **160**, 241-247.
- Dhanjal, S. & Cameotra, S. S.** 2010. Aerobic biogenesis of selenium nanospheres by *Bacillus cereus* isolated from coalmine soil. *Microbial cell Factories*, **9**, 52.
- DiSpirito, A. A., Semrau, J. D., Murrell, J. C., Gallagher, W. H., Dennison, C. & Vuilleumier, S.** 2016. Methanobactin and the Link between Copper and Bacterial Methane Oxidation. *Microbiology and Molecular Biology Reviews : MMBR*, **80**, 387-409.
- DiSpirito, A. A., Zahn, J. A., Graham, D. W., Kim, H. J., Larive, C. K., Derrick, T. S., Cox, C. D. & Taylor, A.** 1998. Copper-binding compounds from *Methylosinus trichosporium* OB3b. *Journal of Bacteriology*, **180**, 3606-3613.
- Dobias, J., Suvorova, E. I. & Bernier-Latmani, R.** 2011. Role of proteins in controlling selenium nanoparticle size. *Nanotechnology*, **22**, 195605.
- Doran, J. W.** 1982. Microorganisms and the biological cycling of selenium. In: *Advances in Microbial Ecology* (Ed. by Anonymous), pp. 1-32. Springer, Boston, MA.
- Doran, J. W. & Alexander, M.** 1977. Microbial transformations of selenium. *Applied and Environmental Microbiology*, **33**, 31-37.
- Dowdle, P. R. & Oremland, R. S.** 1998. Microbial oxidation of elemental selenium in soil slurries and bacterial cultures. *Environmental Science & Technology*, **32**, 3749-3755.
- Dungan, R. S., Yates, S. R. & Frankenberger, W. T.** 2003. Transformations of selenate and selenite by *Stenotrophomonas maltophilia* isolated from a seleniferous agricultural drainage pond sediment. *Environmental Microbiology*, **5**, 287-295.
- Dungan, R. & Frankenberger, W.** 1999. Microbial transformations of selenium and the bioremediation of seleniferous environments. *Bioremediation Journal*, **3**, 171-188.
- El Ghazouani, A., Basle, A., Gray, J., Graham, D. W., Firbank, S. J. & Dennison, C.** 2012. Variations in methanobactin structure influences copper utilization by methane-

oxidizing bacteria. Proceedings of the National Academy of Sciences of the United States of America, **109**, 8400-8404.

El-Batal, A., Omayma, A., Noaman, E. & Effat, S. 2012. Promising antitumor activity of fermented wheat germ extract in combination with selenium nanoparticles. International Journal of Pharmaceutical Science and Health Care, **6**, 1-22.

Enoch, H. G. & Lester, R. L. 1972. Effects of molybdate, tungstate, and selenium compounds on formate dehydrogenase and other enzyme systems in *Escherichia coli*. Journal of Bacteriology, **110**, 1032-1040.

Eswayah, A. S., Smith, T. J. & Gardiner, P. H. 2016. Microbial transformations of selenium species of relevance to bioremediation. Applied and Environmental Microbiology, **82**, 4848-4859.

Eysel, H. & Sunder, S. 1979. Homonuclear bonds in sulfur-selenium mixed crystals: a Raman spectroscopic study. Inorganic Chemistry, **18**, 2626-2627.

Fairweather-Tait, S. J., Collings, R. & Hurst, R. 2010. Selenium bioavailability: current knowledge and future research requirements. The American Journal of Clinical Nutrition, **91**, 1484S-1491S.

Fan, T. W., Lane, A. N. & Higashi, R. M. 1997. Selenium biotransformations by a *euryhaline microalga* isolated from a saline evaporation pond. Environmental Science & Technology, **31**, 569-576.

Fellowes, J., Pattrick, R., Green, D., Dent, A., Lloyd, J. & Pearce, C. 2011. Use of biogenic and abiotic elemental selenium nanospheres to sequester elemental mercury released from mercury contaminated museum specimens. Journal of Hazardous Materials, **189**, 660-669.

Ferreira, I., Ferreira-Strixino, J., Castilho, M. L., Campos, C. B., Tellez, C. & Raniero, L. 2016. Characterization of *Paracoccidioides brasiliensis* by FT-IR spectroscopy and nanotechnology. Spectrochimica Acta Part A: Molecular and Biomolecular Spectroscopy, **152**, 397-403.

Finn, D., Dalal, R. & Klieve, A. 2015. Methane in Australian agriculture: current emissions, sources and sinks, and potential mitigation strategies. Crop and Pasture Science, **66**, 1-22.

Fleming, R. W. & Alexander, M. 1972. Dimethylselenide and dimethyltelluride formation by a strain of *Penicillium*. Applied Microbiology, **24**, 424-429.

Flohe, L., Günzler, W. & Schock, H. 1973. Glutathione peroxidase: a selenoenzyme. FEBS Letters, **32**, 132-134.

Flohé, L. 2011. Selenium and human health: Snapshots from the frontiers of selenium biomedicine. In: Selenium and Tellurium Chemistry (Ed. by Anonymous), pp. 285-302. Springer.

- Forchhammer, K. & Bock, A.** 1991. Selenocysteine synthase from *Escherichia coli*. Analysis of the reaction sequence. *The Journal of biological chemistry*, **266**, 6324-6328.
- Fordyce, F. M.** 2013. Selenium deficiency and toxicity in the environment. In: *Essentials of Medical Geology* (Ed. by Anonymous), pp. 375-416. Springer.
- Forootanfar, H., Adeli-Sardou, M., Nikkhoo, M., Mehrabani, M., Amir-Heidari, B., Shahverdi, A. R. & Shakibaie, M.** 2014. Antioxidant and cytotoxic effect of biologically synthesized selenium nanoparticles in comparison to selenium dioxide. *Journal of Trace Elements in Medicine and Biology*, **28**, 75-79.
- Francis, A. J., Duxbury, J. M. & Alexander, M.** 1974. Evolution of dimethylselenide from soils. *Applied Microbiology*, **28**, 248-250.
- Franke, K. W. & Moxon, A. L.** 1936. A comparison of the minimum fatal doses of selenium, tellurium, arsenic and vanadium. *Journal of Pharmacology and Experimental Therapeutics*, **58**, 454-459.
- Frankenberger, W. T. & Engberg, R. A.** 1998. *Environmental Chemistry of Selenium*. CRC Press.
- Fujita, M., Ike, M., Kashiwa, M., Hashimoto, R. & Soda, S.** 2002. Laboratory-scale continuous reactor for soluble selenium removal using selenate-reducing bacterium, *Bacillus* sp. SF-1. *Biotechnology and Bioengineering*, **80**, 755-761.
- Fujita, M., Ike, M., Nishimoto, S., Takahashi, K. & Kashiwa, M.** 1997. Isolation and characterization of a novel selenate-reducing bacterium, *Bacillus* sp. SF-1. *Journal of Fermentation and Bioengineering*, **83**, 517-522.
- Ge, K. & Yang, G.** 1993. The epidemiology of selenium deficiency in the etiological study of endemic diseases in China. *The American Journal of Clinical Nutrition*, **57**, 259S-263S.
- Gerhardt, M. B., Green, F. B., Newman, R. D., Lundquist, T. J., Tresan, R. B. & Oswald, W. J.** 1991. Removal of selenium using a novel algal-bacterial process. *Research Journal of the Water Pollution Control Federation*, July 1, 799-805.
- Gupta, S., Nagaraja, T. P. G. & Prakash, R. G.** 2012. Studies on the role of microorganisms in mobilization of selenium in seleniferous soils. (Doctoral dissertation, Thapar University, Patiala, India).
- Güven, K., Mutlu, M. B., Çirpan, C. & Kutlu, H. M.** 2013. Isolation and identification of selenite reducing archaea from Tuz (salt) Lake In Turkey. *Journal of Basic Microbiology*, **53**, 397-401.
- Han, X. & Gu, J.** 2010. Sorption and transformation of toxic metals by microorganisms. *Environ Microbiol*, 2nd edn. Wiley, New York, , 153-176.

- Hansen, D., Duda, P. J., Zayed, A. & Terry, N.** 1998. Selenium removal by constructed wetlands: role of biological volatilization. *Environmental Science & Technology*, **32**, 591-597.
- Hanson, R. S. & Hanson, T. E.** 1996. Methanotrophic bacteria. *Microbiological Reviews*, **60**, 439-471.
- Harrison, G., Curle, C. & Laishley, E. J.** 1984. Purification and characterization of an inducible dissimilatory type sulfite reductase from *Clostridium pasteurianum*. *Archives of Microbiology*, **138**, 72-78.
- Haug, A., Graham, R. D., Christophersen, O. A. & Lyons, G. H.** 2007. How to use the world's scarce selenium resources efficiently to increase the selenium concentration in food. *Microbial Ecology in Health and Disease*, **19**, 209-228.
- Haygarth, P. M.** 1994. Global importance and global cycling of selenium. *Selenium in the Environment*, June 10, 1-27.
- Heider, J. & Bock, A.** 1993. Selenium metabolism in micro-organisms. *Advances in Microbial Physiology*, **35**, 71-109.
- Herbel, M. J., Blum, J. S., Oremland, R. S. & Borglin, S. E.** 2003. Reduction of elemental selenium to selenide: experiments with anoxic sediments and bacteria that respire Se-oxyanions. *Geomicrobiology Journal*, **20**, 587-602.
- Higashi, R. M., Cassel, T. A., Skorupa, J. P. & Fan, T. W.** 2005. Remediation and bioremediation of selenium-contaminated waters. *Water Encyclopedia*.
- Hockin, S. L. & Gadd, G. M.** 2003. Linked redox precipitation of sulfur and selenium under anaerobic conditions by sulfate-reducing bacterial biofilms. *Applied and Environmental Microbiology*, **69**, 7063-7072.
- Hsieh, H. S. & Ganther, H. E.** 1975. Acid-volatile selenium formation catalyzed by glutathione reductase. *Biochemistry*, **14**, 1632-1636.
- Huang, J., Suarez, M. C., Yang, S. I., Lin, Z. & Terry, N.** 2013. Development of a constructed wetland water treatment system for selenium removal: incorporation of an algal treatment component. *Environmental Science & Technology*, **47**, 10518-10525.
- Huber, R., Sacher, M., Vollmann, A., Huber, H. & Rose, D.** 2000. Respiration of arsenate and selenate by hyperthermophilic archaea. *Systematic and Applied Microbiology*, **23**, 305-314.
- Hunsaker, D. M., Spiller, H. A. & Williams, D.** 2005. Acute selenium poisoning: suicide by ingestion. *Journal of Forensic Science*, **50**, JFS2004247-5.
- Hunter, R. J.** 2013. *Zeta Potential in Colloid Science: Principles and Applications*. Academic press.

- Hunter, W. J.** 2014a. *Pseudomonas seleniipraecipitans* proteins potentially involved in selenite reduction. *Current Microbiology*, **69**, 69-74.
- Hunter, W. J.** 2007. An *Azospira oryzae* (syn *Dechlorosoma suillum*) strain that reduces selenate and selenite to elemental red selenium. *Current Microbiology*, **54**, 376-381.
- Hunter, W. J. & Manter, D. K.** 2009. Reduction of selenite to elemental red selenium by *Pseudomonas* sp. strain CA5. *Current Microbiology*, **58**, 493-498.
- Hunter, W. J. & Manter, D. K.** 2008. Bio-reduction of selenite to elemental red selenium by *Tetrathiebacter kashmirensis*. *Current Microbiology*, **57**, 83-88.
- Hunter, W.** 2014b. A *Rhizobium selenitireducens* protein showing selenite reductase activity. *Current Microbiology*, **68**, 311-316.
- Ike, M., Soda, S. & Kuroda, M.** 2017. Bioprocess approaches for the removal of selenium from industrial waste and wastewater by *pseudomonas stutzeri* NT-I. In: *Bioremediation of Selenium Contaminated Wastewater* (Ed. by Anonymous), pp. 57-73. Springer.
- Ike, M., Takahashi, K., Fujita, T., Kashiwa, M. & Fujita, M.** 2000. Selenate reduction by bacteria isolated from aquatic environment free from selenium contamination. *Water Research*, **34**, 3019-3025.
- Iranifam, M., Fathinia, M., Rad, T. S., Hanifehpour, Y., Khataee, A. & Joo, S.** 2013. A novel selenium nanoparticles-enhanced chemiluminescence system for determination of dinitrobutylphenol. *Talanta*, **107**, 263-269.
- Jain, R., Jordan, N., Tsushima, S., Hübner, R., Weiss, S. & Lens, P. N.** 2017. Shape change of biogenic elemental selenium nanomaterials from nanospheres to nanorods decreases their colloidal stability. *Environmental Science: Nano*, **4**, 1054-1063.
- Jain, R., Matassa, S., Singh, S., van Hullebusch, E. D., Esposito, G. & Lens, P. N.** 2016. Reduction of selenite to elemental selenium nanoparticles by activated sludge. *Environmental Science and Pollution Research*, **23**, 1193-1202.
- Jain, R., Gonzalez-Gil, G., Singh, V., Van Hullebusch, E., Farges, F. & Lens, P.** 2014. Biogenic selenium nanoparticles: production, characterization and challenges. *Nanobiotechnology*, Studium Press LLC, USA, , 361-390.
- Jain, R., Jordan, N., Schild, D., Van Hullebusch, E. D., Weiss, S., Franzen, C., Farges, F., Hübner, R. & Lens, P. N.** 2015a. Adsorption of zinc by biogenic elemental selenium nanoparticles. *Chemical Engineering Journal*, **260**, 855-863.
- Jain, R., Jordan, N., Weiss, S., Foerstendorf, H., Heim, K., Kacker, R., Hübner, R., Kramer, H., Van Hullebusch, E. D. & Farges, F.** 2015b. Extracellular polymeric substances govern the surface charge of biogenic elemental selenium nanoparticles. *Environmental Science & Technology*, **49**, 1713-1720.

- Janz, D. M.** 2011. 7 - Selenium. *Fish Physiology*, **31, Part A**, 327-374.
- Jiang, H., Chen, Y., Jiang, P., Zhang, C., Smith, T. J., Murrell, J. C. & Xing, X.** 2010. Methanotrophs: multifunctional bacteria with promising applications in environmental bioengineering. *Biochemical Engineering Journal*, **49**, 277-288.
- Jiang, S., Ho, C. T., Lee, J., Van Duong, H., Han, S. & Hur, H.** 2012. Mercury capture into biogenic amorphous selenium nanospheres produced by mercury resistant *Shewanella putrefaciens* 200. *Chemosphere*, **87**, 621-624.
- Johansson, L., Gafvelin, G. & Arnér, E. S.** 2005. Selenocysteine in proteins—properties and biotechnological use. *Biochimica et Biophysica Acta (BBA)-General Subjects*, **1726**, 1-13.
- Johnson, N. C., Manchester, S., Sarin, L., Gao, Y., Kulaots, I. & Hurt, R. H.** 2008. Mercury vapor release from broken compact fluorescent lamps and in situ capture by new nanomaterial sorbents. *Environmental Science & Technology*, **42**, 5772-5778.
- Johnson, P. I., Gersberg, R. M., Rigby, M. & Roy, S.** 2009. The fate of selenium in the Imperial and Brawley constructed wetlands in the Imperial Valley (California). *Ecological Engineering*, **35**, 908-913.
- Kagami, T., Narita, T., Kuroda, M., Notaguchi, E., Yamashita, M., Sei, K., Soda, S. & Ike, M.** 2013. Effective selenium volatilization under aerobic conditions and recovery from the aqueous phase by *Pseudomonas stutzeri* NT-I. *Water Research*, **47**, 1361-1368.
- Kalidass, B.** 2016. Investigating the Impact of Metals and Methanobactin on Gene Expression in *Methylosinus Trichosporium* Ob3b.
- Kamnev, A. A.** 2008. FTIR spectroscopic studies of bacterial cellular responses to environmental factors, plant-bacterial interactions and signalling. *Journal of Spectroscopy*, **22**, 83-95.
- Kamnev, A. A., Mamchenkova, P. V., Dyatlova, Y. A. & Tugarova, A. V.** 2017. FTIR spectroscopic studies of selenite reduction by cells of the rhizobacterium *Azospirillum brasilense* Sp7 and the formation of selenium nanoparticles. *Journal of Molecular Structure*, **1140**, 106-112.
- Karle, J. A. & Shrift, A.** 1986. Use of selenite, selenide, and selenocysteine for the synthesis of formate dehydrogenase by a cysteine-requiring mutant of *Escherichia coli* K-12. *Biological Trace Element Research*, **11**, 27-35.
- Kashiwa, M., Nishimoto, S., Takahashi, K., Ike, M. & Fujita, M.** 2000. Factors affecting soluble selenium removal by a selenate-reducing bacterium *Bacillus* sp. SF-1. *Journal of Bioscience and Bioengineering*, **89**, 528-533.
- Kaur, G., Iqbal, M. & Bakshi, M. S.** 2009. Biomineralization of fine selenium crystalline rods and amorphous spheres. *The Journal of Physical Chemistry C*, **113**, 13670-13676.

Kenney, G. E., Goering, A. W., Ross, M. O., DeHart, C. J., Thomas, P. M., Hoffman, B. M., Kelleher, N. L. & Rosenzweig, A. C. 2016. Characterization of methanobactin from *Methylosinus* sp. LW4. *Journal of the American Chemical Society*, **138**, 11124-11127.

Kessi, J. 2006. Enzymic systems proposed to be involved in the dissimilatory reduction of selenite in the purple non-sulfur bacteria *Rhodospirillum rubrum* and *Rhodobacter capsulatus*. *Microbiology*, **152**, 731-743.

Kessi, J. & Hanselmann, K. W. 2004. Similarities between the abiotic reduction of selenite with glutathione and the dissimilatory reaction mediated by *Rhodospirillum rubrum* and *Escherichia coli*. *The Journal of Biological Chemistry*, **279**, 50662-50669.

Kessi, J., Ramuz, M., Wehrli, E., Spycher, M. & Bachofen, R. 1999. Reduction of selenite and detoxification of elemental selenium by the phototrophic bacterium *Rhodospirillum rubrum*. *Applied and Environmental Microbiology*, **65**, 4734-4740.

Khiralla, G. M. & El-Deeb, B. A. 2015. Antimicrobial and antibiofilm effects of selenium nanoparticles on some foodborne pathogens. *LWT-Food Science and Technology*, **63**, 1001-1007.

Khoei, N. S., Lampis, S., Zonaro, E., Yrjälä, K., Bernardi, P. & Vallini, G. 2017. Insights into selenite reduction and biogenesis of elemental selenium nanoparticles by two environmental isolates of *Burkholderia fungorum*. *New Biotechnology*, **34**, 1-11.

Kieliszek, M. & Błażej, S. 2013. Selenium: significance, and outlook for supplementation. *Nutrition*, **29**, 713-718.

Kikuchi, T., Iwasaki, K., Nishihara, H., Takamura, Y. & Yagi, O. 2002. Quantitative and rapid detection of the trichloroethylene-degrading bacterium *Methylocystis* sp. M in groundwater by real-time PCR. *Applied Microbiology and Biotechnology*, **59**, 731-736.

Kim, H. J., Graham, D. W., DiSpirito, A. A., Alterman, M. A., Galeva, N., Larive, C. K., Asunskis, D. & Sherwood, P. M. 2004. Methanobactin, a copper-acquisition compound from methane-oxidizing bacteria. *Science (New York, N.Y.)*, **305**, 1612-1615.

Klonowska, A., Heulin, T. & Vermeglio, A. 2005. Selenite and tellurite reduction by *Shewanella oneidensis*. *Applied and Environmental Microbiology*, **71**, 5607-5609.

Knapp, C. W., Fowle, D. A., Kulczycki, E., Roberts, J. A. & Graham, D. W. 2007. Methane monooxygenase gene expression mediated by methanobactin in the presence of mineral copper sources. *Proceedings of the National Academy of Sciences of the United States of America*, **104**, 12040-12045. doi: 0702879104 [pii].

Kong, H., Yang, J., Zhang, Y., Fang, Y., Nishinari, K. & Phillips, G. O. 2014. Synthesis and antioxidant properties of gum arabic-stabilized selenium nanoparticles. *International Journal of Biological Macromolecules*, **65**, 155-162.

- Kora, A. J. & Rastogi, L.** 2016. Biomimetic synthesis of selenium nanoparticles by *Pseudomonas aeruginosa* ATCC 27853: An approach for conversion of selenite. *Journal of Environmental Management*, **181**, 231-236.
- Kramer, G. F. & Ames, B. N.** 1988. Mechanisms of mutagenicity and toxicity of sodium selenite (Na_2SeO_3) in *Salmonella typhimurium*. *Mutation Research/Fundamental and Molecular Mechanisms of Mutagenesis*, **201**, 169-180.
- Krentz, B. D., Mulheron, H. J., Semrau, J. D., DiSpirito, A. A., Bandow, N. L., Haft, D. H., Vuilleumier, S., Murrell, J. C., McEllistrem, M. T. & Hartsel, S. C.** 2010. A comparison of methanobactins from *Methylosinus trichosporium* OB3b and *Methylocystis* strain SB2 predicts methanobactins are synthesized from diverse peptide precursors modified to create a common core for binding and reducing copper ions. *Biochemistry*, **49**, 10117-10130.
- Kumar, S., Tomar, M. S. & Acharya, A.** 2015. Carboxylic group-induced synthesis and characterization of selenium nanoparticles and its anti-tumor potential on Dalton's lymphoma cells. *Colloids and Surfaces B: Biointerfaces*, **126**, 546-552.
- Kuroda, M., Notaguchi, E., Sato, A., Yoshioka, M., Hasegawa, A., Kagami, T., Narita, T., Yamashita, M., Sei, K. & Soda, S.** 2011. Characterization of *Pseudomonas stutzeri* NT-I capable of removing soluble selenium from the aqueous phase under aerobic conditions. *Journal of Bioscience and Bioengineering*, **112**, 259-264.
- Kuzmin, P. G., Shafeev, G. A., Voronov, V. V., Raspopov, R. V., Arianova, E., Trushina, E., Gmoshinskii, I. V. & Khotimchenko, S. A.** 2012. Bioavailable nanoparticles obtained in laser ablation of a selenium target in water. *Quantum Electronics*, **42**, 1042.
- Lai, C., Yang, X., Tang, Y., Rittmann, B. E. & Zhao, H.** 2014. Nitrate shaped the selenate-reducing microbial community in a hydrogen-based biofilm reactor. *Environmental Science & Technology*, **48**, 3395-3402.
- Lai, C., Zhong, L., Zhang, Y., Chen, J., Wen, L., Shi, L., Sun, Y., Ma, F., Rittmann, B. E. & Zhou, C.** 2016a. Bio-reduction of chromate in a methane-based membrane biofilm reactor. *Environmental Science & Technology*, **50**(11), 5832-5839.
- Lai, C., Wen, L., Shi, L., Zhao, K., Wang, Y., Yang, X., Rittmann, B. E., Zhou, C., Tang, Y. & Zheng, P.** 2016b. Selenate and nitrate bioreductions using methane as the electron donor in a membrane biofilm reactor. *Environmental Science & Technology*, **50**, 10179-10186.
- Lampis, S., Zonaro, E., Bertolini, C., Cecconi, D., Monti, F., Micaroni, M., Turner, R. J., Butler, C. S. & Vallini, G.** 2017. Selenite biotransformation and detoxification by *Stenotrophomonas maltophilia* SeITE02: novel clues on the route to bacterial biogenesis of selenium nanoparticles. *Journal of Hazardous Materials*, **324**, 3-14.
- Langi, B., Shah, C., Singh, K., Chaskar, A., Kumar, M. & Bajaj, P. N.** 2010. Ionic liquid-induced synthesis of selenium nanoparticles. *Materials Research Bulletin*, **45**, 668-671.

- Lawson, S. & Macy, J.** 1995. Bioremediation of selenite in oil refinery wastewater. *Applied Microbiology and Biotechnology*, **43**, 762-765.
- Lenz, M. & Lens, P. N.** 2009. The essential toxin: the changing perception of selenium in environmental sciences. *Science of the Total Environment*, **407**, 3620-3633.
- Lenz, M., Kolvenbach, B., Gyax, B., Moes, S. & Corvini, P. F.** 2011. Shedding light on selenium biomineralization: proteins associated with bionanominerals. *Applied and Environmental Microbiology*, **77**, 4676-4680.
- Letavayová, L., Vlčková, V. & Brozmanová, J.** 2006. Selenium: from cancer prevention to DNA damage. *Toxicology*, **227**, 1-14.
- Letavayová, L., Vlasáková, D., Spallholz, J. E., Brozmanová, J. & Chovanec, M.** 2008. Toxicity and mutagenicity of selenium compounds in *Saccharomyces cerevisiae*. *Mutation Research/Fundamental and Molecular Mechanisms of Mutagenesis*, **638**, 1-10.
- Li, B., Liu, N., Li, Y., Jing, W., Fan, J., Li, D., Zhang, L., Zhang, X., Zhang, Z. & Wang, L.** 2014a. Reduction of selenite to red elemental selenium by *Rhodopseudomonas palustris* strain N. *PloS one*, **9**, e95955.
- Li, D., Cheng, Y., Wu, C., Li, W., Li, N., Yang, Z., Tong, Z. & Yu, H.** 2014b. Selenite reduction by *Shewanella oneidensis* MR-1 is mediated by fumarate reductase in periplasm. *Scientific Reports*, **4**, 3735.
- Lipman, J. G. & Waksman, S. A.** 1923. The oxidation of selenium by a new group of autotrophic microorganisms. *Science (New York, N.Y.)*, **57**, 60.
- Lontoh, S. & Semrau, J. D.** 1998. Methane and trichloroethylene degradation by *Methylosinus trichosporium* OB3b expressing particulate methane monooxygenase. *Applied and Environmental Microbiology*, **64**, 1106-1114.
- Lortie, L., Gould, W. D., Rajan, S., McCready, R. G. & Cheng, K. J.** 1992. Reduction of selenate and selenite to elemental selenium by a *Pseudomonas stutzeri* isolate. *Applied and Environmental Microbiology*, **58**, 4042-4044.
- Losi, M. & Frankenberger, W.** 1998. Microbial oxidation and solubilization of precipitated elemental selenium in soil. *Journal of Environmental Quality*, **27**, 836-843.
- Losi, M. E. & Frankenberger, W. T.** 1997. Reduction of selenium oxyanions by *Enterobacter cloacae* SLD1a-1: Isolation and growth of the bacterium and its expulsion of selenium particles. *Applied and Environmental Microbiology*, **63**, 3079-3084.
- Lovley, D. R., Fraga, J. L., Coates, J. D. & Blunt-Harris, E. L.** 1999. Humics as an electron donor for anaerobic respiration. *Environmental Microbiology*, **1**, 89-98.

- Lucovsky, G., Mooradian, A., Taylor, W., Wright, G. & Keezer, R.** 1967. Identification of the fundamental vibrational modes of trigonal, α -monoclinic and amorphous selenium. *Solid State Communications*, **5**, 113-117.
- Lukács, R., Veres, M., Shimakawa, K. & Kugler, S.** 2010. On photoinduced volume change in amorphous selenium: Quantum chemical calculation and Raman spectroscopy. *Journal of Applied Physics*, **107**, 073517.
- Macy, J.** 1994. Biochemistry of selenium metabolism by *Thauera selenatis* gen. nov. sp. nov. and use of the organism for bioremediation of selenium oxyanions in San Joaquin Valley drainage water. *Selenium in the Environment*. Marcel Dekker, New York, NY, 421-444.
- Macy, J. M., Lawson, S. & DeMoll-Decker, H.** 1993. Bioremediation of selenium oxyanions in San Joaquin drainage water using *Thauera selenatis* in a biological reactor system. *Applied Microbiology and Biotechnology*, **40**, 588-594.
- Matoba, R., Kimura, H., Uchima, E., Abe, T., Yamada, T., Mitsukuni, Y. & Shikata, I.** 1986. An autopsy case of acute selenium (selenious acid) poisoning and selenium levels in human tissues. *Forensic Science International*, **31**, 87-92.
- McCarthy, S., Chasteen, T., Marshall, M., Fall, R. & Bachofen, R.** 1993. Phototrophic bacteria produce volatile, methylated sulfur and selenium compounds. *FEMS Microbiology Letters*, **112**, 93-97.
- McConnell, K. P. & Portman, O. W.** 1952. Toxicity of dimethyl selenide in the rat and mouse. *Proceedings of the Society for Experimental Biology and Medicine*, **79**, 230-231.
- McCready, R., Campbell, J. & Payne, J.** 1966. Selenite reduction by *Salmonella heidelberg*. *Canadian Journal of Microbiology*, **12**, 703-714.
- Merkx, M., Kopp, D. A., Sazinsky, M. H., Blazyk, J. L., Müller, J. & Lippard, S. J.** 2001. Dioxygen activation and methane hydroxylation by soluble methane monooxygenase: a tale of two irons and three proteins. *Angewandte Chemie International Edition*, **40**, 2782-2807.
- Michalke, K., Wickenheiser, E. B., Mehring, M., Hirner, A. V. & Hensel, R.** 2000. Production of volatile derivatives of metal(loid)s by microflora involved in anaerobic digestion of sewage sludge. *Applied and Environmental Microbiology*, **66**, 2791-2796.
- Mishra, R. R., Prajapati, S., Das, J., Dangar, T. K., Das, N. & Thatoi, H.** 2011. Reduction of selenite to red elemental selenium by moderately halotolerant *Bacillus megaterium* strains isolated from Bhitarkanika mangrove soil and characterization of reduced product. *Chemosphere*, **84**, 1231-1237.
- Moussard, H., Stralis-Pavese, N., Bodrossy, L., Neufeld, J. D. & Murrell, J. C.** 2009. Identification of active methylotrophic bacteria inhabiting surface sediment of a marine estuary. *Environmental Microbiology Reports*, **1**, 424-433.

- Moxon, A. L.** 1937. Alkali disease or selenium poisoning.
- Murrell, J. C., Gilbert, B. & McDonald, I. R.** 2000. Molecular biology and regulation of methane monooxygenase. *Archives of Microbiology*, **173**, 325-332.
- Nancharaiah, Y. V. & Lens, P. N.** 2015a. Selenium biomineralization for biotechnological applications. *Trends in Biotechnology*, **33**, 323-330.
- Nancharaiah, Y. V. & Lens, P. N.** 2015b. Ecology and biotechnology of selenium-respiring bacteria. *Microbiology and Molecular Biology Reviews : MMBR*, **79**, 61-80.
- Narasingarao, P. & Haggblom, M. M.** 2007. Identification of anaerobic selenate-respiring bacteria from aquatic sediments. *Applied and Environmental Microbiology*, **73**, 3519-3527.
- National Research council.** 2005. Mineral Tolerance of Animals. National Academy Press, Washington, DC.
- National Research Council.** 1983. Selenium in Nutrition: Revised Edition. National Academies Press.
- National Research Council (US). Subcommittee on Mineral Toxicity in Animals.** 1980. Mineral Tolerance of Domestic Animals. : National Academies Press.
- Naumann, D., Keller, S., Helm, D., Schultz, C. & Schrader, B.** 1995. FT-IR spectroscopy and FT-Raman spectroscopy are powerful analytical tools for the non-invasive characterization of intact microbial cells. *Journal of Molecular Structure*, **347**, 399-405.
- Neumann, P., De Souza, M., Pickering, I. & Terry, N.** 2003. Rapid microalgal metabolism of selenate to volatile dimethylselenide. *Plant, Cell & Environment*, **26**, 897-905.
- Nuttall, K. L.** 2006. Evaluating selenium poisoning. *Annals of Clinical and Laboratory Science*, **36**, 409-420.
- Oehme, F. W.** 1972. Mechanisms of heavy metal toxicities. *Clinical toxicology*, **5**, 151-167.
- Ojeda, J. J. & Dittrich, M.** 2012. Fourier transform infrared spectroscopy for molecular analysis of microbial cells. *Microbial Systems Biology: Methods and Protocols*, 187-211.
- Ojeda, J. J., Romero-González, M. E., Bachmann, R. T., Edyvean, R. G. & Banwart, S. A.** 2008. Characterization of the cell surface and cell wall chemistry of drinking water bacteria by combining XPS, FTIR spectroscopy, modeling, and potentiometric titrations. *Langmuir*, **24**, 4032-4040.
- Okano, K., Saito, I., Mine, T., Suzuki, Y., Yamada, T., Rupesinghe, N., Amaratunga, G., Milne, W. & Zahn, D.** 2007. Characterizations of a-Se based photodetectors using X-ray

photoelectron spectroscopy and Raman spectroscopy. *Journal of Non-Crystalline Solids*, **353**, 308-312.

Oldfield, J. 2002. A brief history of selenium research: From alkali disease to prostate cancer (from poison to prevention). *J Anim Sci. Online supplement*, **14**.

Oremland, R. S. & Zehr, J. P. 1986. Formation of methane and carbon dioxide from dimethylselenide in anoxic sediments and by a methanogenic bacterium. *Applied and Environmental Microbiology*, **52**, 1031-1036.

Oremland, R. S., Steinberg, N. A., Presser, T. S. & Miller, L. G. 1991. In situ bacterial selenate reduction in the agricultural drainage systems of western Nevada. *Applied and Environmental Microbiology*, **57**, 615-617.

Oremland, R. S., Hollibaugh, J. T., Maest, A. S., Presser, T. S., Miller, L. G. & Culbertson, C. W. 1989. Selenate reduction to elemental selenium by anaerobic bacteria in sediments and culture: biogeochemical significance of a novel, sulfate-independent respiration. *Applied and Environmental Microbiology*, **55**, 2333-2343.

Oremland, R. S., Blum, J. S., Culbertson, C. W., Visscher, P. T., Miller, L. G., Dowdle, P. & Strohmaier, F. E. 1994. Isolation, growth, and metabolism of an obligately anaerobic, selenate-respiring bacterium, strain SES-3. *Applied and Environmental Microbiology*, **60**, 3011-3019.

Oremland, R. S., Herbel, M. J., Blum, J. S., Langley, S., Beveridge, T. J., Ajayan, P. M., Sutto, T., Ellis, A. V. & Curran, S. 2004. Structural and spectral features of selenium nanospheres produced by Se-respiring bacteria. *Applied and Environmental Microbiology*, **70**, 52-60.

Oyamada, N., Takahashi, G. & Ishizaki, M. 1991. Methylation of inorganic selenium compounds by freshwater green algae, *Ankistrodesmus* sp., *Chlorella vulgaris* and *Selenastrum* sp. *Eisei Kagaku*, **37**, 83-88.

Painter, E. P. 1941. The chemistry and toxicity of selenium compounds, with special reference to the selenium problem. *Chemical Reviews*, **28**, 179-213.

Pandey, V. C., Singh, J. S., Singh, D. & Singh, R. P. 2014. Methanotrophs: promising bacteria for environmental remediation. *International Journal of Environmental Science and Technology*, **11**, 241-250.

Papp, L. V., Lu, J., Holmgren, A. & Khanna, K. K. 2007. From selenium to selenoproteins: synthesis, identity, and their role in human health. *Antioxidants & Redox Signaling*, **9**, 775-806.

Patching, S. & Gardiner, P. 1999. Recent developments in selenium metabolism and chemical speciation: a review. *Journal of Trace Elements in Medicine and biology*, **13**, 193-214.

- Pearce, C. I., Pattrick, R. A., Law, N., Charnock, J. M., Coker, V. S., Fellowes, J. W., Oremland, R. S. & Lloyd, J. R.** 2009. Investigating different mechanisms for biogenic selenite transformations: *Geobacter sulfurreducens*, *Shewanella oneidensis* and *Veillonella atypica*. *Environmental Technology*, **30**, 1313-1326.
- Pearce, C. I., Coker, V. S., Charnock, J. M., Pattrick, R. A., Mosselmans, J. F. W., Law, N., Beveridge, T. J. & Lloyd, J. R.** 2008. Microbial manufacture of chalcogenide-based nanoparticles via the reduction of selenite using *Veillonella atypica*: an in situ EXAFS study. *Nanotechnology*, **19**, 155603.
- Pereg, L., de-Bashan, L. E. & Bashan, Y.** 2016. Assessment of affinity and specificity of *Azospirillum* for plants. *Plant and Soil*, **399**, 389-414.
- Pester, M., Friedrich, M. W., Schink, B. & Brune, A.** 2004. *pmoA*-based analysis of methanotrophs in a littoral lake sediment reveals a diverse and stable community in a dynamic environment. *Applied and Environmental Microbiology*, **70**, 3138-3142.
- Pickering, I., George, G. N., Van Fleet-Stalder, V., Chasteen, T. G. & Prince, R. C.** 1999. X-ray absorption spectroscopy of selenium-containing amino acids. *Journal of Biological Inorganic Chemistry*, **4**, 791-794.
- Pickering, I. J., Brown, G. E. & Tokunaga, T. K.** 1995. Quantitative speciation of selenium in soils using X-ray absorption spectroscopy. *Environmental Science & Technology*, **29**, 2456-2459.
- Pinsent, J.** 1954. The need for selenite and molybdate in the formation of formic dehydrogenase by members of the coli-aerogenes group of bacteria. *The Biochemical Journal*, **57**, 10-16.
- Prakash, N. T., Sharma, N., Prakash, R., Raina, K. K., Fellowes, J., Pearce, C. I., Lloyd, J. R. & Pattrick, R. A.** 2009. Aerobic microbial manufacture of nanoscale selenium: exploiting nature's bio-nanomineralization potential. *Biotechnology Letters*, **31**, 1857.
- Prasad, G.** 2009. Biomedical applications of nanoparticles. In: *Safety of Nanoparticles* (Ed. by Anonymous), pp. 89-109. Springer.
- Presser, T. S. & Ohlendorf, H. M.** 1987. Biogeochemical cycling of selenium in the San Joaquin Valley, California, USA. *Environmental Management*, **11**, 805-821.
- Pyrzynska, K.** 1998. Speciation of selenium compounds. *Analytical Sciences*, **14**, 479-483.
- Qin, H., Zhu, J., Liang, L., Wang, M. & Su, H.** 2013. The bioavailability of selenium and risk assessment for human selenium poisoning in high-Se areas, China. *Environment International*, **52**, 66-74.
- Quadrani, D. A., Spiller, H. A. & Steinhorn, D.** 2000. A fatal case of gun blue ingestion in a toddler. *Veterinary and Human Toxicology*, **42**, 96-98.

- Quintana, M., Haro-Poniatowski, E., Morales, J. & Batina, N.** 2002. Synthesis of selenium nanoparticles by pulsed laser ablation. *Applied Surface Science*, **195**, 175-186.
- Rael, R. & Frankenberger, W.** 1996. Influence of pH, salinity, and selenium on the growth of *Aeromonas veronii* in evaporation agricultural drainage water. *Water Research*, **30**, 422-430.
- Rajalakshmi, M. & Arora, A. K.** 1999. Vibrational spectra of selenium nanoparticles dispersed in a polymer. *Nanostructured materials*, **11**, 399-405.
- Ramos, J. F.** 2012. Selenium Nanoparticles for the Prevention of Polyvinyl Chloride-related Medical Infections. (Doctoral dissertation, Division of Engineering, Brown University).
- Ramos, J. F. & Webster, T. J.** 2012. Cytotoxicity of selenium nanoparticles in rat dermal fibroblasts. *International Journal of Nanomedicine*, **7**, 3907-3914.
- Ramya, S., Shanmugasundaram, T. & Balagurunathan, R.** 2015. Biomedical potential of actinobacterially synthesized selenium nanoparticles with special reference to anti-biofilm, anti-oxidant, wound healing, cytotoxic and anti-viral activities. *Journal of Trace Elements in Medicine and Biology*, **32**, 30-39.
- Ranjard, L., Prigent-Combaret, C., Favre-Bonté, S., Monnez, C., Nazaret, S. & Cournoyer, B.** 2004. Characterization of a novel selenium methyltransferase from freshwater bacteria showing strong similarities with the calicheamicin methyltransferase. *Biochimica et Biophysica Acta (BBA)-Gene Structure and Expression*, **1679**, 80-85.
- Ranjard, L., Nazaret, S. & Cournoyer, B.** 2003. Freshwater bacteria can methylate selenium through the thiopurine methyltransferase pathway. *Applied and Environmental Microbiology*, **69**, 3784-3790.
- Ranjard, L., Prigent-Combaret, C., Nazaret, S. & Cournoyer, B.** 2002. Methylation of inorganic and organic selenium by the bacterial thiopurine methyltransferase. *Journal of Bacteriology*, **184**, 3146-3149.
- Rasigraf, O., Kool, D. M., Jetten, M. S., Sinninghe Damste, J. S. & Ettwig, K. F.** 2014. Autotrophic carbon dioxide fixation via the Calvin-Benson-Bassham cycle by the denitrifying methanotroph "*Candidatus* Methylomirabilis oxyfera". *Applied and Environmental Microbiology*, **80**, 2451-2460.
- Reamer, D. C. & Zoller, W. H.** 1980. Selenium biomethylation products from soil and sewage sludge. *Science (New York, N.Y.)*, **208**, 500-502. doi: 208/4443/500 [pii].
- Ren, Y., Zhao, T., Mao, G., Zhang, M., Li, F., Zou, Y., Yang, L. & Wu, X.** 2013. Antitumor activity of hyaluronic acid-selenium nanoparticles in Heps tumor mice models. *International Journal of Biological Macromolecules*, **57**, 57-62.

- Ressler, T.** 1998. WinXAS: a program for X-ray absorption spectroscopy data analysis under MS-Windows. *Journal of Synchrotron Radiation*, **5**, 118-122.
- Rezvanfar, M. A., Rezvanfar, M. A., Shahverdi, A. R., Ahmadi, A., Baeeri, M., Mohammadirad, A. & Abdollahi, M.** 2013. Protection of cisplatin-induced spermatotoxicity, DNA damage and chromatin abnormality by selenium nano-particles. *Toxicology and Applied Pharmacology*, **266**, 356-365.
- Ridley, H., Watts, C. A., Richardson, D. J. & Butler, C. S.** 2006. Resolution of distinct membrane-bound enzymes from *Enterobacter cloacae* SLD1a-1 that are responsible for selective reduction of nitrate and selenate oxyanions. *Applied and Environmental Microbiology*, **72**, 5173-5180.
- Rossberg, A., Reich, T. & Bernhard, G.** 2003. Complexation of uranium (VI) with protocatechuic acid—application of iterative transformation factor analysis to EXAFS spectroscopy. *Analytical and Bioanalytical Chemistry*, **376**, 631-638.
- Rotruck, J. T., Pope, A. L., Ganther, H. E., Swanson, A. B., Hafeman, D. G. & Hoekstra, W. G.** 1973. Selenium: biochemical role as a component of glutathione peroxidase. *Science (New York, N.Y.)*, **179**, 588-590.
- Roux, M., Sarret, G., Pignot-Paintrand, I., Fontecave, M. & Coves, J.** 2001. Mobilization of selenite by *Ralstonia metallidurans* CH34. *Applied and Environmental Microbiology*, **67**, 769-773.
- Roy, A. B. & Trudinger, P. A.** 1970. *The Biochemistry of Inorganic Compounds of Sulphur*. Cambridge University Press.
- Santos, S., Ungureanu, G., Boaventura, R. & Botelho, C.** 2015. Selenium contaminated waters: an overview of analytical methods, treatment options and recent advances in sorption methods. *Science of the Total Environment*, **521**, 246-260.
- Sarathchandra, S. U. & Watkinson, J. H.** 1981. Oxidation of elemental selenium to selenite by *Bacillus megaterium*. *Science (New York, N.Y.)*, **211**, 600-601.
- Sarret, G., Avoscan, L., Carriere, M., Collins, R., Geoffroy, N., Carrot, F., Coves, J. & Gouget, B.** 2005. Chemical forms of selenium in the metal-resistant bacterium *Ralstonia metallidurans* CH34 exposed to selenite and selenate. *Applied and Environmental Microbiology*, **71**, 2331-2337.
- Saulou, C., Jamme, F., Girbal, L., Maranges, C., Fourquaux, I., Coccagn-Bousquet, M., Dumas, P. & Mercier-Bonin, M.** 2013. Synchrotron FTIR microspectroscopy of *Escherichia coli* at single-cell scale under silver-induced stress conditions. *Analytical and Bioanalytical Chemistry*, **405**, 2685-2697.
- Scheinost, A. C. & Charlet, L.** 2008. Selenite reduction by mackinawite, magnetite and siderite: XAS characterization of nanosized redox products. *Environmental Science & Technology*, **42**, 1984-1989.

Scheinost, A. C., Kirsch, R., Banerjee, D., Fernandez-Martinez, A., Zaenker, H., Funke, H. & Charlet, L. 2008. X-ray absorption and photoelectron spectroscopy investigation of selenite reduction by Fe II-bearing minerals. *Journal of Contaminant Hydrology*, **102**, 228-245.

Schmidt, R., Tantoyotai, P., Fakra, S. C., Marcus, M. A., Yang, S. I., Pickering, I. J., Bañuelos, G. S., Hristova, K. R. & Freeman, J. L. 2013. Selenium biotransformations in an engineered aquatic ecosystem for bioremediation of agricultural wastewater via brine shrimp production. *Environmental Science & Technology*, **47**, 5057-5065.

Schrauzer, G. N. 2000. Selenomethionine: a review of its nutritional significance, metabolism and toxicity. *The Journal of Nutrition*, **130**, 1653-1656.

Schröder, I., Rech, S., Krafft, T. & Macy, J. M. 1997. Purification and characterization of the selenate reductase from *Thauera selenatis*. *Journal of Biological Chemistry*, **272**, 23765-23768.

Schwarz, K. & Foltz, C. M. 1957. Selenium as an integral part of factor 3 against dietary necrotic liver degeneration. *Journal of the American Chemical Society*, **79**, 3292-3293.

Scopigno, T., Steurer, W., Yannopoulos, S., Chrissanthopoulos, A., Krisch, M., Ruocco, G. & Wagner, T. 2011. Vibrational dynamics and surface structure of amorphous selenium. *Nature Communications*, **2**, 195.

Semrau, J. D., Jagadevan, S., DiSpirito, A. A., Khalifa, A., Scanlan, J., Bergman, B. H., Freemeier, B. C., Baral, B. S., Bandow, N. L. & Vorobev, A. 2013. Methanobactin and MmoD work in concert to act as the 'copper-switch' in methanotrophs. *Environmental Microbiology*, **15**, 3077-3086.

Semrau, J. D., DiSpirito, A. A. & Yoon, S. 2010. Methanotrophs and copper. *FEMS Microbiology Reviews*, **34**, 496-531.

Shah, C. P., Dwivedi, C., Singh, K. K., Kumar, M. & Bajaj, P. N. 2010. Riley oxidation: A forgotten name reaction for synthesis of selenium nanoparticles. *Materials Research Bulletin*, **45**, 1213-1217.

Shakibaie, M., Forootanfar, H., Golkari, Y., Mohammadi-Khorsand, T. & Shakibaie, M. R. 2015. Anti-biofilm activity of biogenic selenium nanoparticles and selenium dioxide against clinical isolates of *Staphylococcus aureus*, *Pseudomonas aeruginosa*, and *Proteus mirabilis*. *Journal of Trace Elements in Medicine and Biology*, **29**, 235-241.

Shakibaie, M., Khorramizadeh, M. R., Faramarzi, M. A., Sabzevari, O. & Shahverdi, A. R. 2010. Biosynthesis and recovery of selenium nanoparticles and the effects on matrix metalloproteinase-2 expression. *Biotechnology and Applied Biochemistry*, **56**, 7-15.

Shamberger, R. 2012. *Biochemistry of Selenium (Vol. 2)*: Springer Science & Business Media.

- Shirsat, S., Kadam, A., Naushad, M. & Mane, R. S.** 2015. Selenium nanostructures: microbial synthesis and applications. *Rsc Advances*, **5**, 92799-92811.
- Shoeibi, S. & Mashreghi, M.** 2017. Biosynthesis of selenium nanoparticles using *Enterococcus faecalis* and evaluation of their antibacterial activities. *Journal of Trace Elements in Medicine and Biology*, **39**, 135-139.
- Shum, A. C. & Murphy, J. C.** 1972. Effects of selenium compounds on formate metabolism and coincidence of selenium-75 incorporation and formic dehydrogenase activity in cell-free preparations of *Escherichia coli*. *Journal of Bacteriology*, **110**, 447-449.
- Siddique, T., Zhang, Y., Okeke, B. C. & Frankenberger, W. T.** 2006. Characterization of sediment bacteria involved in selenium reduction. *Bioresource Technology*, **97**, 1041-1049.
- Singh, J. S., Pandey, V. C., Singh, D. & Singh, R. P.** 2010. Influence of pyrite and farmyard manure on population dynamics of soil methanotroph and rice yield in saline rain-fed paddy field. *Agriculture, Ecosystems & Environment*, **139**, 74-79.
- Skotti, E., Kountouri, S., Bouchagier, P., Tsitsigiannis, D. I., Polissiou, M. & Tarantilis, P. A.** 2014. FTIR spectroscopic evaluation of changes in the cellular biochemical composition of the phytopathogenic fungus *Alternaria alternata* induced by extracts of some Greek medicinal and aromatic plants. *Spectrochimica Acta Part A: Molecular and Biomolecular Spectroscopy*, **127**, 463-472.
- Slobodkina, G. B., Lebedinsky, A. V., Chernyh, N. A., Bonch-Osmolovskaya, E. A. & Slobodkin, A. I.** 2015. *Pyrobaculum ferrireducens* sp. nov., a hyperthermophilic Fe (III)-, selenate- and arsenate-reducing crenarchaeon isolated from a hot spring. *International Journal of Systematic and Evolutionary Microbiology*, **65**, 851-856.
- Smith, T. J. & Murrell, J.** 2011. Mutagenesis of Soluble Methane Monooxygenase. *Methods in enzymology*, **495**, 135.
- Smith, T. & Murrell, C.** 2009. Methanotrophy/methane oxidation. *Encyclopedia of Microbiology*. Elsevier: Oxford, 293-298.
- Smith, T. J. & Foster, S. J.** 1995. Characterization of the involvement of two compensatory autolysins in mother cell lysis during sporulation of *Bacillus subtilis* 168. *Journal of Bacteriology*, **177**, 3855-3862.
- Soda, S., Takahashi, H., Kagami, T., Miyake, M., Notaguchi, E., Sei, K., Iwasaki, N. & Ike, M.** 2012. Biotreatment of selenium refinery wastewater using pilot-scale granular sludge and swim-bed bioreactors augmented with a selenium-reducing bacterium *Pseudomonas stutzeri* NT-I. *Journal [of] Japan Biological Society of Water and Waste*, **48**, 63-71.
- Song, C., Sun, X., Xing, S., Xia, P., Shi, Y. & Wang, S.** 2014. Characterization of the interactions between tetracycline antibiotics and microbial extracellular polymeric

substances with spectroscopic approaches. *Environmental Science and Pollution Research*, **21**, 1786-1795.

Song, D., Li, X., Cheng, Y., Xiao, X., Lu, Z., Wang, Y. & Wang, F. 2017. Aerobic biogenesis of selenium nanoparticles by *Enterobacter cloacae* Z0206 as a consequence of fumarate reductase mediated selenite reduction. *Scientific Reports*, **7**, 3239-017-03558-3.

Sonkusre, P., Nanduri, R., Gupta, P. & Cameotra, S. S. 2014. Improved extraction of intracellular biogenic selenium nanoparticles and their specificity for cancer chemoprevention. *J Nanomed Nanotechnol*, **5**, 1-9.

Srivastava, N. & Mukhopadhyay, M. 2013. Biosynthesis and structural characterization of selenium nanoparticles mediated by *Zooglea ramigera*. *Powder Technology*, **244**, 26-29.

Stadtman, T. 1991. Biosynthesis and function of selenocysteine-containing enzymes. *J Biol Chem*, **266**, 16257-16260.

Stadtman, T. C. 1990. Selenium biochemistry. *Annual Review of Biochemistry*, **59**, 111-127.

Staicu, L. C. & Barton, L. L. 2017. Bacterial metabolism of Selenium—For survival or profit. In: *Bioremediation of Selenium Contaminated Wastewater* (Ed. by Anonymous), pp. 1-31. Springer.

Staicu, L. C., Oremland, R. S., Tobe, R. & Mihara, H. 2017. Bacteria versus selenium: A view from the inside out. In: *Selenium in Plants* (Ed. by Anonymous), pp. 79-108. Springer.

Stanley, S., Prior, S., Leak, D. & Dalton, H. 1983. Copper stress underlies the fundamental change in intracellular location of methane mono-oxygenase in methane-oxidizing organisms: studies in batch and continuous cultures. *Biotechnology Letters*, **5**, 487-492.

Stolz, J. F., Gugliuzza, T., Blum, J. S., Oremland, R. & Murillo, F. M. 1997. Differential cytochrome content and reductase activity in *Geospirillum barnesii* strain SeS3. *Archives of Microbiology*, **167**, 1-5.

Stolz, J. F., Ellis, D. J., Blum, J. S., Ahmann, D., Lovley, D. R. & Oremland, R. S. 1999. Note: *Sulfurospirillum barnesii* sp. nov. and *Sulfurospirillum arsenophilum* sp. nov., new members of the *Sulfurospirillum* clade of the ϵ -Proteobacteria. *International Journal of Systematic and Evolutionary Microbiology*, **49**, 1177-1180.

Stolz, J. F. & Oremland, R. S. 1999. Bacterial respiration of arsenic and selenium. *FEMS Microbiology Reviews*, **23**, 615-627.

- Sun, X., Wang, S., Zhang, X., Chen, J. P., Li, X., Gao, B. & Ma, Y.** 2009. Spectroscopic study of Zn²⁺ and Co²⁺ binding to extracellular polymeric substances (EPS) from aerobic granules. *Journal of Colloid and Interface Science*, **335**, 11-17.
- Switzer Blum, J., Stolz, J. F., Oren, A. & Oremland, R. S.** 2001. *Selenihalanaerobacter shriftii* gen. nov., sp. nov., a halophilic anaerobe from Dead Sea sediments that respire selenate. *Archives of Microbiology*, **175**, 208-219.
- Switzer Blum, J., Burns Bindi, A., Buzzelli, J., Stolz, J. F. & Oremland, R. S.** 1998. *Bacillus arsenicoselenatis*, sp. nov., and *Bacillus selenitireducens*, sp. nov.: two haloalkaliphiles from Mono Lake, California that respire oxyanions of selenium and arsenic. *Archives of Microbiology*, **171**, 19-30.
- Tastet, L., Schaumlöffel, D. & Lobinski, R.** 2008. ICP-MS-assisted proteomics approach to the identification of selenium-containing proteins in selenium-rich yeast. *Journal of Analytical Atomic Spectrometry*, **23**, 309-317.
- Taylor, D., Dalton, C., Hall, A., Woodroffe, M. & Gardiner, P.** 2009. Recent developments in selenium research. *British Journal of Biomedical Science*, **66**, 107-116.
- Tellez, C. M., Gaus, K. P., Graham, D. W., Arnold, R. G. & Guzman, R. Z.** 1998. Isolation of copper biochelates from *Methylosinus trichosporium* OB3b and soluble methane monooxygenase mutants. *Applied and Environmental Microbiology*, **64**, 1115-1122.
- Terry, N., Carlson, C., Raab, T. & Zayed, A. M.** 1992. Rates of selenium volatilization among crop species. *Journal of Environmental Quality*, **21**, 341-344.
- Theisen, A. R., Ali, M. H., Radajewski, S., Dumont, M. G., Dunfield, P. F., McDonald, I. R., Dedysh, S. N., Miguez, C. B. & Murrell, J. C.** 2005. Regulation of methane oxidation in the facultative methanotroph *Methylocella silvestris* BL2. *Molecular microbiology*, **58**, 682-692.
- Thompson-Eagle, E. T., Frankenberger, W. T. & Karlson, U.** 1989. Volatilization of Selenium by *Alternaria alternata*. *Applied and Environmental Microbiology*, **55**, 1406-1413.
- Tian, B., Van den Bossche, J. & Kostarelos, K.** 2012. Design and engineering of multifunctional quantum dot-based nanoparticles for simultaneous therapeutic-diagnostic applications. In: *Multifunctional Nanoparticles for Drug Delivery Applications* (Ed. by Anonymous), pp. 345-365. Springer.
- Tiwari, S., Singh, J. S. & Singh, D. P.** 2015. Methanotrophs and CH₄ sink: effect of human activity and ecological perturbations. *Climate Change Environ.Sustain*, **3**, 35-50.
- Tolu, J., Le Hécho, I., Bueno, M., Thiry, Y. & Potin-Gautier, M.** 2011. Selenium speciation analysis at trace level in soils. *Analytica Chimica Acta*, **684**, 126-133.

- Tomei, F. A., Barton, L. L., Lemanski, C. L. & Zocco, T. G.** 1992. Reduction of selenate and selenite to elemental selenium by *Wolinella succinogenes*. Canadian Journal of Microbiology, **38**, 1328-1333.
- Tomei, F. A., Barton, L. L., Lemanski, C. L., Zocco, T. G., Fink, N. H. & Sillerud, L. O.** 1995. Transformation of selenate and selenite to elemental selenium by *Desulfovibrio desulfuricans*. Journal of industrial microbiology & biotechnology, **14**, 329-336.
- Torma, A. E. & Habashi, F.** 1972. Oxidation of copper (II) selenide by *Thiobacillus ferrooxidans*. Canadian journal of microbiology, **18**, 1780-1781.
- Tran, P. A. & Webster, T. J.** 2011. Selenium nanoparticles inhibit *Staphylococcus aureus* growth. International Journal of Nanomedicine, **6**, 1553-1558.
- Tugarova, A. V. & Kamnev, A. A.** 2017. Proteins in microbial synthesis of selenium nanoparticles. Talanta, **174**, 539-547.
- Tugarova, A. V., Mamchenkova, P. V., Dyatlova, Y. A. & Kamnev, A. A.** 2017. FTIR and Raman spectroscopic studies of selenium nanoparticles synthesised by the bacterium *Azospirillum thiophilum*. Spectrochimica Acta Part A: Molecular and Biomolecular Spectroscopy, **192**, 458-463.
- Tugarova, A. V., Vetchinkina, E. P., Loshchinina, E. A., Burov, A. M., Nikitina, V. E. & Kamnev, A. A.** 2014. Reduction of selenite by *Azospirillum brasilense* with the formation of selenium nanoparticles. Microbial Ecology, **68**, 495-503.
- Tugarova, A., Vetchinkina, E., Loshchinina, E., Shchelochkov, A., Nikitina, V. & Kamnev, A.** 2013. The ability of the rhizobacterium *Azospirillum brasilense* to reduce selenium (IV) to selenium (0). Microbiology, **82**, 352-355.
- Turner, R. J., Borghese, R. & Zannoni, D.** 2012. Microbial processing of tellurium as a tool in biotechnology. Biotechnology Advances, **30**, 954-963.
- Turner, R. J., Weiner, J. H. & Taylor, D. E.** 1998. Selenium metabolism in *Escherichia coli*. Biometals, **11**, 223-227.
- Unden, G., Becker, S., Bongaerts, J., Holighaus, G., Schirawski, J. & Six, S.** 1995. O₂-sensing and O₂-dependent gene regulation in facultatively anaerobic bacteria. Archives of Microbiology, **164**, 81-90.
- Van Fleet-Stalder, V. & Chasteen, T. G.** 1998. Using fluorine-induced chemiluminescence to detect organo-metalloids the headspace of phototrophic bacterial cultures amended with selenium and tellurium. Journal of Photochemistry and Photobiology B: Biology, **43**, 193-203.
- Van Overschelde, O., Guisbiers, G. & Snyders, R.** 2013. Green synthesis of selenium nanoparticles by excimer pulsed laser ablation in water. Apl Materials, **1**, 042114.

- Vekariya, K. K., Kaur, J. & Tikoo, K.** 2012. ER α signaling imparts chemotherapeutic selectivity to selenium nanoparticles in breast cancer. *Nanomedicine: Nanotechnology, Biology and Medicine*, **8**, 1125-1132.
- Vogel, M., Fischer, S., Maffert, A., Hübner, R., Scheinost, A., Franzen, C. & Steudtner, R.** 2017. Biotransformation and detoxification of selenite by microbial biogenesis of selenium-sulfur nanoparticles. *Journal of Hazardous Materials*, .
- Wadhvani, S. A., Shedbalkar, U. U., Singh, R. & Chopade, B. A.** 2016. Biogenic selenium nanoparticles: current status and future prospects. *Applied Microbiology and Biotechnology*, **100**, 2555-2566.
- Wallar, B. J. & Lipscomb, J. D.** 1996. Dioxygen activation by enzymes containing binuclear non-heme iron clusters. *Chemical Reviews*, **96**, 2625-2658.
- Wang, J., Zhang, Y., Yuan, Y. & Yue, T.** 2014. Immunomodulatory of selenium nanoparticles decorated by sulfated *Ganoderma lucidum* polysaccharides. *Food and Chemical Toxicology*, **68**, 183-189.
- Wang, T., Yang, L., Zhang, B. & Liu, J.** 2010. Extracellular biosynthesis and transformation of selenium nanoparticles and application in H₂ O₂ biosensor. *Colloids and Surfaces B: Biointerfaces*, **80**, 94-102.
- Watts, C. A., Ridley, H., Condie, K. L., Leaver, J. T., Richardson, D. J. & Butler, C. S.** 2003. Selenate reduction by *Enterobacter cloacae* SLD1a-1 is catalysed by a molybdenum-dependent membrane-bound enzyme that is distinct from the membrane-bound nitrate reductase. *FEMS Microbiology Letters*, **228**, 273-279.
- Webb, S.** 2005. SIXpack: a graphical user interface for XAS analysis using IFEFFIT. *Physica Scripta*, **2005**, 1011.
- Weeks, M. E.** 1932. The discovery of the elements. VI. Tellurium and selenium. *J.Chem.Educ*, **9**, 474.
- Weres, O., Jaouni, A. & Tsao, L.** 1989. The distribution, speciation and geochemical cycling of selenium in a sedimentary environment, Kesterson Reservoir, California, USA. *Applied Geochemistry*, **4**, 543-563.
- Whittenbury, R., Phillips, K. & Wilkinson, J.** 1970. Enrichment, isolation and some properties of methane-utilizing bacteria. *Microbiology*, **61**, 205-218.
- Wilber, C. G.** 1980. Toxicology of selenium: a review. *Clinical toxicology*, **17**, 171-230.
- Williams, K. H., Wilkins, M. J., N'Guessan, A., Arey, B., Dodova, E., Dohnalkova, A., Holmes, D., Lovley, D. R. & Long, P. E.** 2013. Field evidence of selenium bioreduction in a uranium-contaminated aquifer. *Environmental Microbiology reports*, **5**, 444-452.

- Yadav, V., Sharma, N., Prakash, R., KK, R., Bharadwaj, L. & Prakash, N. T.** 2008. Generation of selenium containing nano-structures by soil bacterium *Pseudomonas Aeruginosa*. *Biotechnology*, **7**, 299-304.
- Yang, K., Cui, Q., Hou, Y., Liu, B., Zhou, Q., Hu, J., Mao, H. & Zou, G.** 2007. Pressure-induced crystallization and phase transformation of amorphous selenium: Raman spectroscopy and x-ray diffraction studies. *Journal of Physics: Condensed Matter*, **19**, 425220.
- Yanke, L., Bryant, R. & Laishley, E.** 1995. Hydrogenase I of *Clostridium pasteurianum* functions as a novel selenite reductase. *Anaerobe*, **1**, 61-67.
- Yazdi, M. H., Mahdavi, M., Setayesh, N., Esfandyar, M. & Shahverdi, A. R.** 2013. Selenium nanoparticle-enriched *Lactobacillus brevis* causes more efficient immune responses *in vivo* and reduces the liver metastasis in metastatic form of mouse breast cancer. *DARU Journal of Pharmaceutical Sciences*, **21**, 33.
- Yee, N., Ma, J., Dalia, A., Boonfueng, T. & Kobayashi, D. Y.** 2007. Se(VI) reduction and the precipitation of Se(0) by the facultative bacterium *Enterobacter cloacae* SLD1a-1 are regulated by FNR. *Applied and Environmental Microbiology*, **73**, 1914-1920.
- Yu, R., Coffman, J. P., van Fleet-Stalder, V. & Chasteen, T. G.** 1997. Toxicity of oxyanions of selenium and of a proposed bioremediation intermediate, dimethyl selenone. *Environmental Toxicology and Chemistry*, **16**, 140-145.
- Yuan, S., Sun, M., Sheng, G., Li, Y., Li, W., Yao, R. & Yu, H.** 2010. Identification of key constituents and structure of the extracellular polymeric substances excreted by *Bacillus megaterium* TF10 for their flocculation capacity. *Environmental Science & Technology*, **45**, 1152-1157.
- Zannoni, D., Borsetti, F., Harrison, J. J. & Turner, R. J.** 2007. The bacterial response to the chalcogen metalloids Se and Te. *Advances in Microbial Physiology*, **53**, 1-312.
- Zehr, J. P. & Oremland, R. S.** 1987. Reduction of selenate to selenide by sulfate-respiring bacteria: experiments with cell suspensions and estuarine sediments. *Applied and Environmental Microbiology*, **53**, 1365-1369.
- Zhang, J., Gao, X., Zhang, L. & Bao, Y.** 2001. Biological effects of a nano red elemental selenium. *Biofactors*, **15**, 27-38.
- Zhang, L., Li, D. & Gao, P.** 2012. Expulsion of selenium/protein nanoparticles through vesicle-like structures by *Saccharomyces cerevisiae* under microaerophilic environment. *World Journal of Microbiology and Biotechnology*, **28**, 3381-3386.
- Zhang, L. & Chasteen, T. G.** 1994. Amending cultures of selenium-resistant bacteria with dimethyl selenone. *Applied Organometallic Chemistry*, **8**, 501-508.

Zhang, W., Chen, Z., Liu, H., Zhang, L., Gao, P. & Li, D. 2011. Biosynthesis and structural characteristics of selenium nanoparticles by *Pseudomonas alcaliphila*. *Colloids and Surfaces B: Biointerfaces*, **88**, 196-201.

Zhang, Y., Okeke, B. C. & Frankenberger, W. T. 2008. Bacterial reduction of selenate to elemental selenium utilizing molasses as a carbon source. *Bioresource Technology*, **99**, 1267-1273.

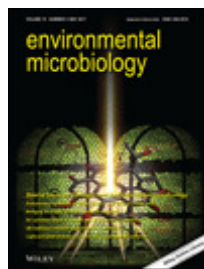
Zhou, X., Yuan, Y., Yang, Y., Rutzke, M., Thannhauser, T. W., Kochian, L. V. & Li, L. 2009. Involvement of a broccoli COQ5 methyltransferase in the production of volatile selenium compounds. *Plant Physiology*, **151**, 528-540.

Zioła-Frankowska, A., Kuta, J. & Frankowski, M. 2015. Application of a new HPLC-ICP-MS method for simultaneous determination of Al³⁺ and aluminium fluoride complexes. *Heliyon*, **1**, e00035.

Appendix



RightsLink®

[Home](#)
[Account Info](#)
[Help](#)


Title: Methanobactin and MmoD work in concert to act as the 'copper-switch' in methanotrophs

Author: Jeremy D. Semrau, Sheeja Jagadevan, Alan A. DiSpirito, et al

Publication: Environmental Microbiology

Publisher: John Wiley and Sons

Date: May 20, 2013

Copyright © 2013, John Wiley and Sons

Logged in as:
Abdurrahman Eswayah
Sheffield Hallam University

Account #:
3001184825

[LOGOUT](#)

Order Completed

Thank you for your order.

This Agreement between Sheffield Hallam University -- Abdurrahman Eswayah ("You") and John Wiley and Sons ("John Wiley and Sons") consists of your license details and the terms and conditions provided by John Wiley and Sons and Copyright Clearance Center.

Your confirmation email will contain your order number for future reference.

[printable details](#)

License Number	4317600817289
License date	Mar 28, 2018
Licensed Content Publisher	John Wiley and Sons
Licensed Content Publication	Environmental Microbiology
Licensed Content Title	Methanobactin and MmoD work in concert to act as the 'copper-switch' in methanotrophs
Licensed Content Author	Jeremy D. Semrau, Sheeja Jagadevan, Alan A. DiSpirito, et al
Licensed Content Date	May 20, 2013
Licensed Content Volume	15
Licensed Content Issue	11
Licensed Content Pages	10
Type of use	Dissertation/Thesis
Requestor type	University/Academic
Format	Print
Portion	Figure/table
Number of figures/tables	1
Original Wiley figure/table number(s)	1
Will you be translating?	No
Title of your thesis / dissertation	Bioremediation of Selenium Containing Species in Solution by Methanotrophic Bacteria
Expected completion date	Apr 2018
Expected size (number of pages)	200
Attachment	
Requestor Location	Sheffield Hallam University BMRC
	Howard Street Sheffield, S1 1WB

	United Kingdom
	Attn: Sheffield Hallam University
Publisher Tax ID	EU826007151
Total	0.00 GBP

Would you like to purchase the full text of this article? If so, please continue on to the content ordering system located here: [Purchase PDF](#)

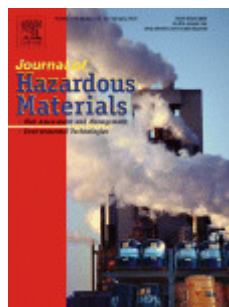
If you click on the buttons below or close this window, you will not be able to return to the content ordering system.

ORDER MORE CLOSE WINDOW

Copyright © 2018 [Copyright Clearance Center, Inc.](#) All Rights Reserved. [Privacy statement](#). [Terms and Conditions](#).
Comments? We would like to hear from you. E-mail us at customercare@copyright.com



RightsLink®

[Home](#)
[Account Info](#)
[Help](#)


Title: Biotransformation and detoxification of selenite by microbial biogenesis of selenium-sulfur nanoparticles

Author: M. Vogel, S. Fischer, A. Maffert, R. Hübner, A.C. Scheinost, C. Franzen, R. Steudtner

Publication: Journal of Hazardous Materials

Publisher: Elsevier

Date: 15 February 2018

© 2017 Elsevier B.V. All rights reserved.

Logged in as:
Abdurrahman Eswayah
Sheffield Hallam University

Account #:
3001184825

[LOGOUT](#)

Order Completed

Thank you for your order.

This Agreement between Sheffield Hallam University -- Abdurrahman Eswayah ("You") and Elsevier ("Elsevier") consists of your license details and the terms and conditions provided by Elsevier and Copyright Clearance Center.

Your confirmation email will contain your order number for future reference.

[printable details](#)

License Number	4317600271919
License date	Mar 28, 2018
Licensed Content Publisher	Elsevier
Licensed Content Publication	Journal of Hazardous Materials
Licensed Content Title	Biotransformation and detoxification of selenite by microbial biogenesis of selenium-sulfur nanoparticles
Licensed Content Author	M. Vogel, S. Fischer, A. Maffert, R. Hübner, A.C. Scheinost, C. Franzen, R. Steudtner
Licensed Content Date	Feb 15, 2018
Licensed Content Volume	344
Licensed Content Issue	n/a
Licensed Content Pages	9
Type of Use	reuse in a thesis/dissertation
Portion	figures/tables/illustrations
Number of figures/tables/illustrations	1
Format	print
Are you the author of this Elsevier article?	No
Will you be translating?	No
Original figure numbers	Graphical abstract
Title of your thesis/dissertation	Bioremediation of Selenium Containing Species in Solution by Methanotrophic Bacteria
Expected completion date	Apr 2018
Estimated size (number of pages)	200
Attachment	
Requestor Location	Sheffield Hallam University BMRC Howard Street Sheffield, S1 1WB

	United Kingdom
	Attn: Sheffield Hallam University
Publisher Tax ID	GB 494 6272 12
Total	0.00 GBP

ORDER MORE **CLOSE WINDOW**

Copyright © 2018 [Copyright Clearance Center, Inc.](#) All Rights Reserved. [Privacy statement.](#) [Terms and Conditions.](#)
Comments? We would like to hear from you. E-mail us at customercare@copyright.com